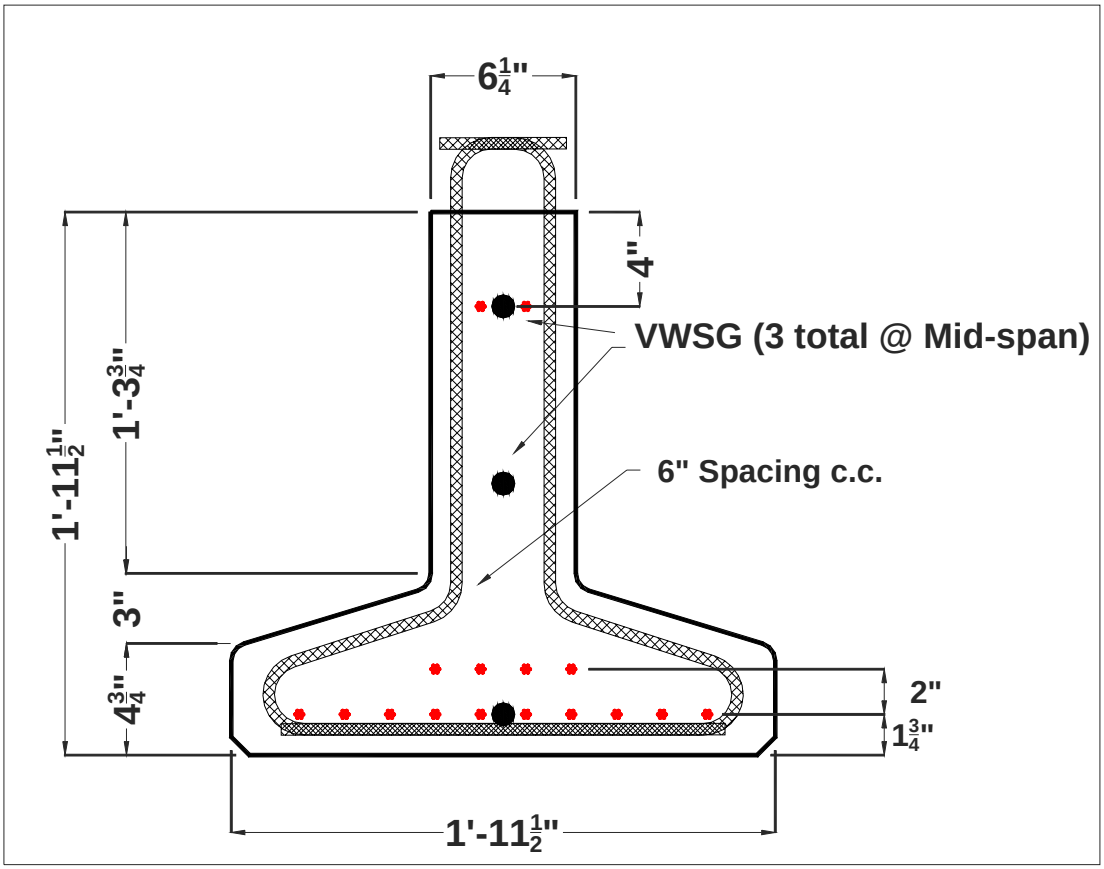

Figure 8.1: Cross section of IT600

Table 8.1: Geometric properties of IT600

A	=	256	$inch^2$	I	=	12,822	$inch^4$
E_{ci}	=	3,600	ksi	E_c	=	5,300	ksi
f_{ci}	=	6,280	psi	f_c	=	7,880	psi
Y_{bot}	=	8.45	inch	*e*	=	3.86	inch
H	=	23.5	inch	L	=	12	feet
M_{sw}	=	4.41	kip-ft	V/S	=	2.87	inch
f_{pj}	=	198	ksi	A_{ps}	=	2.448	$inch^2$
E_{ps}	=	28,500	ksi	RH	=	65	%

The remaining two specimens, used to determine the effect of shrinkage alone, had the prestressing strand tensioned to a “hand-tight” condition. Designations of these specimens were UT #1 and UT #2, where UT stands for untensioned. The same

number of strands were used in the untensioned specimens as in the fully tensioned specimens so that both specimen types had identical transformed section properties.

Long-term strains were recorded by use of embedded, vibrating-wire strain gages (VWSGs), Figure 8.2. The strain gages selected were the Model VCE-4200 Vibrating Wire-Embedded Strain Gage, manufactured by Geokon, Inc., Lebanon, New Hampshire. The manufacturer recommended this gage type for this project for its long-term strain and temperature-measuring capabilities of the concrete. Strains were measured using the vibrating-wire principle: a length of steel wire is tensioned between two end blocks that are embedded directly in the concrete. Deformations of the concrete mass will cause the two end blocks to move relative to one another, thus altering the tension in the steel wire. The tension is measured by plucking the wire and measuring its resonant frequency of vibration using an electromagnetic coil. (GeoKan, Inc.) The gages are connected to a data-acquisition system, and strain and temperature recordings are taken periodically. A correction calculation is needed to convert the strain reading into a true mechanical strain. (Ramakrishnam, 2001)

$$\mu_{actual} = \left(R_1 - R_0\right)B + \left(T_1 - T_0\right)\left(C_1\right) \tag{8.1}$$

where

$\mu_{actual} = \text{actual strain}\left(in/in\right)$;
$R_0 = \text{initial strain reading}\left(in/in\right)$;
$R_1 = \text{next strain reading}\left(in/in\right)$;
$B = \text{batch calibration factor given by manufacturer}$;
$T_0 = \text{initial temperature reading}\left({}^{o}C\right)$;
$T_1 = \text{next temperature reading}\left({}^{o}C\right)$; and
$C_1 = \text{coefficient of expansion of steel (wire)}\left(12.2\,\mu\varepsilon/{}^{o}C\right)$.

Three VWSGs were placed at mid span of each specimen. One was placed at a depth of four inches from the top (location of the top strands), another at 8.25 inches from the bottom (neutral axis of the cross section), and the final one at two inches from the bottom (location of bottom layer of strands), Figure 8.3. Strains from the gage at the bottom strand height were converted to stress and used for comparison purposes with code expressions. The other two gages were used to make sure the strains in the section remained linear and the bottom gage was reading correctly. To determine the stress from the corrected strain values, Hooke's Law was used.

$$\sigma = E_{ps}\varepsilon \tag{8.2}$$

where

E_{ps} = modulus of elasticity of prestressing strand (ksi) and
ε= corrected strain value (in/in).

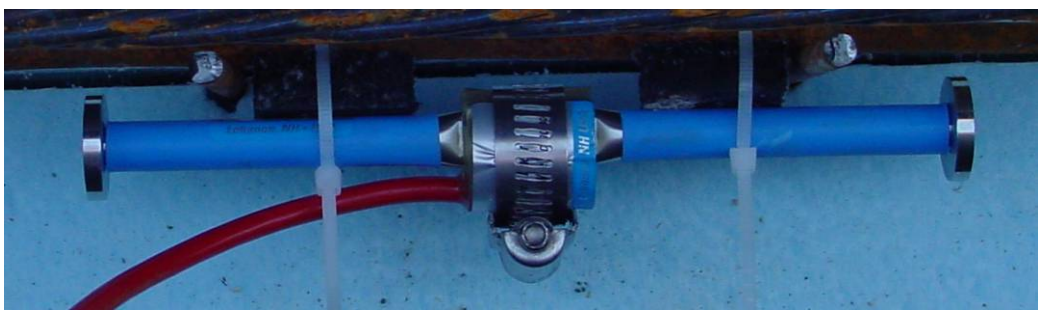

Figure 8.2: VWSG closeup

Figure 8.3: VWSGs at mid span

A load cell was placed at the “dead” end of the prestressing bed, Figure 8.4, in order to get an exact tensile force of the prestressing strand after jacking. The nominal value of the jacking stress, f_{pj}, was calculated to be 202.5 ksi. However, experimentally it was found to be 198 ksi and this value will be used as the jacking stress (f_{pj}) for all comparison calculations against code expressions. Strains were zeroed just prior to detensioning. Therefore, subsequent strain changes were due to prestress losses and not the concrete hardening during the setting process.

Figure 8.4: Load cell at dead end

Elastic shortening losses occur at the time the prestress force is transferred to the concrete and can be eliminated from long-term calculations. With use of low-relaxation prestressing strands, the increase in relaxation losses from transfer to final losses is very small compared to creep and shrinkage losses. Hence, individual relaxation losses were not isolated experimentally. Values for relaxation losses were calculated using code expressions. Elastic shortening losses were determined using two fully tensioned specimens and taking the change in stress at the center of gravity of the prestressing strands from just prior to detensioning to just after detensioning.

Long-term, time-dependent prestress losses (creep and shrinkage) were determined by use of both sets of specimens. Prestress loss due to shrinkage was obtained from the two untensioned specimens. Losses due to creep were determined by taking the losses of the fully tensioned specimens and subtracting the above noted

shrinkage loss in the untensioned specimens, the elastic shortening loss, and the calculated relaxation loss.

To compare experimental results with design code estimates, intermediate losses needed to be calculated. Most common methods (ACI, PCI, AASHTO) only calculate losses at transfer and at the end of the service life of the member. In order to estimate creep and shrinkage values for periods less than two years, the expression by Corley and Sozen was used. The following equation made it possible to compare creep and shrinkage values for periods less than two years.

$$R = 0.13 \ln\left(t + 1\right) \tag{8.3}$$

where

R = the total time-dependent proportion and
t = time (days).

This equation made it possible to calculate losses the member was experiencing at different selected days. Other more complex models could have been used to estimate creep and shrinkage values at intermediate time steps. However, since the applicability of these models to SCC has not been established, the general expression as shown in the previous equation 8.3 was chosen.

8.2 IT Fabrication

Fabrication of all IT specimens was performed at Prestressed Concrete Inc., Newton, Kansas. They were cast in the afternoon on February 10, 2005, and detensioned the next morning, February 11, 2005. As was the case with the flexural specimens, inverted-slump flow (spread), VSI, J-Ring, and L-Box tests were performed at the time of casting. The two fully tensioned specimens were cast on the rollaway bed (Figure 8.5) and the two untensioned specimens (Figure 8.6) on a utility bed. After all

internal shear reinforcement was tied into place, the VWSGs were tied into place. After that, the side walls were folded into place, Figure 8.7. Concrete was then poured into the forms, and no internal or external vibration was used on the SCC, Figure 8.8. The following morning, the walls were removed (Figure 8.9) and Whittemoe points (Figure 8.10) were glued onto the concrete two inches from the bottom. Once all the Whittemore points were installed and initial readings were taken, the strands were detensioned by flame cutting, Figure 8.11. Post-detensioning readings were taken and the specimens were placed on a flat bed trailer and shipped to Manhattan, Kansas. They were then monitored for their time-dependent deformations.

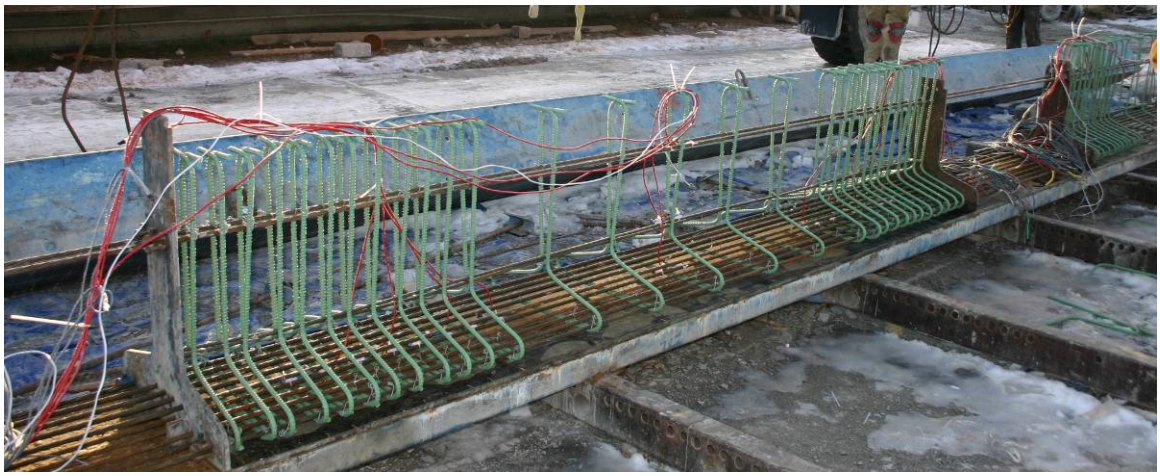

Figure 8.5: Tensioned IT specimen

Figure 8.6: Untensioned IT600 specimen

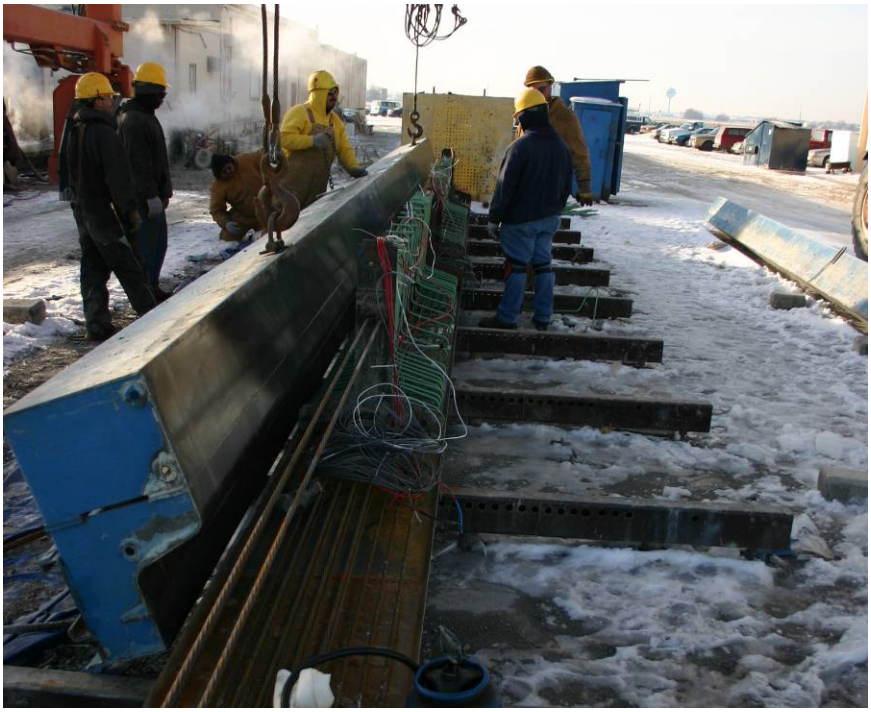

Figure 8.7: Side-form placement for IT600

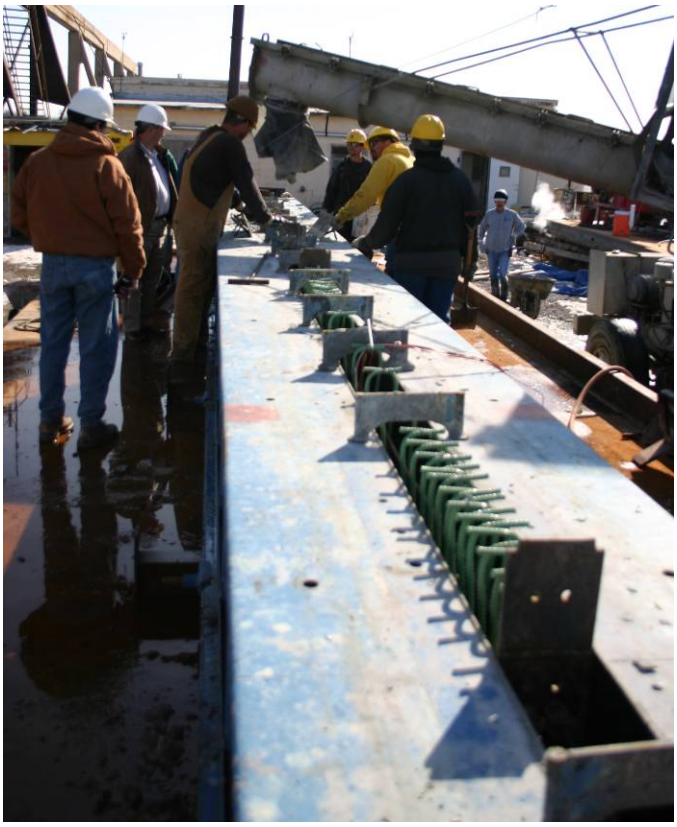

Figure 8.8: Placement of SCC

Figure 8.9: Side-form removal

Figure 8.10: Application of Whittemore points

Figure 8.11: Flame cutting of strands

CHAPTER NINE - IT SPECIMEN RESULTS

9.1 Material Properties

Inverted-slump flow (spread), VSI, J-Ring, and L-Box tests were performed before the casting of all IT specimens. Also, cylinder breaks that were matched-cured until detensioning were completed at the time of prestress release and at 28 days. Values for compressive strengths and modulus of elasticity for the SCC mixture can be seen in Table 8.1. The inverted-slump flow was measured to be 24 inches, J-Ring 22 inches, and the ratio of h_2/h_1 for the L-Box was 0.85. The VSI was determined by the author to be 0.

9.2 Transfer Length Results

Transfer lengths of the IT specimens were determined by use of concrete surface strains. The procedure for this method is detailed in section 5.2. The concrete strain profile versus specimen length for both FT #1 and FT #2 was plotted to determine transfer lengths. FT #1, Figure 9.1, had transfer lengths of 32 inches on one end and 23 inches on the other end. FT #2, Figure 9.2, had transfer lengths of 24 inches on one end and 28 inches on the other. Ends of the specimens with the greatest transfer lengths were both flame cut at detensioning, while ends with the smaller values underwent a gradual release during detensioning. Transfer length, as predicted by equation 1.1, was 24 inches. The value of 145 ksi was used for f_{se} (calculation shown in A.8). Using the expression for shear design for ACI (50-strand diameters as described in section 11.4.3 of the ACI Building Code), transfer length is 25 inches and 30 inches when using 60-strand diameters as stated by the AASHTO code (eq 5.11.4.1).

Experimental values for transfer length were all in general accordance with the values recommended by code equations.

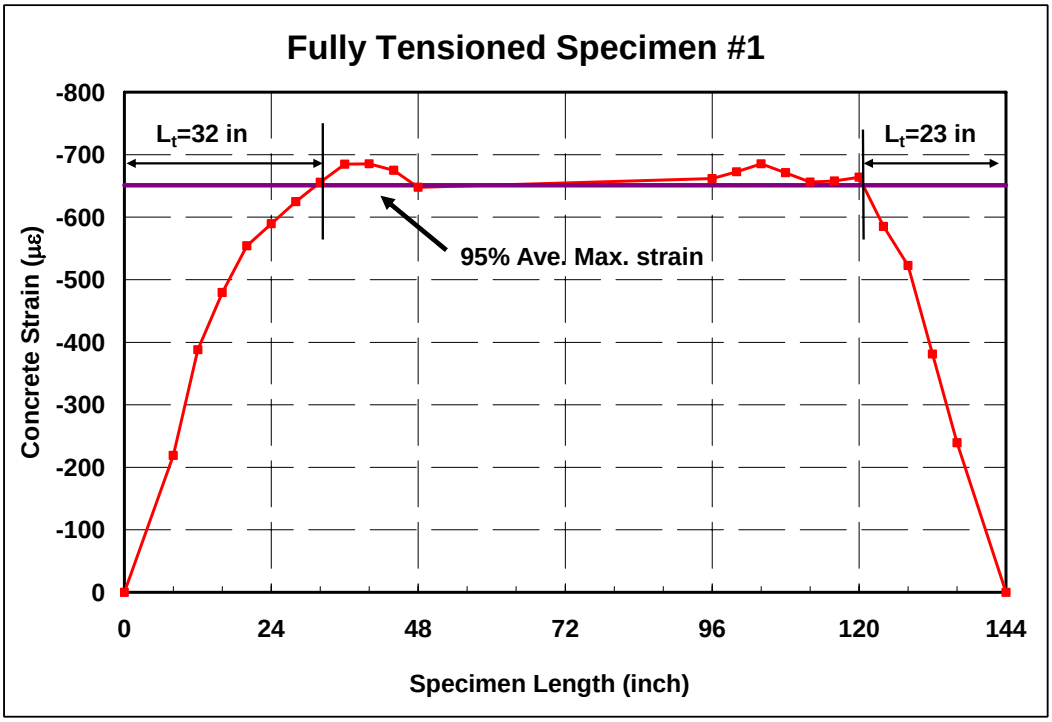

Figure 9.1: Concrete strain versus specimen length for FT #1

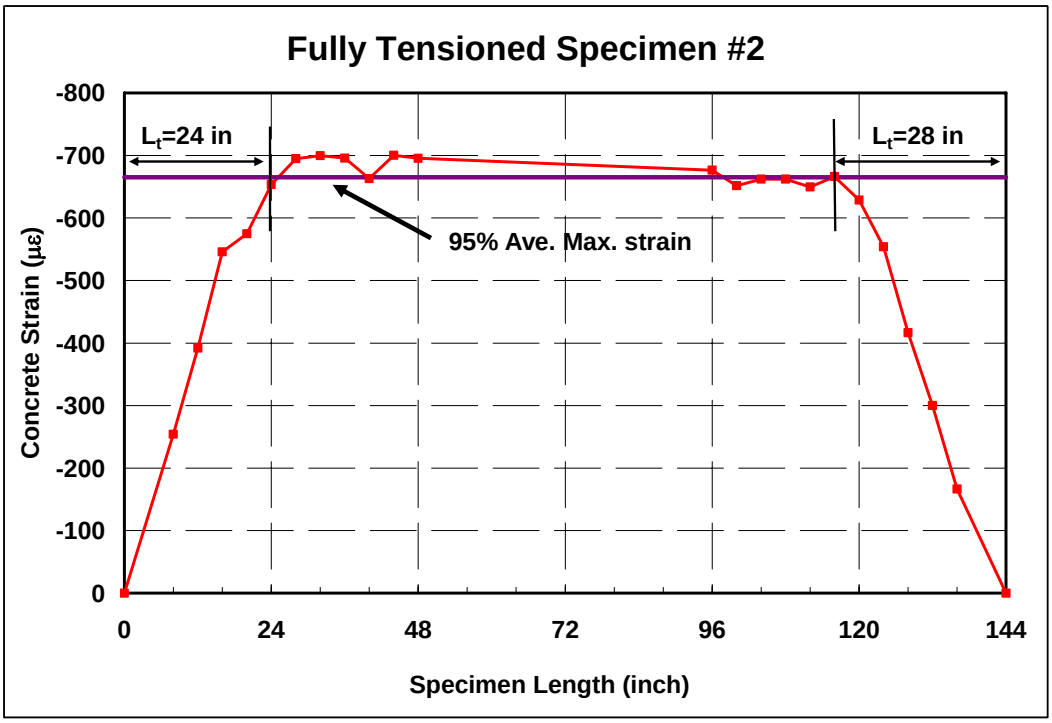

Figure 9.2: Concrete strain versus specimen length for FT #2

9.3 Prestress Loss Results

Using methods for determining prestress losses as described in Chapter Two and presented in section A.8, all values for elastic shortening, creep, shrinkage, and relaxation were calculated, see Table 9.1. Experimental results for modulus of elasticity for the concrete (E_{ci} & E_c) were used for calculations using code expressions. Experimental values recorded from the two fully tensioned IT specimens are also presented. (The average of the two specimens is given.) It was found that ACI and PCI methods gave the same results; therefore, they are presented in the same row. Experimental values for elastic shortening, creep, shrinkage, and relaxation are also given.

Table 9.1: Summary of time-dependent losses

Method	Elastic Shortening	Creep	Shrinkage	Relaxation	Effective Prestress Stress
AASHTO	19.3	29.3	7.3	1.5	141
ACI/PCI	17.3	23.6	6.8	3.1	147
KDOT	18.9	29.3	7.3	1.3	141
Experimental*	18.8	23.5	0.7	--	155

all values in ksi
* Data recorded at 514 days

Strains have been recorded throughout the life of the specimens. By using equation 8.3, time-dependent losses were estimated at several intermediate days and compared to the experimentally determined values. Results are shown in Table 9.2 and Figure 9.3 in graphical form.

Table 9.2: Strand stress predictions at various days

Time (Days)	AASHTO	ACI/PCI	KDOT	Experimental
Transfer	175	176	175	180
25	162	165	162	170
50	159	162	159	166
75	157	161	157	163
96	156	160	156	162
120	155	159	155	161
144	153	158	154	158
200	152	157	153	158
240	151	156	152	157
340	149	155	150	156
450	148	154	149	156
514	148	153	148	155
Long Term	141	147	141	--

all values in ksi

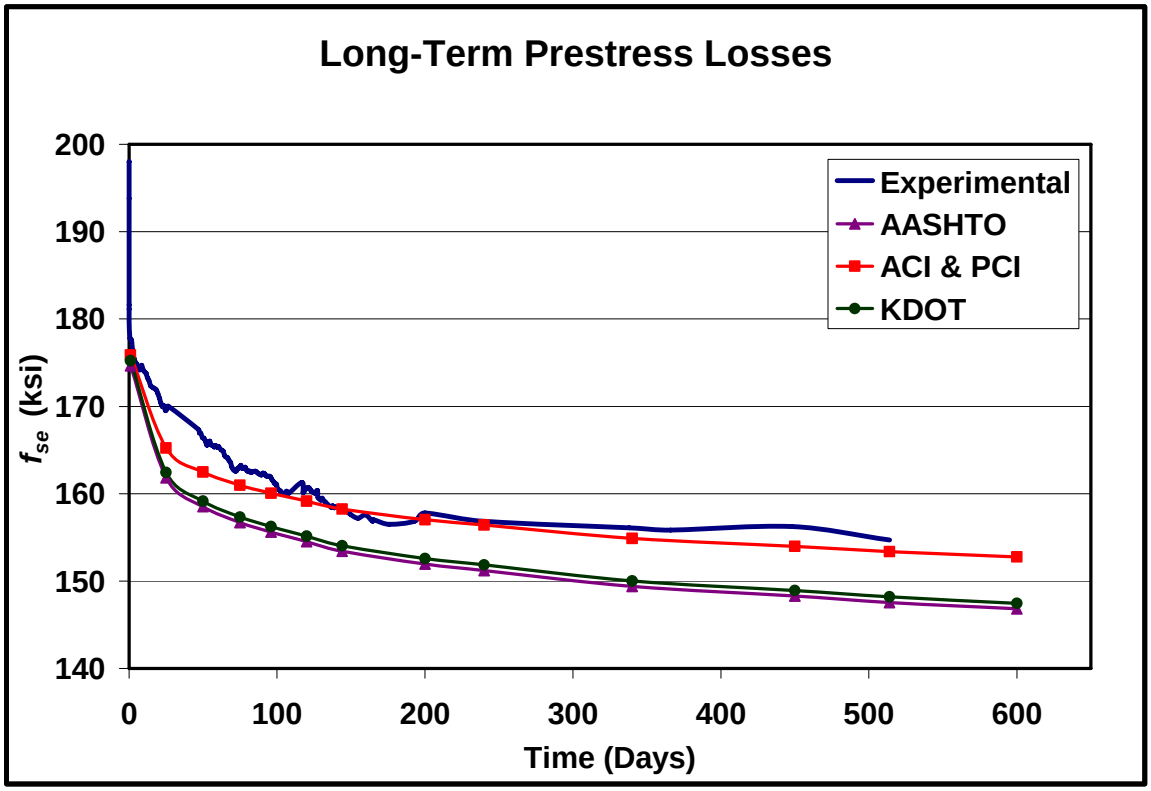

Figure 9.3: Strand stress predictions at various days

It can be seen from Table 9.1 that the experimental specimens did not experience as much of the prestress loss due to shrinkage as predicted by code equations. The two untensioned specimens were used to isolate the shrinkage loss, and the resulting values along with the PCI predicted values can be seen in Figure 9.4 (average of both specimens are shown). The maximum range for shrinkage was 3 ksi, but 0.7 ksi was used at 514 days because that was the present value. The erratic nature of the experimental results is due to the fact that the specimens were kept in the open and were able to experience more moisture and sunlight than normal bridge girders.

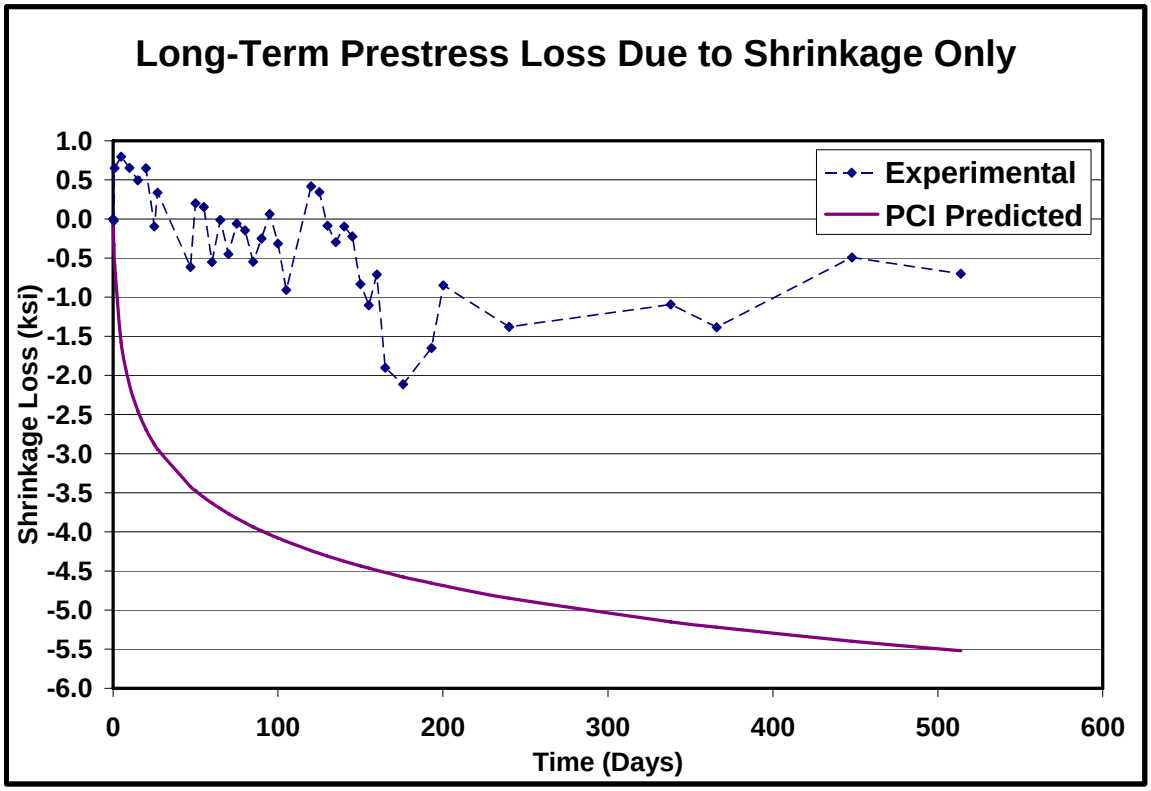

Figure 9.4: Prestress loss due to shrinkage only

Since three VWSGs were placed at mid span of the specimens at varying depths the concrete strains versus depth for both fully tensioned specimens could be plotted. From Figures 9.5 and 9.6, it can be seen that the strains remained linear throughout the life of the specimens, as expected.

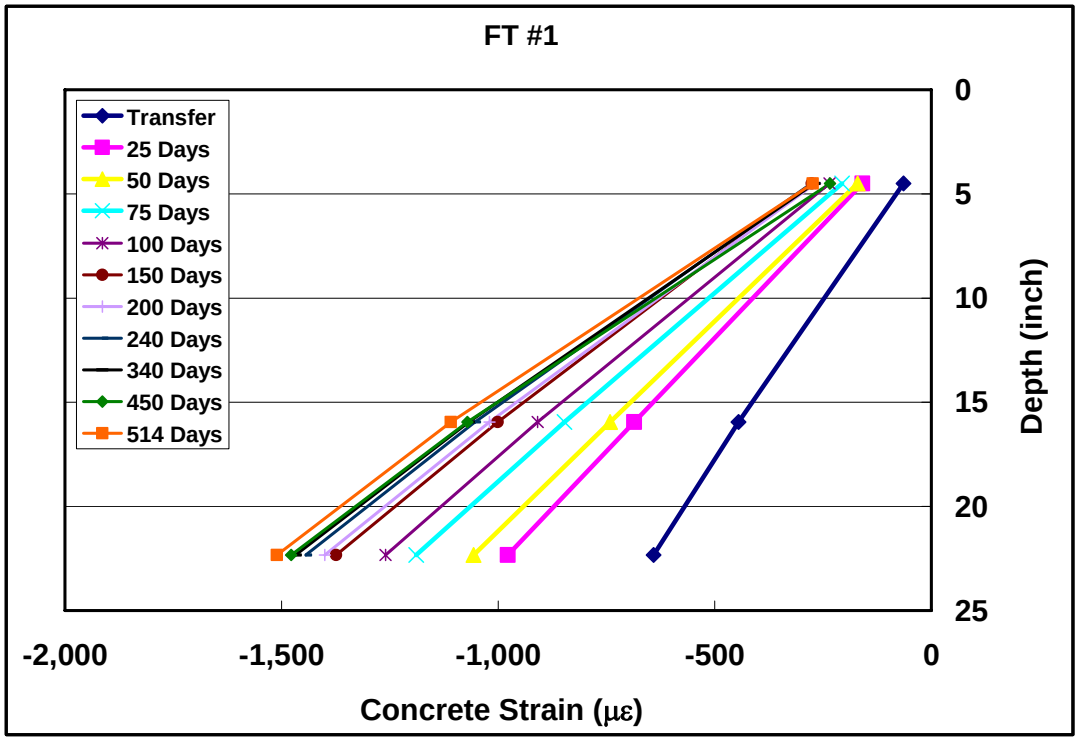

Figure 9.5: Concrete strain versus depth for FT #1

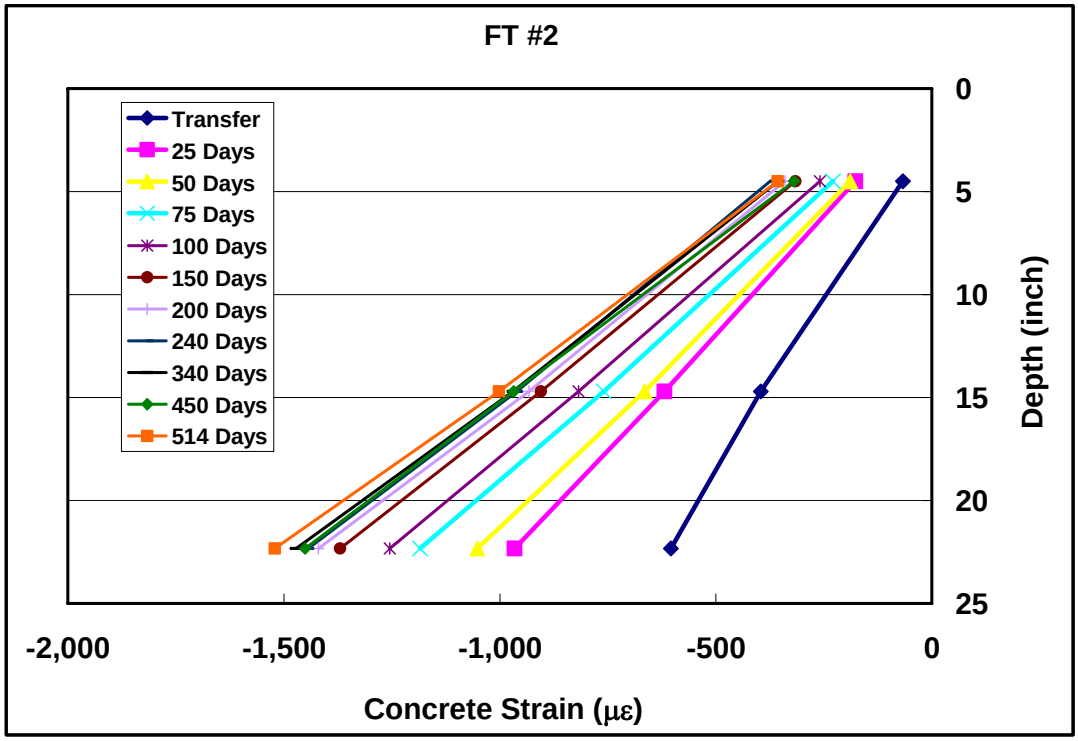

Figure 9.6: Concrete strain versus depth for FT #2

CHAPTER TEN - CREEP AND SHRINKAGE PRISMS

Creep and shrinkage are important factors in determining time-dependent deformations of precast members. ACI Committee 209 released a report which presented a unified approach to predicting the effect of moisture changes, sustained loading, and temperature on prestressed concrete structures. Creep is defined as the time-dependent deformation of hardened concrete subjected to sustained stress. Creep values are obtained by subtracting from the total measured strain of a loaded specimen the sum of the initial instantaneous (elastic) strain due to the sustained stress and shrinkage strain in an identical load-free specimen, which is subjected to the same relative humidity and temperature conditions. Shrinkage is defined as the contraction of concrete due to drying and physiochemical changes, dependent on time but not on stresses induced by external loading. (Mokhtarzadeh, 2000) Shrinkage is expressed as a dimensionless strain (inch/inch) under steady conditions of relative humidity and temperature. There are three types of shrinkage: drying shrinkage, autogenous shrinkage, and carbonation shrinkage. (ACI 209, 1997) Drying shrinkage is due to moisture loss in the concrete. Autogenous shrinkage is caused by the hydration of cement. Carbonation shrinkage results as various cement hydration products are carbonated in the presence of CO.

10.1 ACI 209 Creep Model

ACI Committee 209 presents the following equation for predicting the creep coefficient (ratio of creep strain to initial elastic strain) of concrete at any time

$$v_t = \frac{t^{\Psi}}{d + t^{\Psi}} v_u \tag{10.1}$$

where

v_t = creep coefficient at any time t;
t = time in days after loading;
Ψ = constant, $(0.40 < \Psi < 0.80)$;
d = constant, $(6 < d\ 30$ days); and
v_u = ultimate creep coefficient, $(1.30 < v_u < 4.15)$.

Creep tests were conducted as outlined in ASTM C512, Standard Test Method for Creep of Concrete in Compression. Specimens measuring four inches x four inches x 24 inches (square specimens) and 4.5 inches diameter x 24 inches (cylindrical specimens) were used in determining the ultimate creep coefficient. Ends of each specimen were capped with a sulfur-based, high-strength capping compound. The specimens were then loaded into the creep frame (Figure 10.1) and loaded to 40 percent of the compressive strength. Three specimens with four-inch x four-inch ends, along with one specimen with a 4.5-inch-diameter end were loaded to 40% of the compressive (release) strength while the specimens were one-day old. Four of the four-inch x four-inch ends were then loaded at 28 days to a stress of 40% of the 28-day compressive strength. The four specimens that were loaded at 28 days were kept in a moist room. Surface strains of the concrete were measured using Whittemore locating points (Figure 10.2 for square specimens and Figure 10.3 for cylindrical specimens). Each specimen had six strain measurements taken, three on each side. For the duration of the test, strain measurements of the creep specimens were measured and recorded periodically. In the 4.5-inch-diameter specimen and one of the specimens loaded at 28 days, a VWSG was embedded in the center to also measure creep strain.

Values of Ψ, *d*, and v_u can be determined by fitting the data obtained from the tests performed.

Figure 10.1: Specimen loaded in creep apparatus

Figure 10.2: Square specimen for creep and shrinkage

Figure 10.3: Cylindrical specimen for creep and shrinkage

10.2 ACI 209 Shrinkage Model

ACI Committee 209 presents the following equation for predicting shrinkage strain of concrete at any time:

$$\left(\varepsilon_{sh}\right)_t = \frac{t^{\alpha}}{f + t^{\alpha}}\left(\varepsilon_{sh}\right)_u \tag{10.2}$$

where

$\left(\varepsilon_{sh}\right)_t =$ shrinkage strain at any time t;
$t =$ time in days after loading;
$\alpha =$ constant $(0.90 < \alpha < 1.10)$;
$f =$ constant $(20 < f < 130$ days); and
$\left(\varepsilon_{sh}\right)_u =$ ultimate shrinkage strain $(415\,x10^{-6} < \left(\varepsilon_{sh}\right)_u < 1070\,x10^{-6})$.

Companion shrinkage specimens were cast at the same time as the creep specimens were made. To provide the same exposed surface area as the creep specimens, the shrinkage specimens were also capped. This prevented the shrinkage specimens from exchanging moisture with the environment through their ends. Four, four-inch x four-inch x 24-inch and one 4.5-inch-diameter by 24-inch specimens were used to measure shrinkage strains. Shrinkage specimens were stored in the vertical position, similar to the creep specimens. Identical to the creep specimens, surface strains were recorded using a Whittemore gage. Similar to the creep specimens, a VWSG was embedded into one of the four-inch x four-inch and one 4.5-inch-diameter end specimen. Both creep and shrinkage specimens were stored in the laboratory where the temperature was close to 75 degrees Fahrenheit with approximate 50% relative humidity. No controlled environment was provided to prevent fluctuation of the temperature and relative humidity.

CHAPTER ELEVEN - CREEP AND SHRINKAGE PRISM RESULTS

11.1 Creep

Creep tests were conducted for a duration of more than 500 days for the proposed SCC mixture. Immediately after loading, the initial deformation, representing the elastic response, was measured. Creep strains were then calculated by subtracting from the total strain, the initial elastic strain, and the average shrinkage of the unloaded companion specimens.

The experimental creep coefficient was found by the procedure described in ACI 209. The coefficient was found by deducting the initial elastic strain and also the shrinkage strains from the measured value and dividing by the initial elastic strain. Adjusting the parameters in equation 10.1, the ultimate creep coefficient can be determined by plotting the experimental data against the values obtained from equation 10.1. This adjustment was implemented to match the predicted curve with the experimental curve. Using this trial-and-error approach, the creep parameters for the square specimens were determined to be 0.7 for □, 16 for d, and 1.75 for v_u for the specimens loaded at day one; and 0.6 for □, 24 for d, and 2.00 for v_u for the specimens loaded at 28 days; for the SCC mixture. Values of the constants determined were all within the given ranges suggested by ACI 209. Results of the square specimens can be seen in Figures 11.1 and 11.2 for both “different loading days” cases.

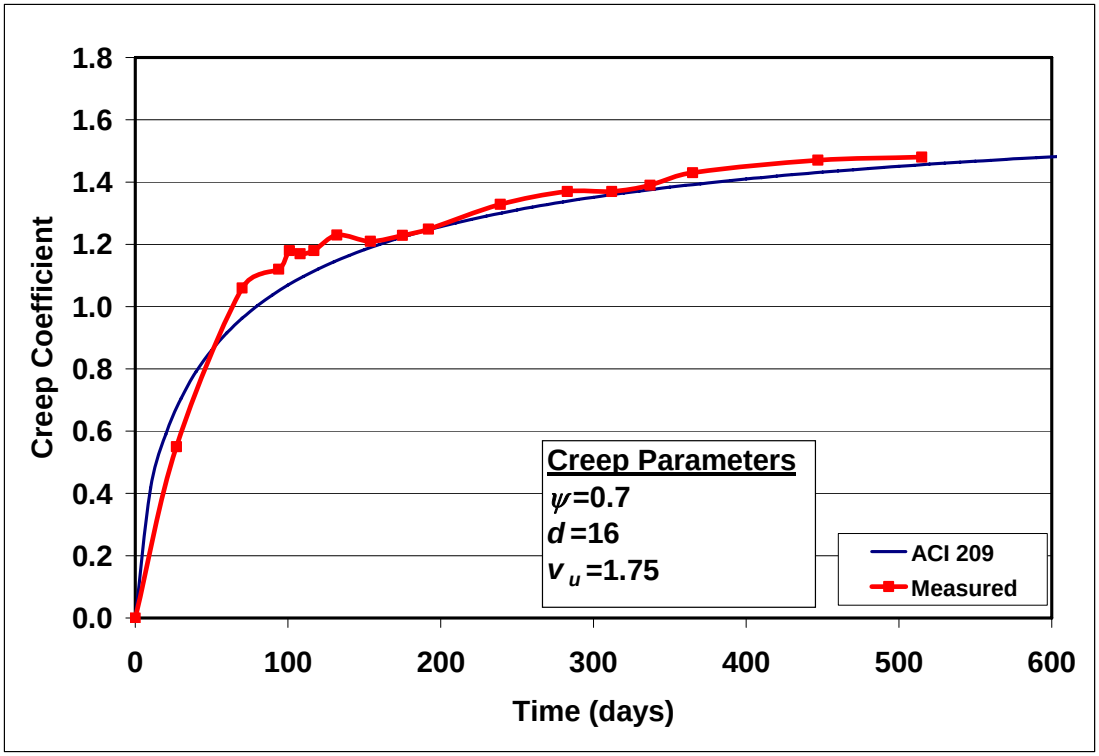

Figure 11.1: Creep coefficient for square specimens loaded at day one

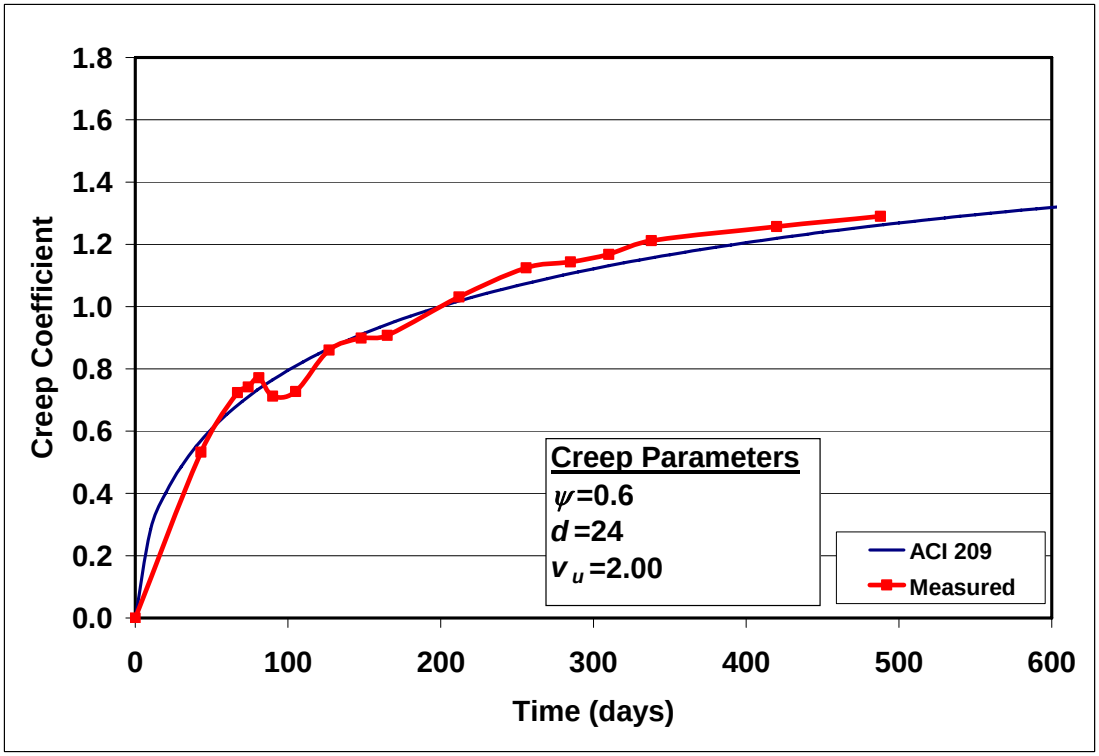

Figure 11.2: Creep coefficient for square specimens loaded at day 28

Figure 11.3 compares the creep coefficient predicted by ACI 209, to the experimental values measured for square, cylindrical, and cylindrical specimen with an embedded VWSG, all for a “day-one loaded” case. Figure 11.4 is an identical comparison for a “day-28 loaded” case. It can be seen in both cases that the specimen with the VWSG in the center had a larger creep coefficient. This can be attributed to the fact that the center of the specimen was experiencing more of the creep effect than the surface of the specimen.

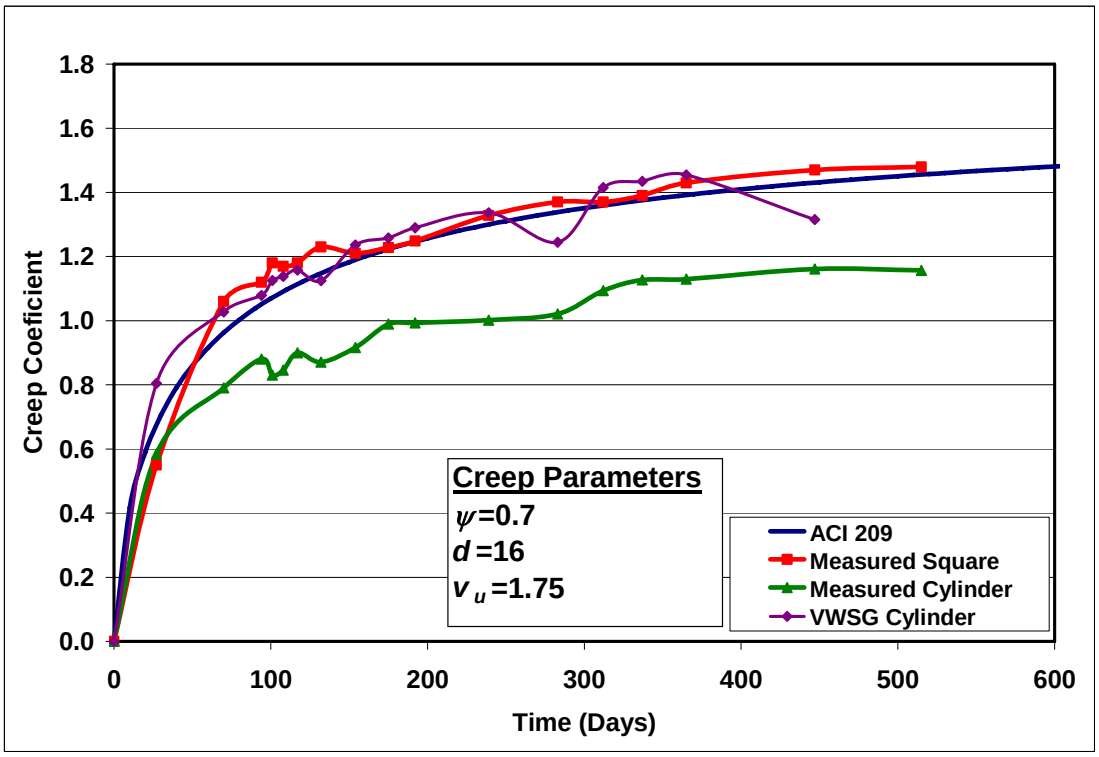

Figure 11.3: Creep coefficient for square and cylindrical (+VWSG) specimens loaded at day one

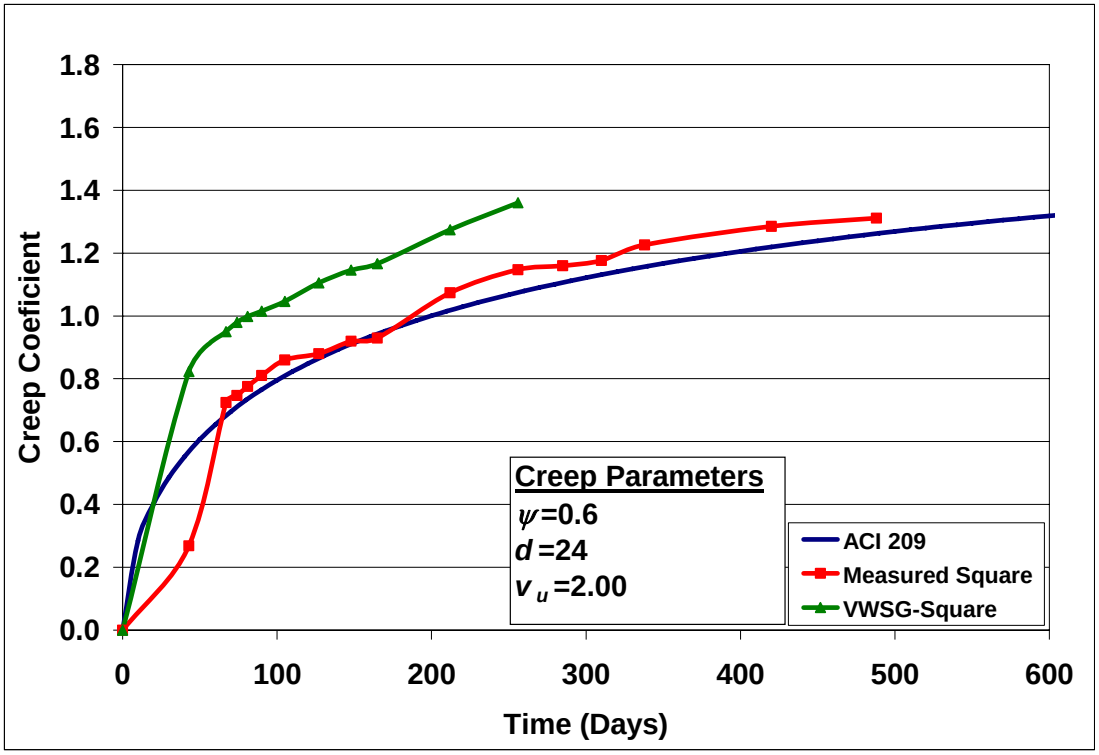

Figure 11.4: Creep coefficient for square (+VWSG) specimens at day 28

11.2 Shrinkage

Figure 11.5 shows the measured shrinkage strains of the square specimens with respect to time for the proposed SCC mixture. Predicted shrinkage strains are calculated from equation 10.2. Along with the predicted ACI 209 value and measured strains, the strain results of an embedded VWSG are also shown. It can be seen that the dip in strain values occurred for the strains measured with both the Whittemore points and the VWSG. This suggests that temperature and relative humidity changed during this portion. Shrinkage specimen parameters used in determining the predicted curve were 1.0 for □, 20 for f, and 550 x 10^6, for the ultimate shrinkage value $(\square_{sh})_u$. Figure 11.6 shows the measured shrinkage strains of the cylindrical specimen with respect to time for the proposed SCC mixture. The predicted shrinkage strains are calculated from equation 10.2. Along with the strains measured and predicted by ACI-

209 strains recorded by the embedded VWSG are presented in Figure 11.5. Shrinkage specimen parameters used in determining the predicted curve were 1.0 for □, 20 for f, and 600 x 10^6, for the ultimate shrinkage value $(\square_{sh})_u$. Figures 11.5 and 11.6 show that the surface of the specimens experienced more shrinkage than center of the specimens.

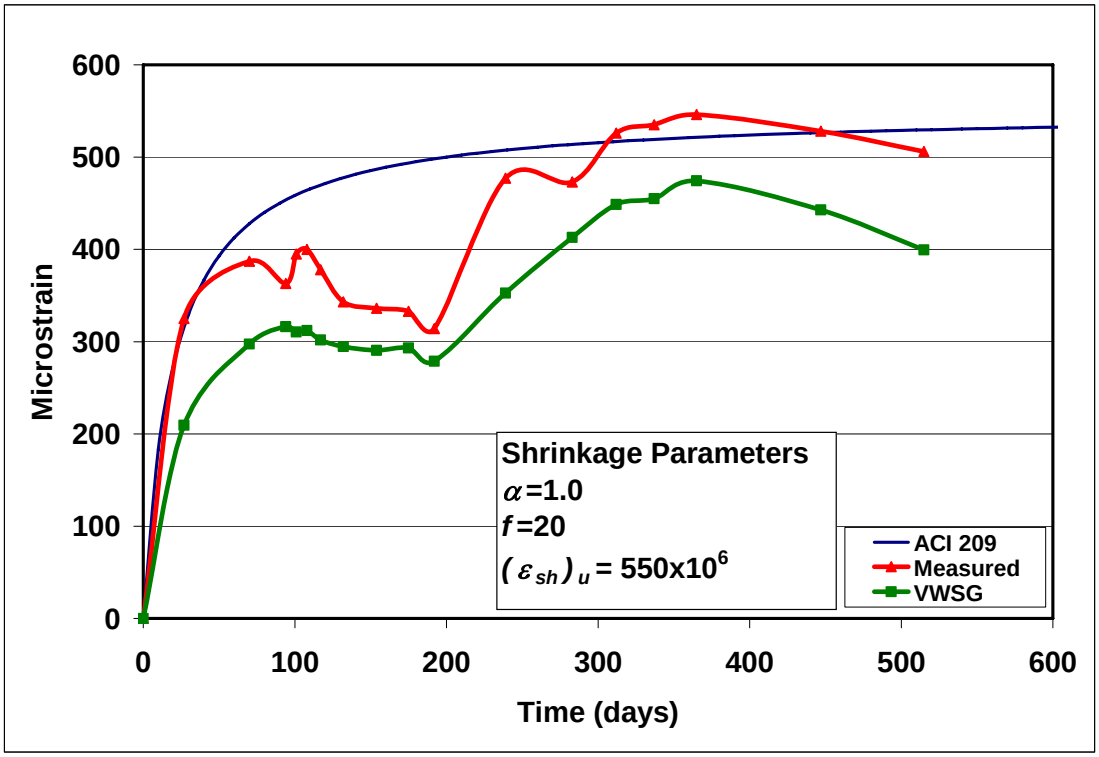

Figure 11.5: Shrinkage strains for square (+VWSG) specimens

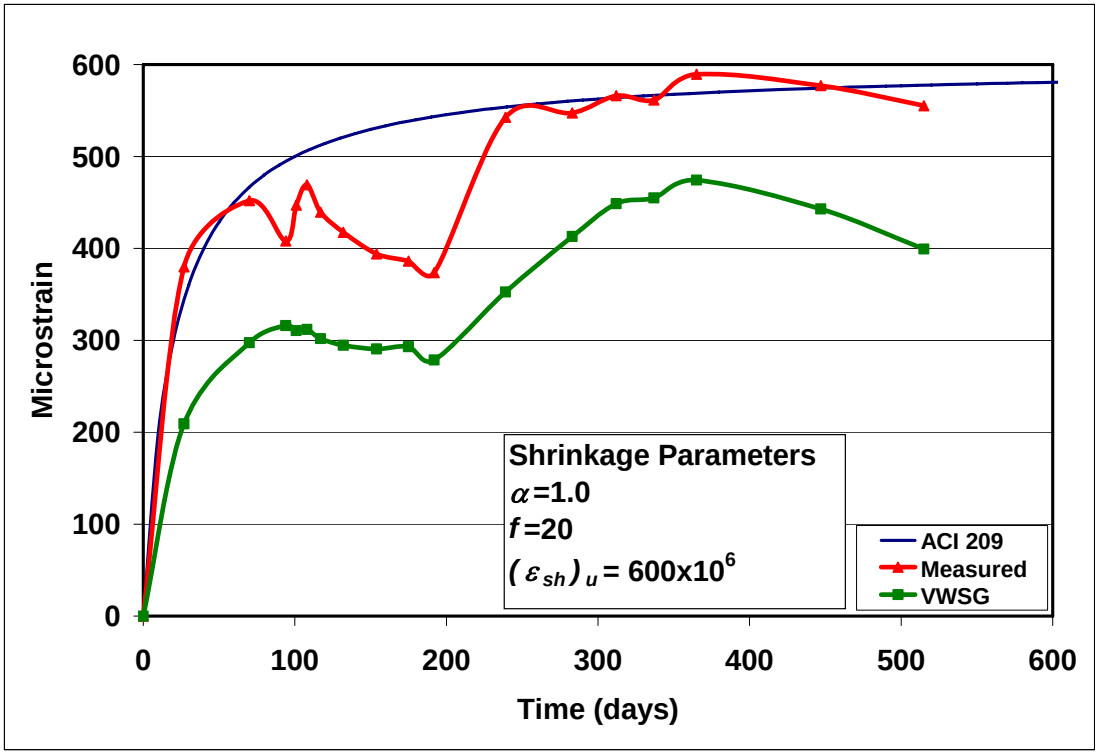

Figure 11.6: Shrinkage strains for cylindrical (+VWSG) specimens

Figure 11.7 shows the comparison of shrinkage strains for the square and cylindrical specimens. The cylindrical specimen experienced slightly larger strains than the square specimens. This was unexpected because the square specimens had a larger surface-to-volume ratio than the cylindrical specimens.

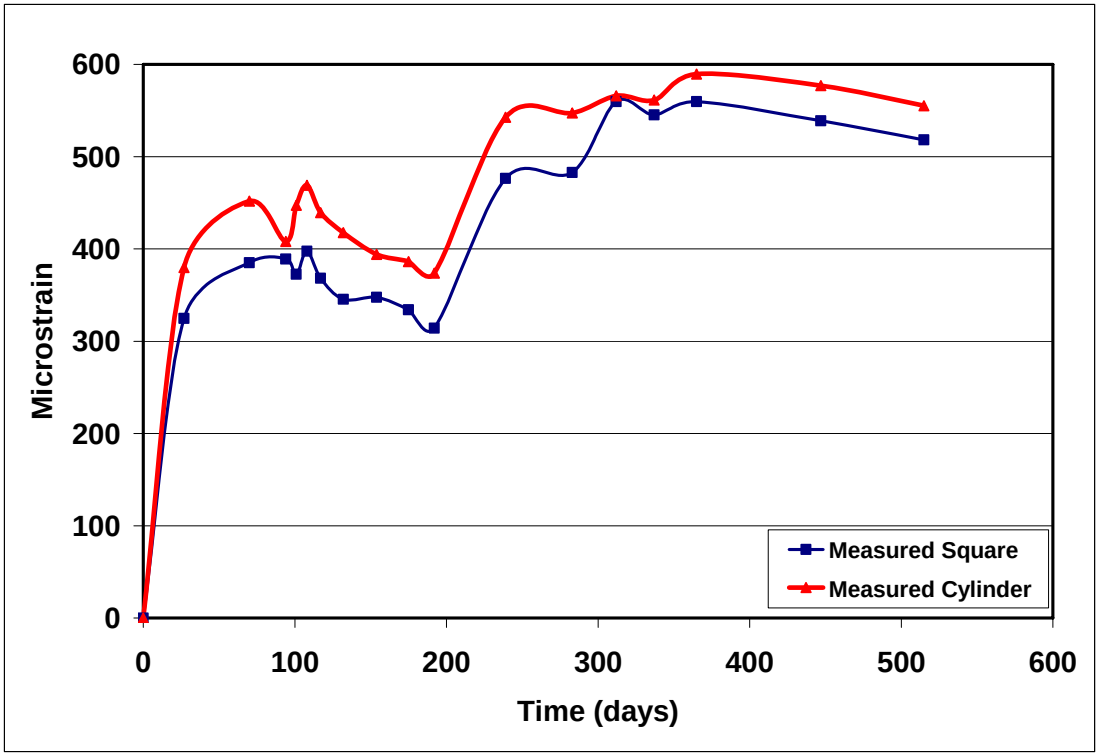

Figure 11.7: Comparison of square versus cylindrical specimen shrinkage strains

11.3 Comparison of ACI 209 Prestress Loss Predictions

The ACI 209 document, shown in section A.9, also has a procedure for calculating time-dependent losses. The creep and shrinkage loss terms utilize the creep coefficient (one day) and shrinkage strains that were determined in the previous sections. By using the results obtained from equations 10.1 and 10.2, the effective prestress was determined using the ACI 209 method (Table 11.1 and Figure 11.8) and compared to the experimental results of the IT specimens. It can be seen that the overall losses are fairly close to that of the experimental results. However, if each individual term is calculated separately, the creep predictions by ACI-209 will be much lower than the experimental results, and the shrinkage predictions will be much higher than the

experimental results. Table 11.2 shows this, along with the values predicted by the PCI method.

Table 11.1: Prestress loss predictions using ACI-209 method

Day	Elastic Shortening	Creep	Shrinkage	Relaxation	Total Losses	ACI 209 Predicted	Experimental Stress
Release	19.9	0.0	0.0	1.2	21.1	176.9	180.0
25	19.9	11.0	7.5	2.8	41.2	156.8	170.0
50	19.9	14.5	9.7	3.1	47.1	150.9	166.0
75	19.9	16.5	10.7	3.2	50.3	147.7	163.0
96	19.9	17.9	11.2	3.3	52.3	145.7	162.0
120	19.9	18.9	11.6	3.4	53.8	144.2	161.0
144	19.9	19.7	11.9	3.5	55.0	143.0	158.0
200	19.9	21.3	12.3	3.6	57.1	140.9	158.0
240	19.9	21.9	12.5	3.7	58.1	139.9	157.0
340	19.9	23.3	12.8	3.9	59.8	138.2	156.0
450	19.9	24.1	13.0	4.0	61.0	137.0	156.0
514	19.9	24.6	13.0	4.1	61.6	136.4	155.0
Ultimate	19.9	29.5	13.5	5.0	68.0	130.0	--

* all values reported in ksi

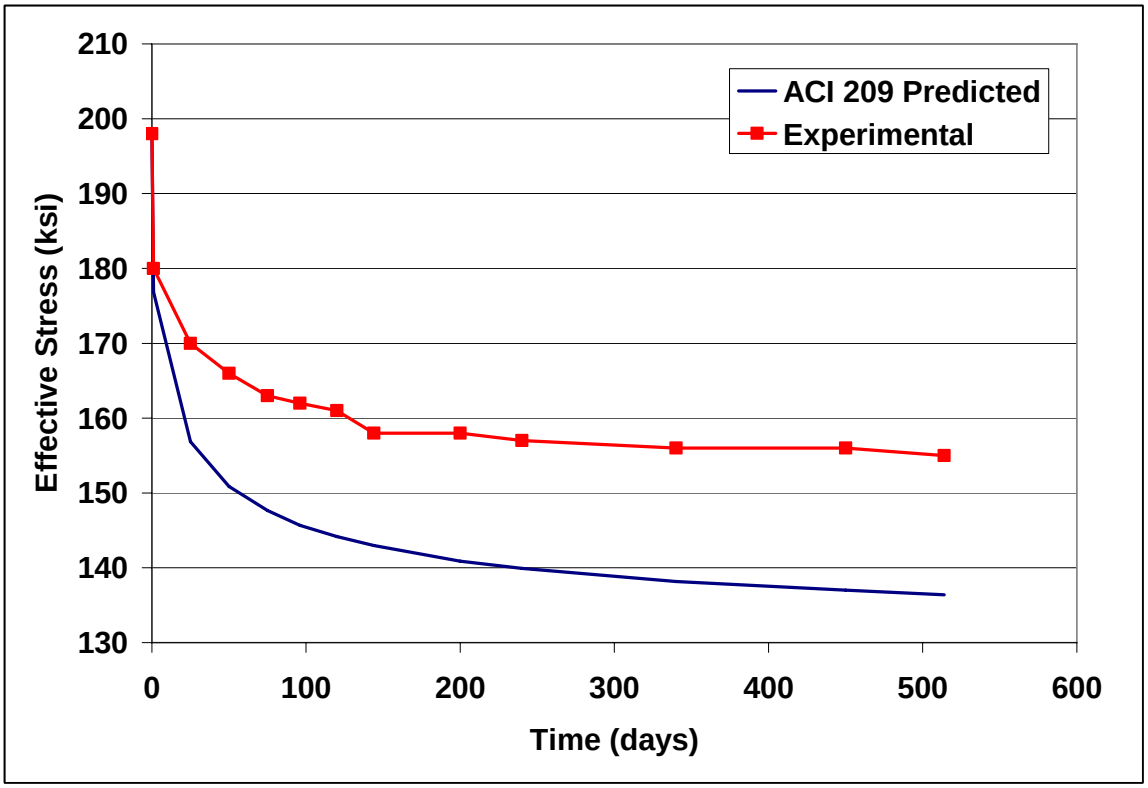

Figure 11.8: Effective stress versus time for ACI-209 prediction method

Table 11.2: Creep and shrinkage loss predictions using ACI-209 and PCI methods

Day	ACI-209 Creep	PCI Creep	Experimental Creep	ACI-209 Shrinkage	PCI Shrinkage	Experimental Shrinkage
Release	0.0	0.0	0.0	0.0	0.0	0.0
25	11.0	9.9	9.9	7.5	2.9	0.1
50	14.5	12.0	13.2	9.7	3.5	-0.2
75	16.5	13.2	16.1	10.7	3.8	-0.1
96	17.9	13.9	17.1	11.2	4.0	-0.1
120	18.9	14.6	19.4	11.6	4.2	-0.4
144	19.7	15.3	20.8	11.9	4.4	0.2
200	21.3	16.3	20.2	12.3	4.7	0.8
240	21.9	16.8	20.6	12.5	4.8	1.4
340	23.3	17.9	21.9	12.8	5.2	1.1
450	24.1	18.6	22.5	13.0	5.4	0.5
514	24.6	19.1	23.3	13.0	5.5	0.7
Ultimate	29.5	23.6	--	13.5	6.8	--

* all values reported in ksi

CHAPTER TWELVE - SCC BRIDGE MONITORING

A five-span bridge containing 35 girders was chosen to be instrumented, and long-term strain values were recorded. Of the 35 girders, 21 were cast with conventional concrete and the remaining 14 girders with SCC. The bridge was located on US Highway 160 in Cowley County just west of Winfield, Kansas. To determine the time-dependent losses, VWSGs were embedded into seven of the girders, four with conventional concrete and three with SCC. This was one of the first bridges with SCC to be monitored for long-term prestress losses. The girders used in this project were KDOT standard Type K3 girders, shown in Figure 12.1. Table 12.1 lists the geometric properties for this girder type.

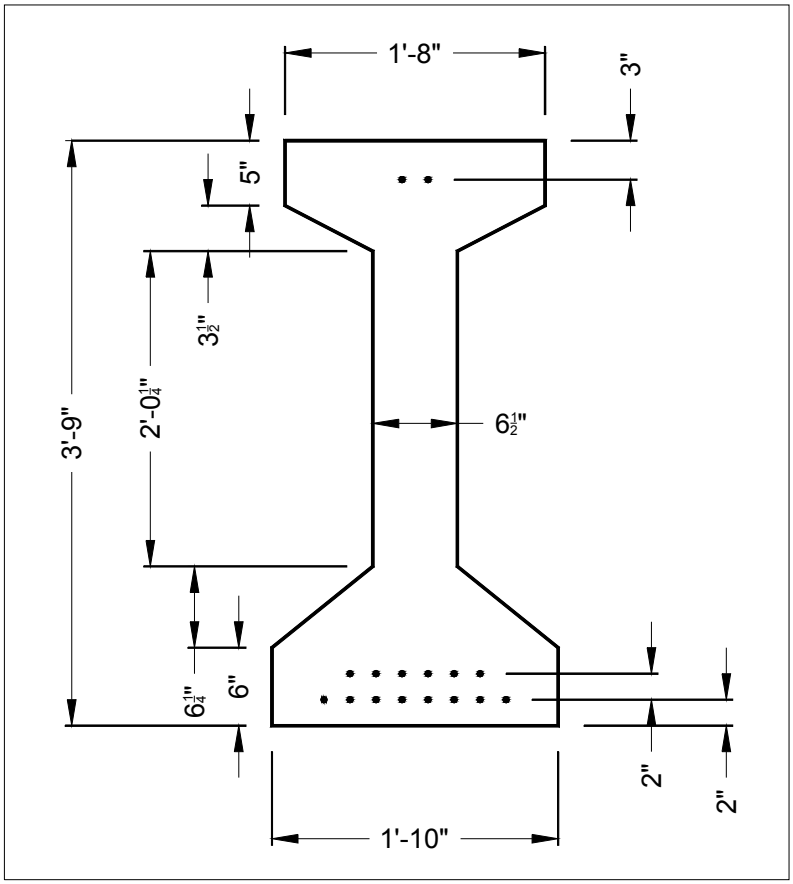

Figure 12.1: Cross section of K3 girder

Table 12.1: Geometric properties of K3 girder

A=	525	$inch^2$	I=	127,490	$inch^4$
Y_{bot}=	21	inch	*e* =	13.27	inch
H=	45	inch	L=	50	feet
w_o=	547	plf	V/S=	3.56	inch
f_{pj}=	202.5	ksi	A_{ps}=	2.448	$inch^2$
E_{ps}=	28,500	ksi	RH=	65	%

12.1 Girder Fabrication and Instrumentation

In order to determine the long-term strains experienced by the girders, VWSGs were selected for use in this project. Strain gages selected were the Model VCE-4200 Vibrating Wire-Embedded Strain Gage, identical to those used in the IT specimens.

Bridge instrumentation involved selecting seven girders and placing the VWSGs at various depths in each girder. Two different patterns of placing the gages at different depths were used. The first had three total gages embedded in the girder, with one being at the height of the top strand, one at 21 inches from the bottom (neutral axis of the section), and one at the bottom strand height, Figure 12.2. Girders with this depth pattern were A3, C3, and E3. The other gage pattern had six total gages embedded, one being at the height of the top strands, one at 21 inches from the bottom (neutral axis of the composite section, including the deck), one at 21 inches from the bottom (neutral axis of the section), one at four inches from the bottom, and two gages at the bottom strand height, Figure 12.2. The gage pattern was similar to the one used by Yang and Myers (2005). Two gages were placed at the bottom in case one of the gages broke. All gages were placed at mid span of the seven selected girders.

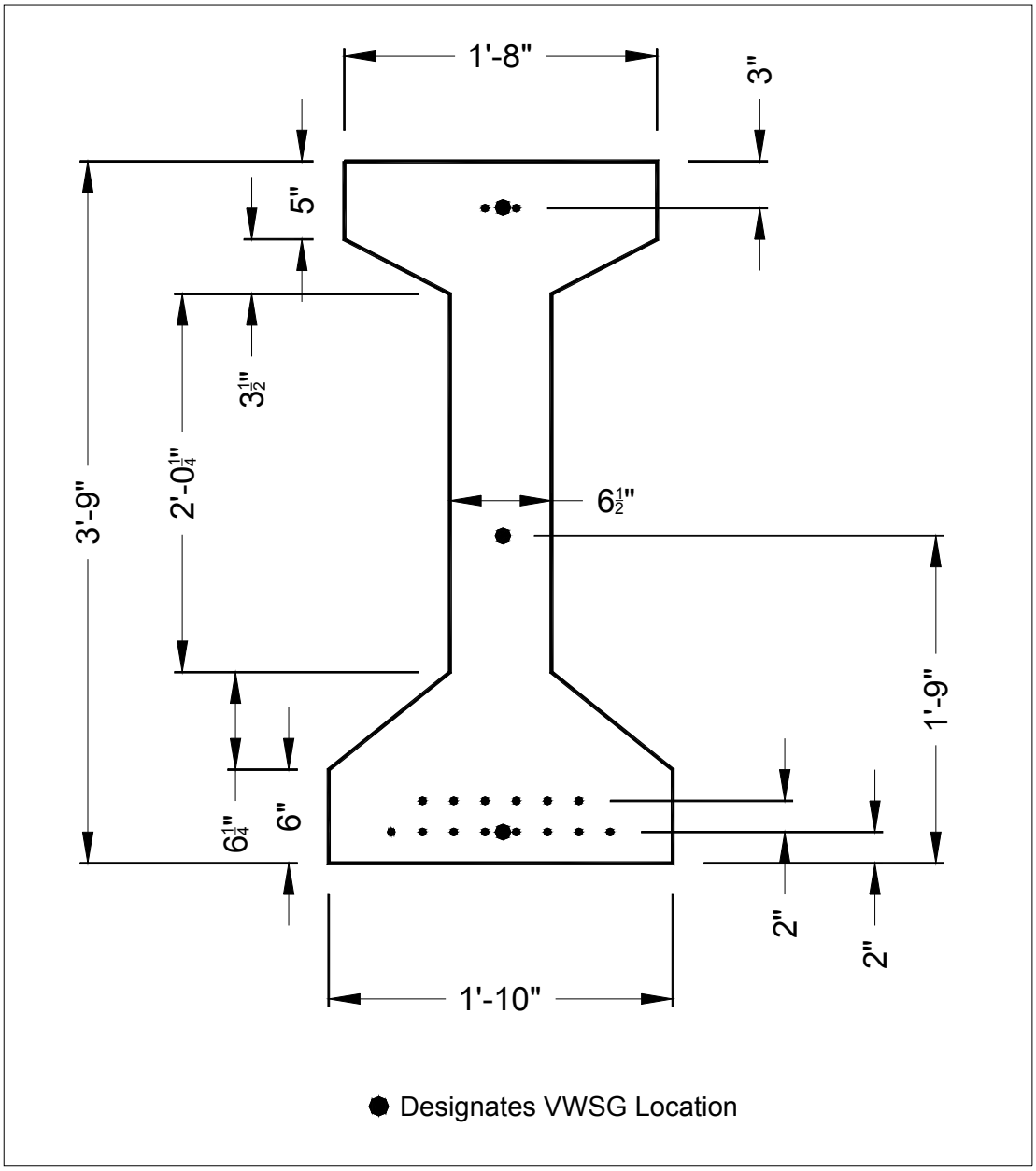

Figure 12.2: VWSG placement for girders with three gages

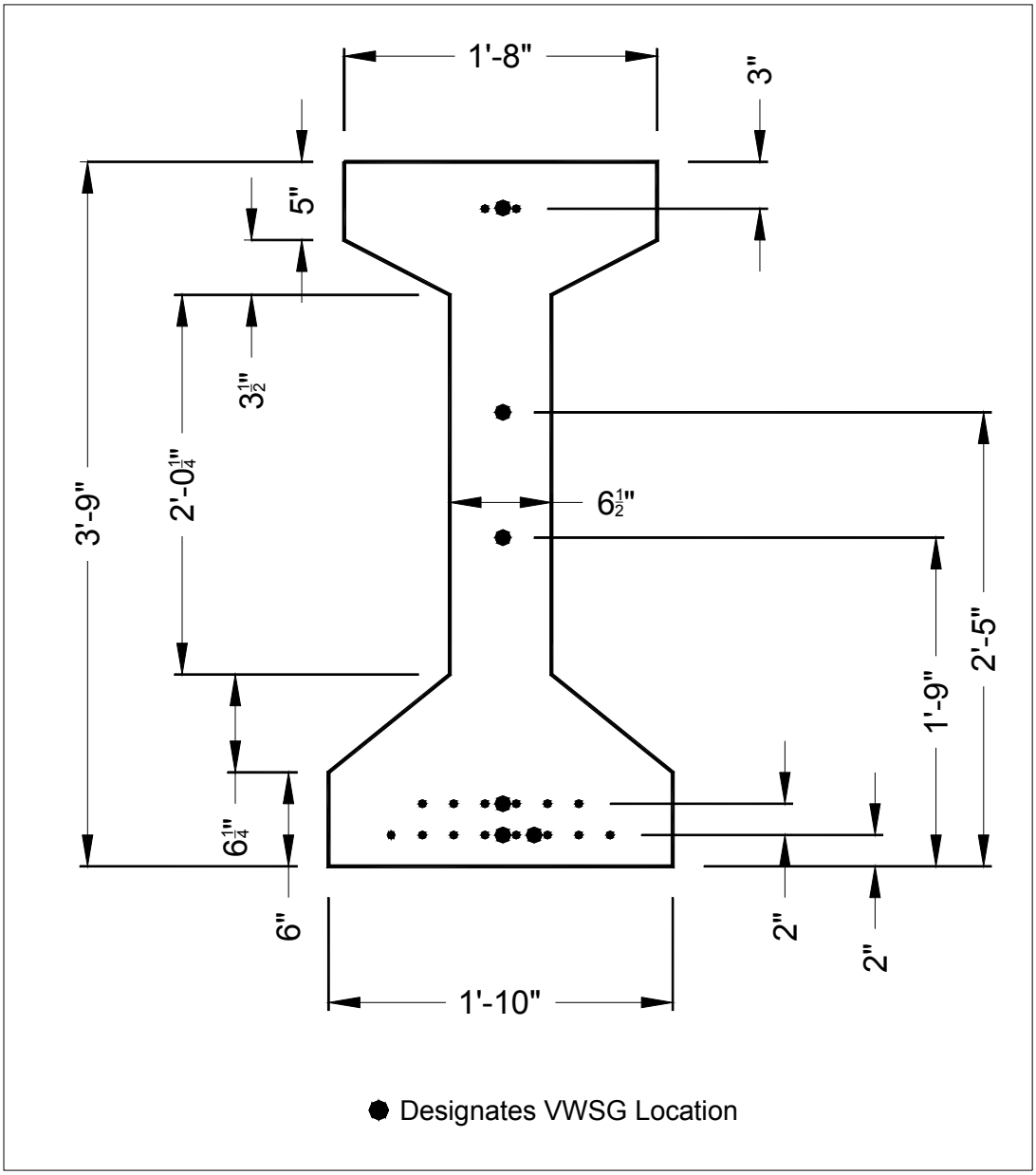

Figure 12.3: VWSG placement for girders with six gages

Figure 12.4 and 12.5 show the VWSGs tied to the internal rebar for the girders with three and six gages, respectively.

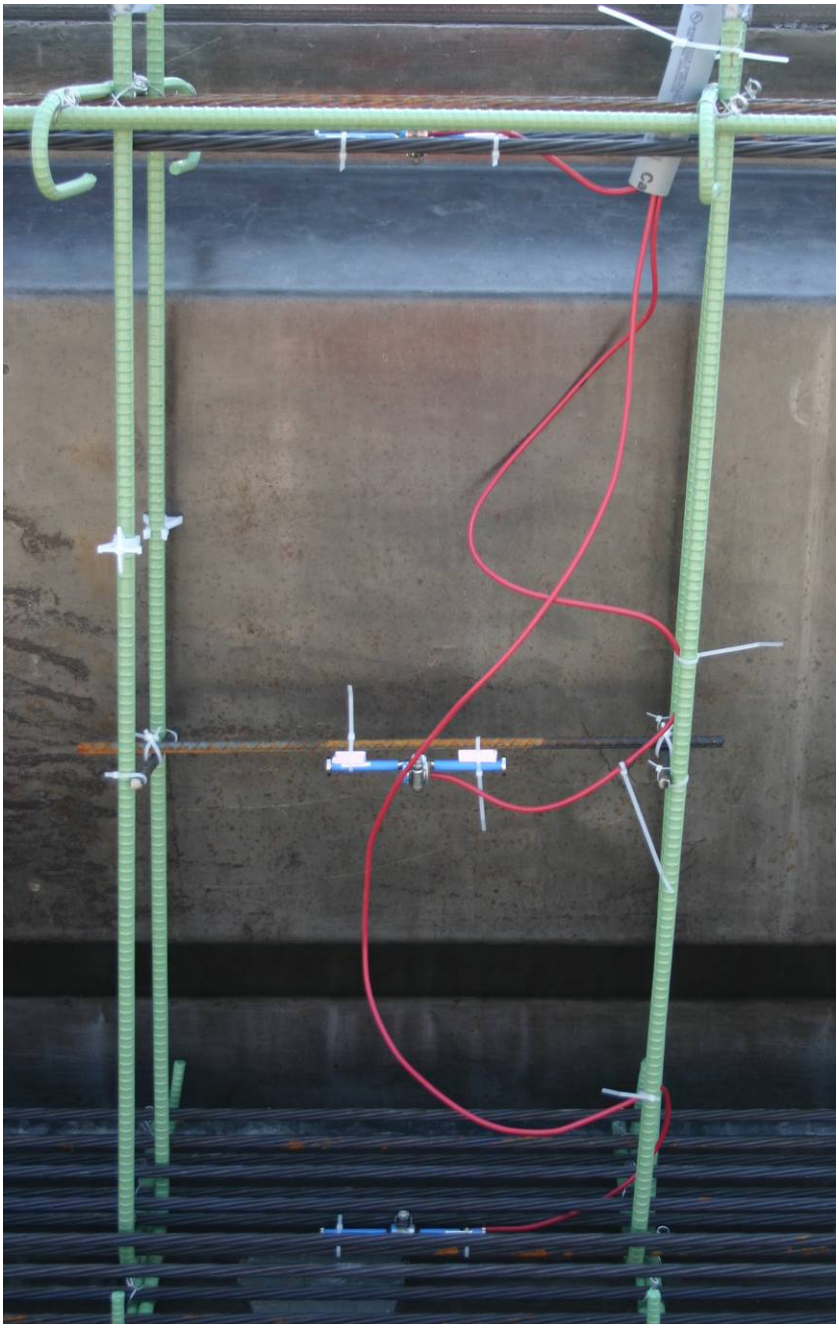

Figure 12.4: Location of VWSG's throughout cross-section

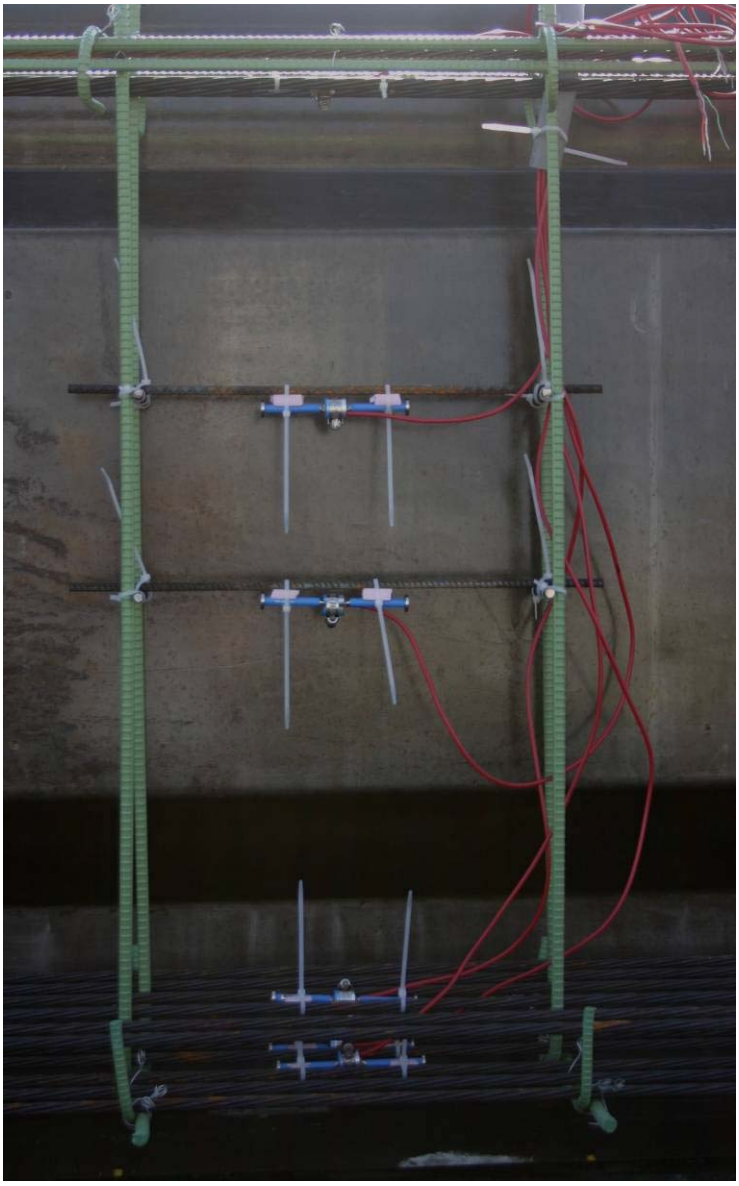

Figure 12.5: Location of VWSG's throughout cross-section

Casting of the K3 girders started August 3, 2005. Fabrication of all K3 girders was performed at Prestressed Concrete Inc., Newton, Kansas, the same precast plant where the flexural and IT specimens were cast. Forms at the precast plant allowed them to cast three girders at a time. Prestressing strand used in all the girders was 0.5-inch-diameter, Grade 270 ksi. Modulus of elasticity (E_{ps}) for the prestressing strand was reported as 28,500 ksi by the manufacturer. A straight-strand profile was used for every

girder. The procedure began with an empty prestressing bed, Figure 12.6. The prestressing strand was then pulled to 202.5 ksi and the internal shear stirrups were tied into place, Figure 12.7. Figure 12.8 shows the girders after all the steel had been tied into place and after one side wall had been put into place. The other form wall was then put into place (Figure 12.9) and concrete placement was ready to begin. Vibration was needed for the girders with conventional concrete, Figure 12.10. and girders with SCC did not require any vibration, Figure 12.11. Standard slump tests were performed on the conventional concrete mixture, Figure 12.12. Inverted-slump flow (spread) and L-Box tests were performed on the SCC mixtures, Figures 12.13 and 12.14, respectively. Figure 12.15 shows that the SCC mixture had good aggregate distribution and there was no large aggregate missing from the leading edge.

Figure 12.6: Empty prestressing bed

Figure 12.7: Tying of internal shear stirrups

Figure 12.8: Forms after one side wall has been set into place

Figure 12.9: Prestressing bed after walls have been set into place

Figure 12.10: Vibration of conventional concrete mixture

Figure 12.11: Laborers not having to vibrate SCC mixture

Figure 12.12: Slump test of conventional concrete mixture

Figure 12.13: Inverted-slump flow test for SCC mixture

Figure 12.14: L-Box test for SCC mixture

Figure 12.15: SCC mixture showing no excess paste and presence of aggregate on leading edge

The morning after casting concrete a set of three concrete cylinders were tested for compressive strength, the prestressing strand was detensioned as soon as the release strengths were achieved. To detension, the walls were removed and the strand was torched, Figure 12.16. The presence of “bug” holes can be seen in the girders with conventional concrete mixture, Figures 12.17 and 12.18 while the girders with the SCC mixture had a smooth exterior finish, Figures 12.19 and 12.20.

Figure 12.16: Detensioning of strands with a torch

Figure 12.17: Presence of "bug" holes in girder with conventional concrete

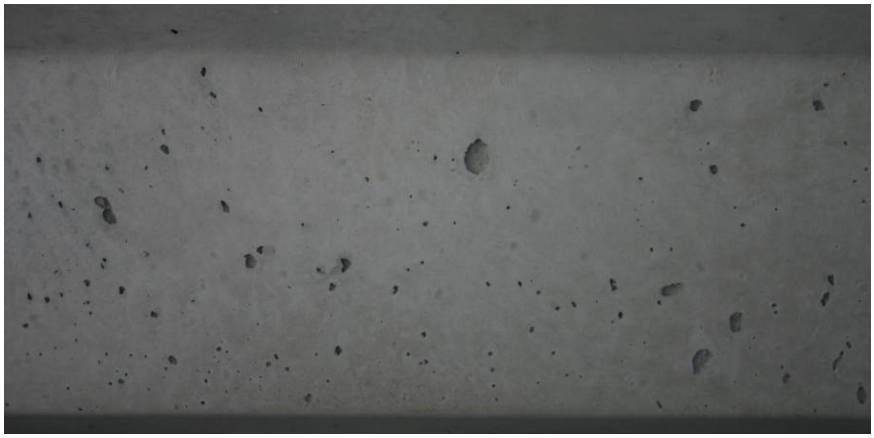

Figure 12.18: Closeup view of "bug" holes in girder with conventional concrete

Figure 12.19: Smooth exterior of SCC girder

Figure 12.20: Closeup of smooth SCC finish

12.2 Bridge Layout

As noted previously, the bridge consisted of 35 girders. The girder layout is shown in Figure 12.21. Spans A-C were all cast with conventional concrete, and spans D-E were cast with the proposed SCC mixture. The bridge was erected in two phases. All of the girders embedded with VWSGs, lines 1-3, were part of phase I. Girder lines 4-7

were part of phase II. The girders with embedded VWSGs were A3, B1, B3, C3, D1, D3, and E3.

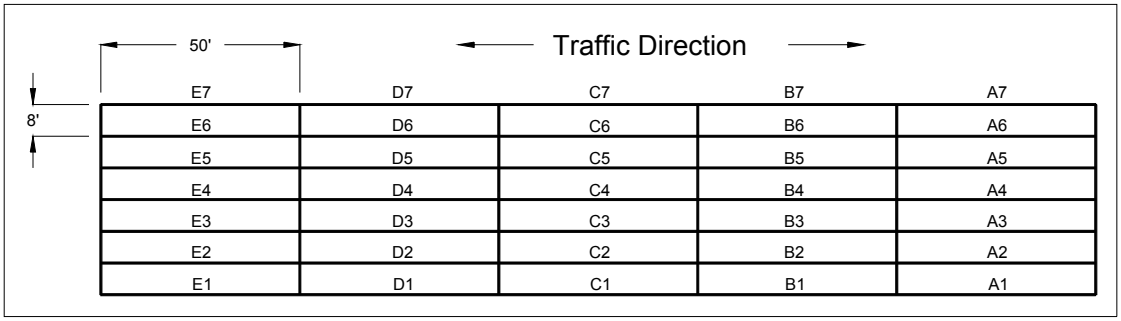

Figure 12.21: Layout and designation of bridge girders

12.3 Bridge Erection

The construction process at the bridge site started in mid July 2005. Having a 2-phase construction made it possible to keep one lane of traffic open during the whole process. Removal of the north half of the existing bridge was followed by construction of the first phase. After phase I was completed, the road was opened to traffic and the rest of the existing bridge was removed followed by the second construction phase. The entire bridge was opened to traffic after this phase.

As noted earlier, during construction of phase I, one lane of traffic remained open, Figure 12.22. Since the bridge had been altered, temporary support for the existing structure was needed, Figure 12.23. Once the old bridge had been removed, the first step was to drill new piles, Figure 12.24. Once the piles were in place, the abutment walls were cast, Figure 12.25. After all the supports were completed, it was time to set the girders into place. Figures 12.26, 12.27, and 12.28 show different views of the girders after they had been set. Placing shoring for the deck construction was the next step, Figures 12.29 and 12.30. After all the shoring was in place, the deck steel was

tied into place, Figures 12.31 and 12.32. During this time, wires from the VWSGs were hooked up to a multi-plexor, Figure 12.33, which were in turn connected to the data logger. Conduit was cast into the abutments to allow for the wires to run through them, Figure 12.34. Once all the wires were connected, casting of the deck started by using a concrete pump truck to pump the concrete to the bridge deck, Figure 12.35. The concrete was vibrated and finished, Figures 12.36 and 12.37.

Figure 12.22: One lane open to traffic during phase I construction

Figure 12.23: Temporary supports for existing bridge

Figure 12.24: Placement of cages for piles

Figure 12.25: Abutment wall

Figure 12.26: Placement of girders

Figure 12.27: Underneath view of placed girders

Figure 12.28: Underneath view of placed girders

Figure 12.29: Placement of shoring for deck casting

Figure 12.30: Placement of shoring for deck casting-II

Figure 12.31: Placement of deck reinforcement

Figure 12.32: Tying of deck reinforcement into place

Figure 12.33: Wires extending into multi-plexor

Figure 12.34: Wires extending through abutment wall

Figure 12.35: Pump truck for pumping concrete to bridge deck

Figure 12.36: Vibrating concrete

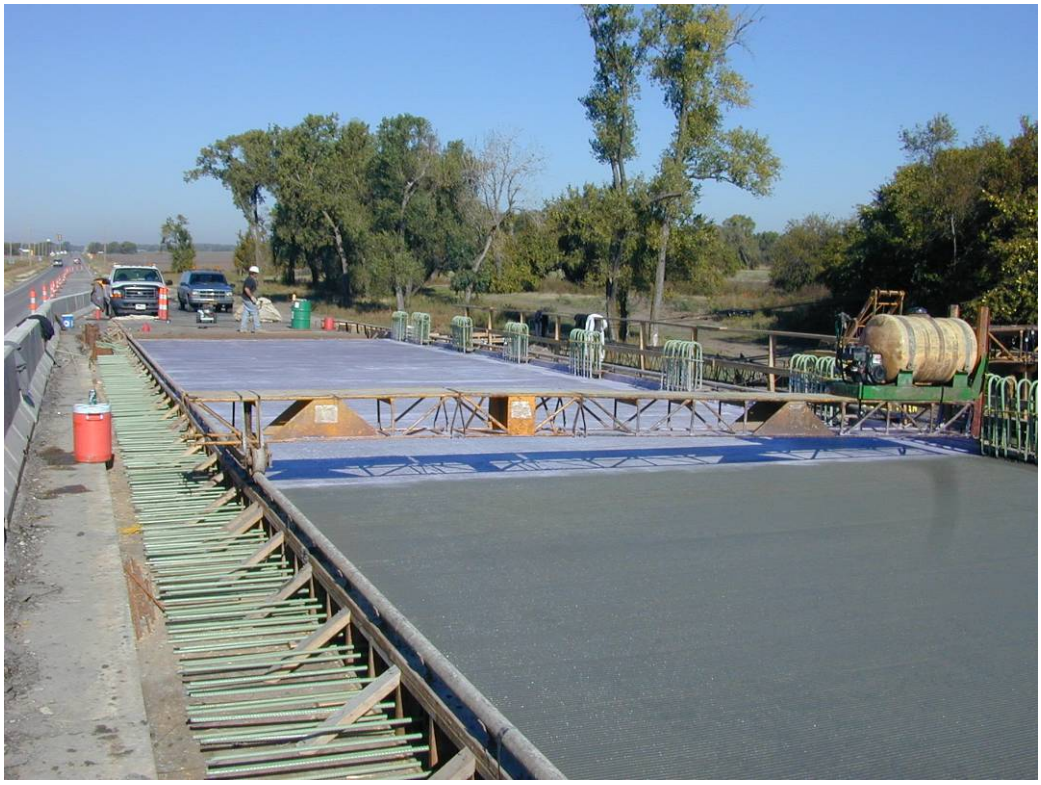

Figure 12.37: Finishing of concrete

Once the deck had cured, phase I was opened for traffic, Figure 12.38. The remaining part of the existing bridge was removed and construction on phase II began, Figure 12.39. After the girders of phase II were set into place, shoring for the deck was erected, Figure 12.40. Once the shoring and deck steel were all in place, the deck was cast, Figure 12.41. All remaining tasks were finished and traffic in both directions was opened in early April 2006, Figure 12.42. Restoration around the site was completed (Figure 12.43) and a solar panel was installed on the side rail to provide power to the data logger, Figure 12.44. A side view of the completed bridge is shown in Figure 12.45.

Figure 12.38: Opened lane of phase I and beginning of phase II

Figure 12.39: Groundwork for phase II

Figure 12.40: Shoring for phase II

Figure 12.41: Deck completion of phase II

Figure 12.42: Finished bridge and approach

Figure 12.43: Side restoration

Figure 12.44: Solar panel on side railing

Figure 12.45: Side view of completed project

CHAPTER THIRTEEN - PRESTRESS LOSS RESULTS OF SCC BRIDGE

13.1 Material Properties

13.1.1 Girder Properties

As noted earlier, conventional and self-consolidating concrete, as two separate concrete mixtures, were used in the bridge girders. The hardened concrete properties were different for these two mixtures. This difference plays an important role when comparing experimental results to code predictions. Figure 13.1 shows the measured modulus of elasticity for release and 28-day modulus for both mixes. Figure 13.2 shows the measured compressive strength for release and 28-day strength for both mixes. At the time of casting for the SCC girders with the VWSGs, the release strengths were lower than normal. However, the average release strengths of the remaining ungaged girders with SCC were much higher than those girders with conventional concrete, Figure 13.3. This figure shows the release compressive strength for all the girders containing SCC and conventional concrete for all 35 girders cast. The lower modulus of elasticity for the SCC mixture was expected due to more “fines” in the mixture. For the girders with the SCC mixture, the slump flow ranged from 24 inches to 29 inches. The slumps ranged from 4.5 inches to nine inches for the girders with the conventional concrete mixture. Currently KDOT recommends a three to nine-inch slump for conventional concrete in bridge girders and does not have a range for girders with SCC.

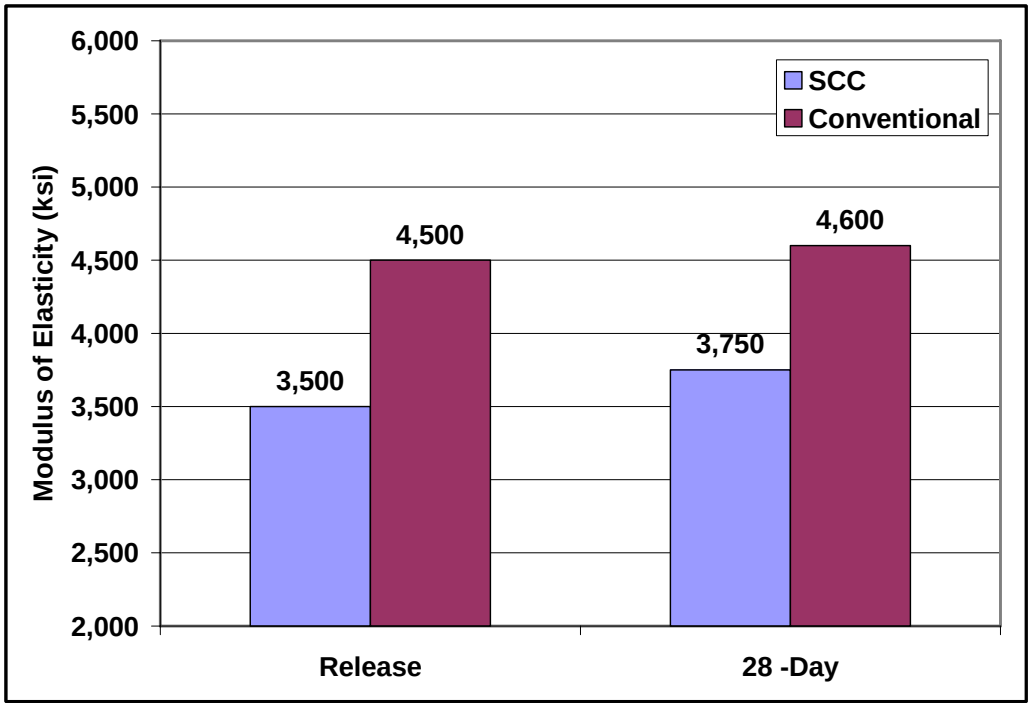

Figure 13.1: Modulus of elasticity for girders gaged with VWSGs

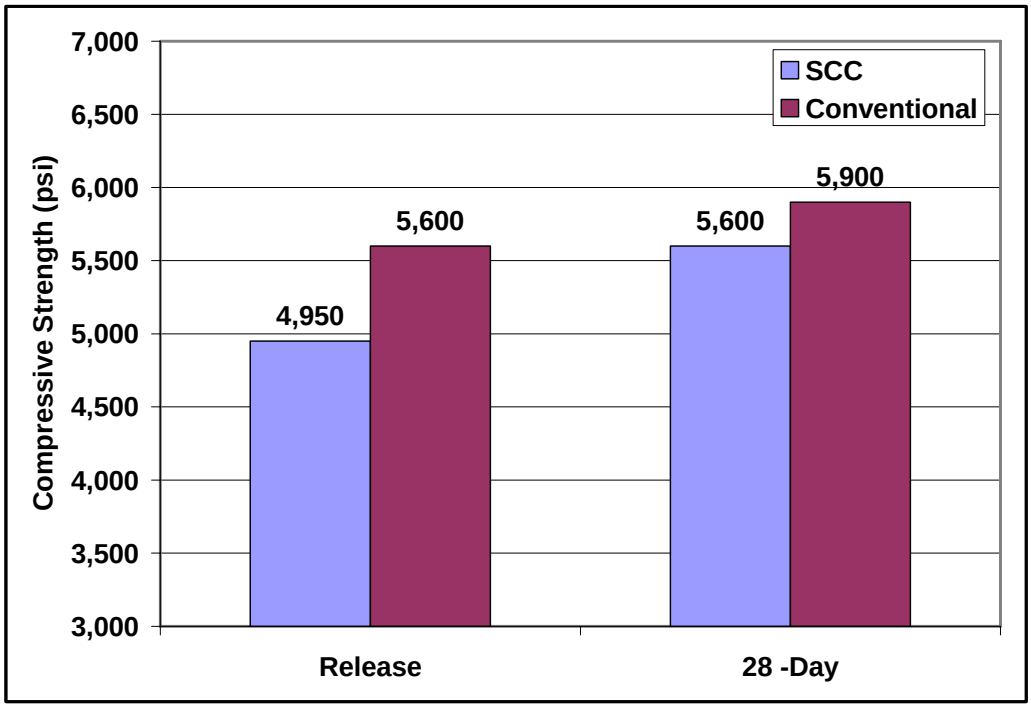

Figure 13.2: Compressive strength for girders gaged with VWSGs

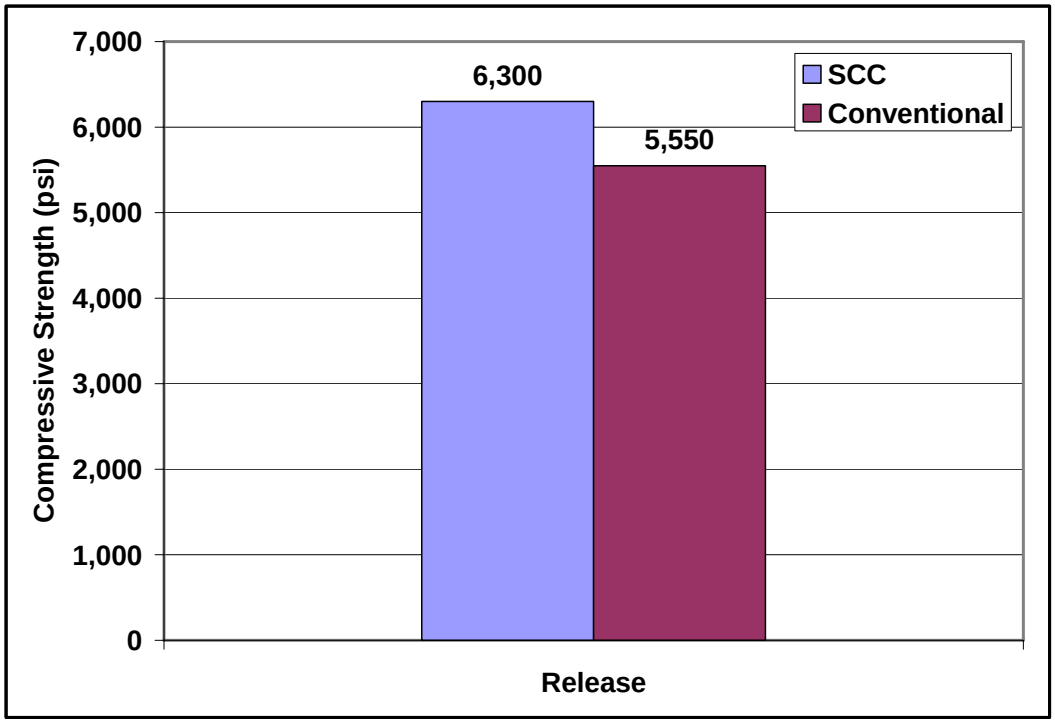

Figure 13.3: Release compressive strength for all girders cast

13.1.2 Deck Properties

The deck for phase I was cast on October 18, 2005. The 28-day compressive strength was found to be 4,500 psi with a modulus of elasticity of 5,150 ksi. Split-cylinder tests were also performed at 28 days and tensile strength was found to be 350 psi. The deck thickness was 8.5-inches.

13.2 Experimental Stress Results

The VWSGs yielded results in strain. To compare these values with the code equations, the strain values were converted to stress. Equation 8.2 was used for this calculation. The code equations computed the prestress loss values at the center of gravity of the prestressing strands. Hence, strain values located at the level of the bottom strand height were used for direct comparison. The total time-dependent losses as predicted by the PCI method, yielded 173 ksi and 168 ksi for the girders with

conventional concrete and SCC, respectively. The calculations can be seen in section A.10. The major difference between these two values was the elastic shortening loss which was impacted by the modulus of elasticity of the concrete at release.

13.2.1 Girders with Conventional Concrete

Figures 13.4–13..7 shows the effective stress versus time for the girders cast with conventional concrete. Figures 13.8—13.10 present the strains in concrete versus depth. It must be noted that a strain versus depth profile was not available for girder B3, due to a problem with some of the gages. The strains however did remain linear with depth.

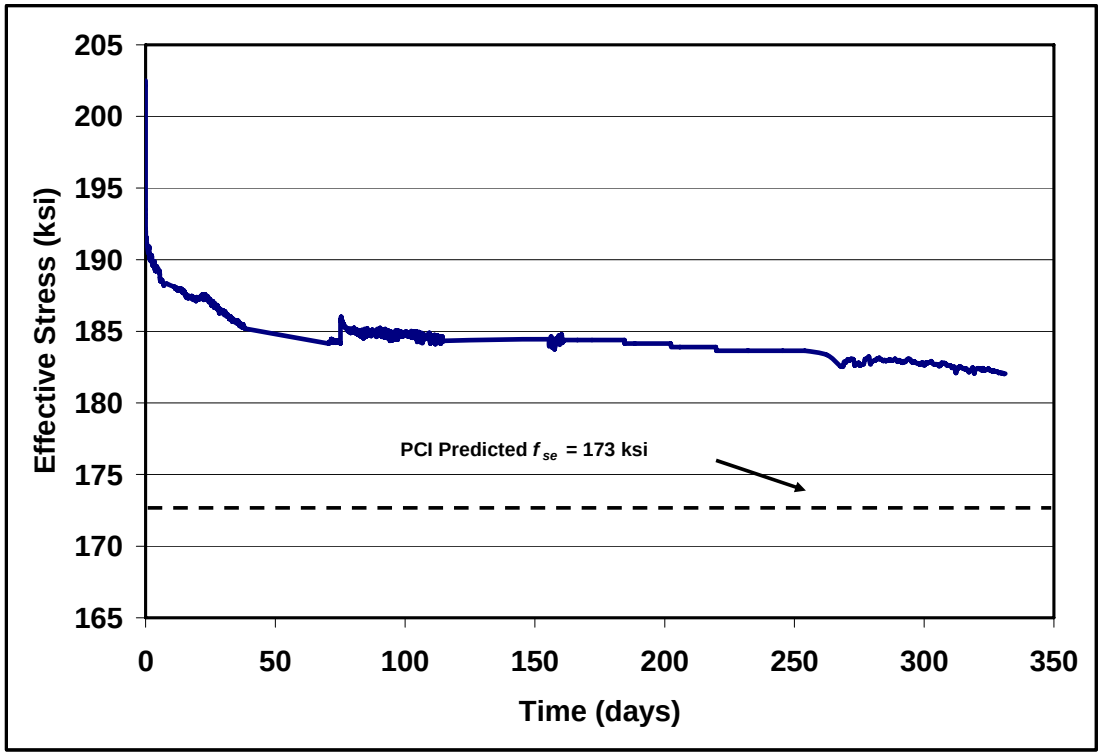

Figure 13.4: Effective stress for girder A3

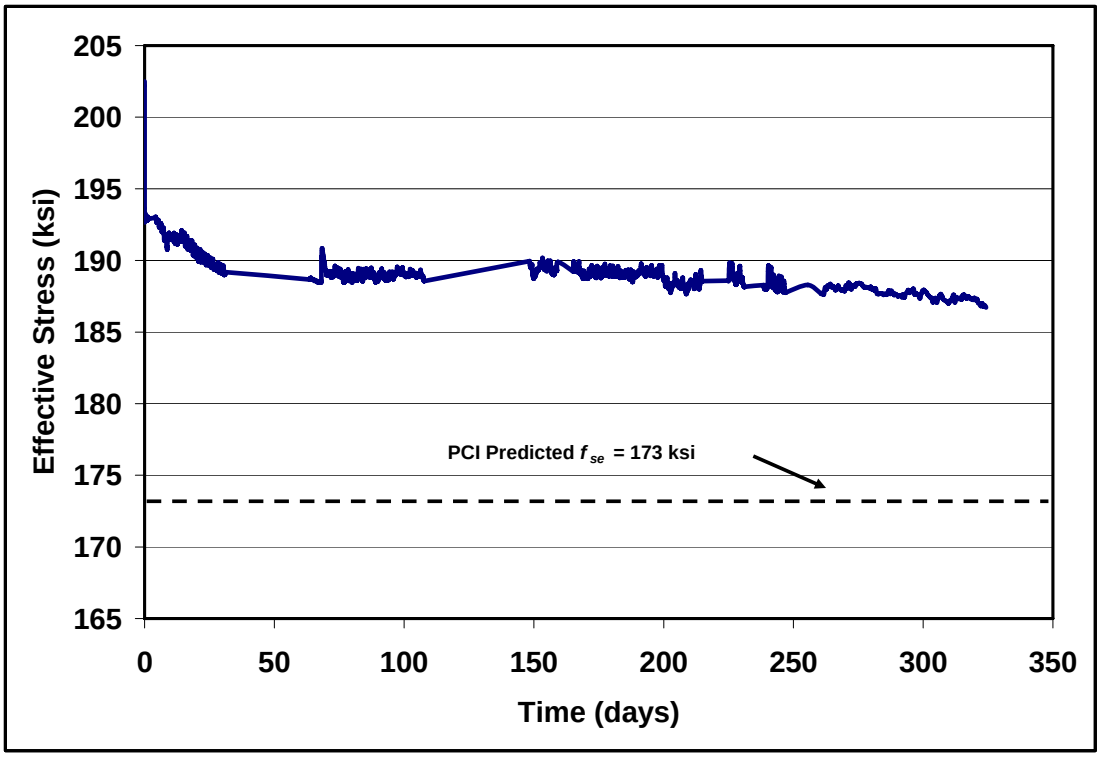

Figure 13.5: Effective stress for girder B1

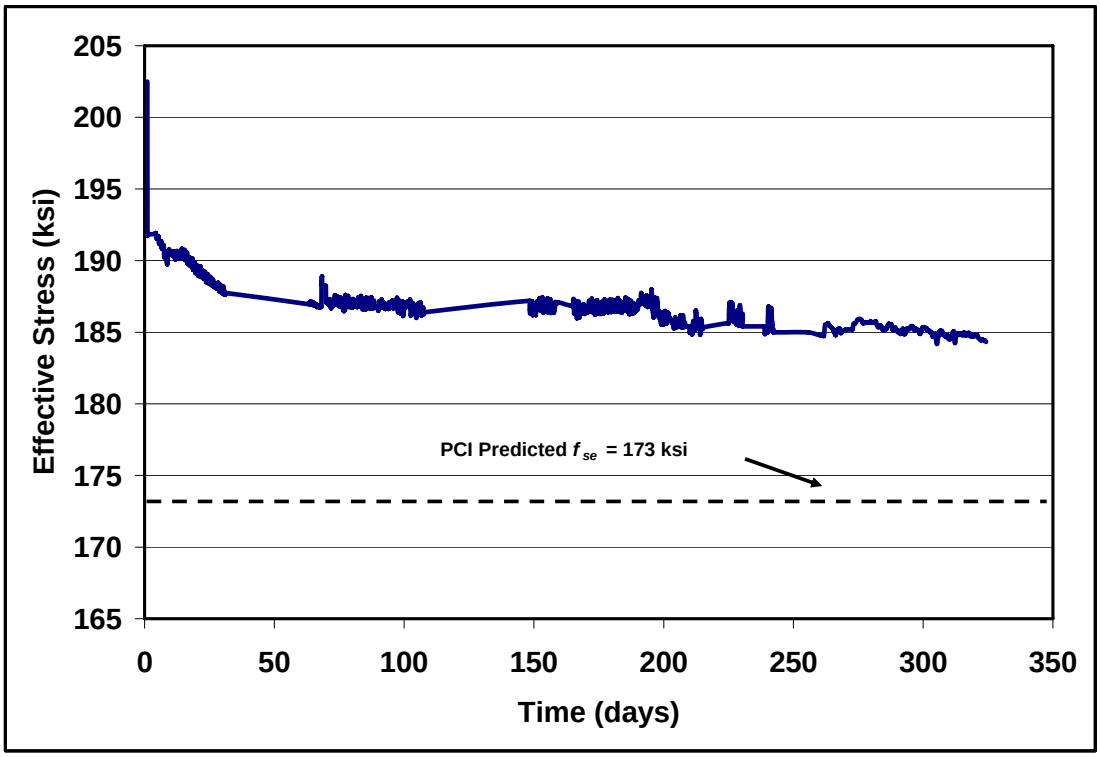

Figure 13.6: Effective stress for girder B3

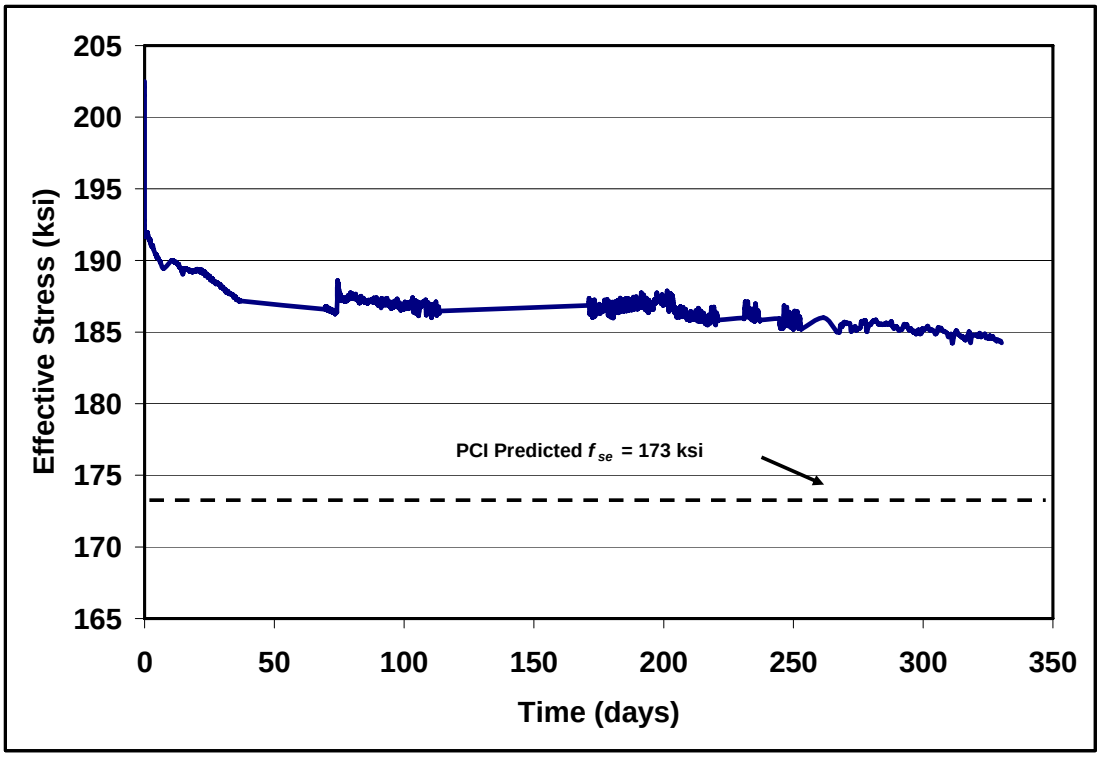

Figure 13.7: Effective stress for girder C3

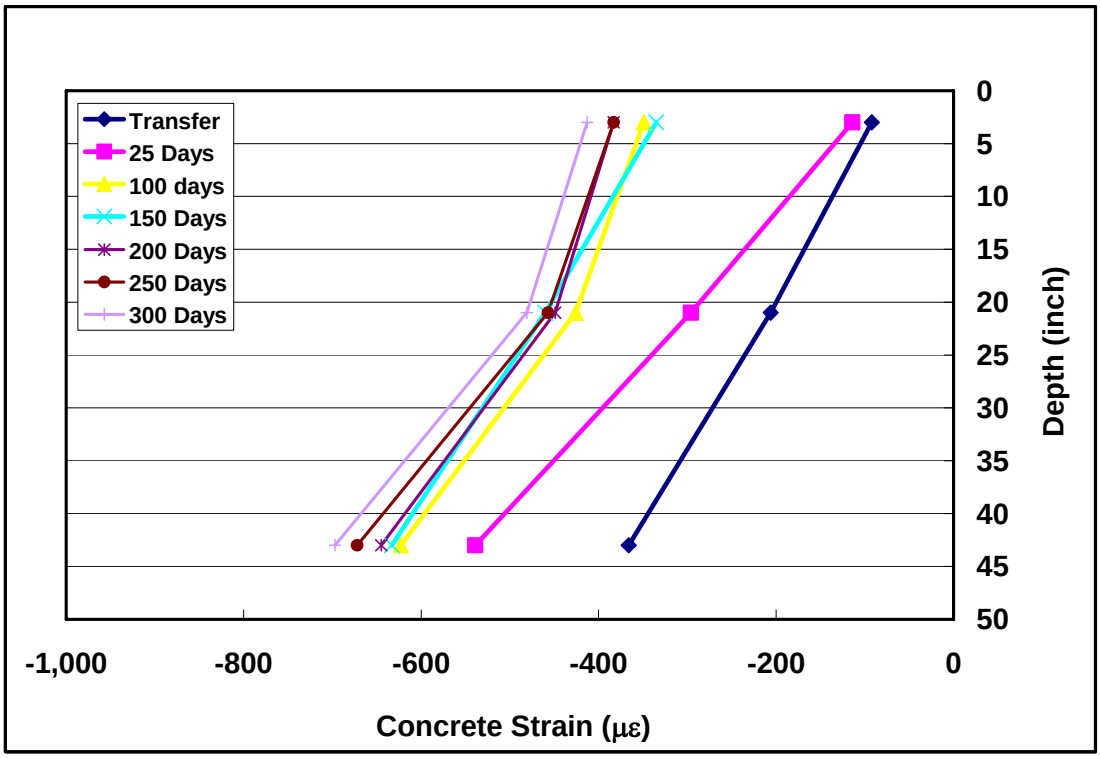

Figure 13.8: Concrete versus depth for girder A3

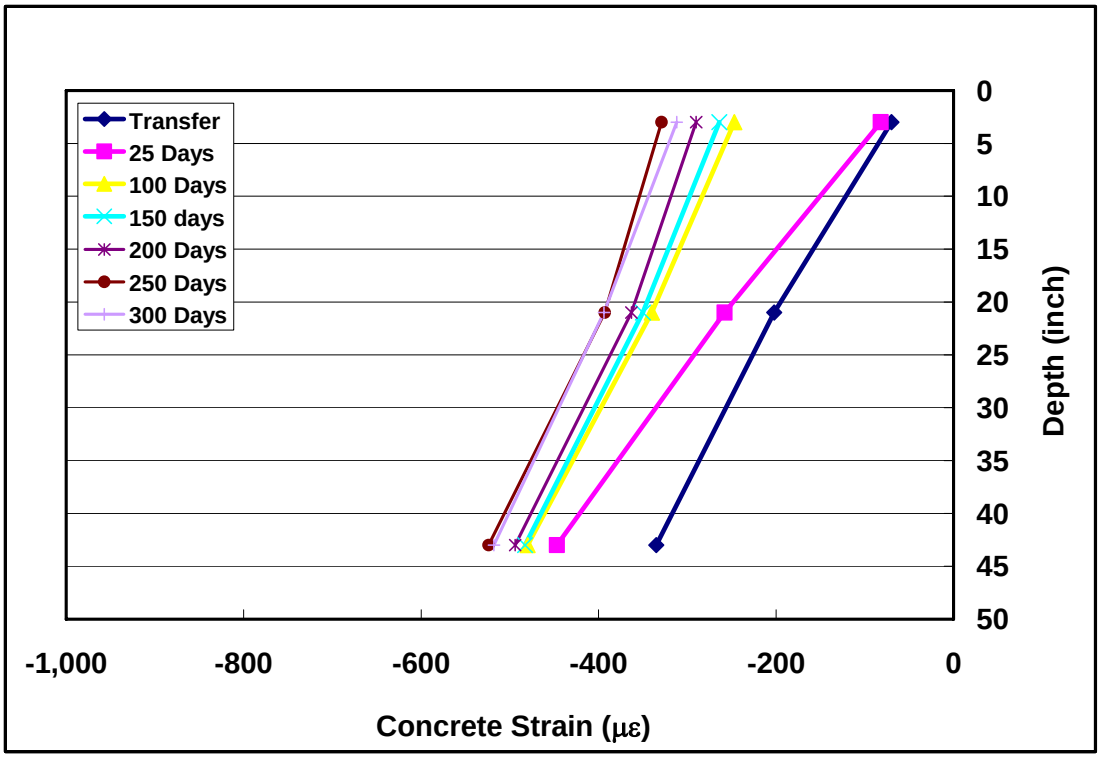

Figure 13.9: Concrete versus depth for girder B1

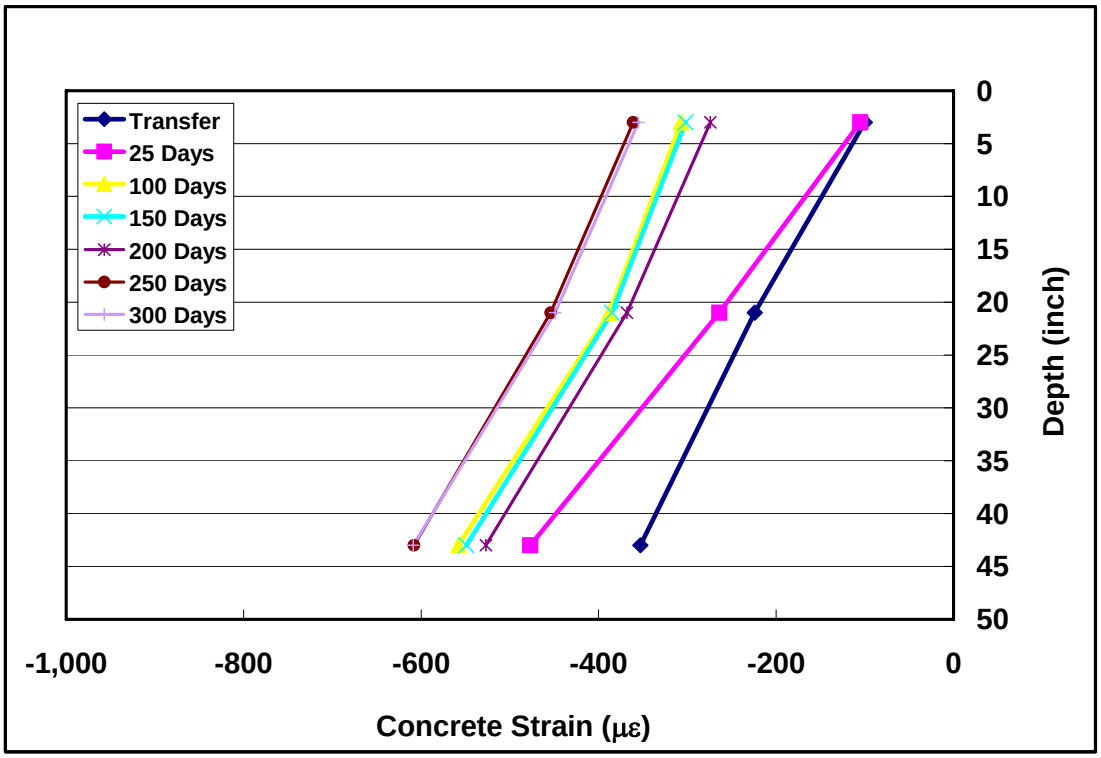

Figure 13.10: Concrete versus depth for girder C3

13.2.2 Girders with Self-Consolidating Concrete

Figures 13.11–13.13 show the effective stress versus time for the girders cast with self-consolidating concrete. Figures 13.14—13.16 present the strains in the concrete versus the depth.

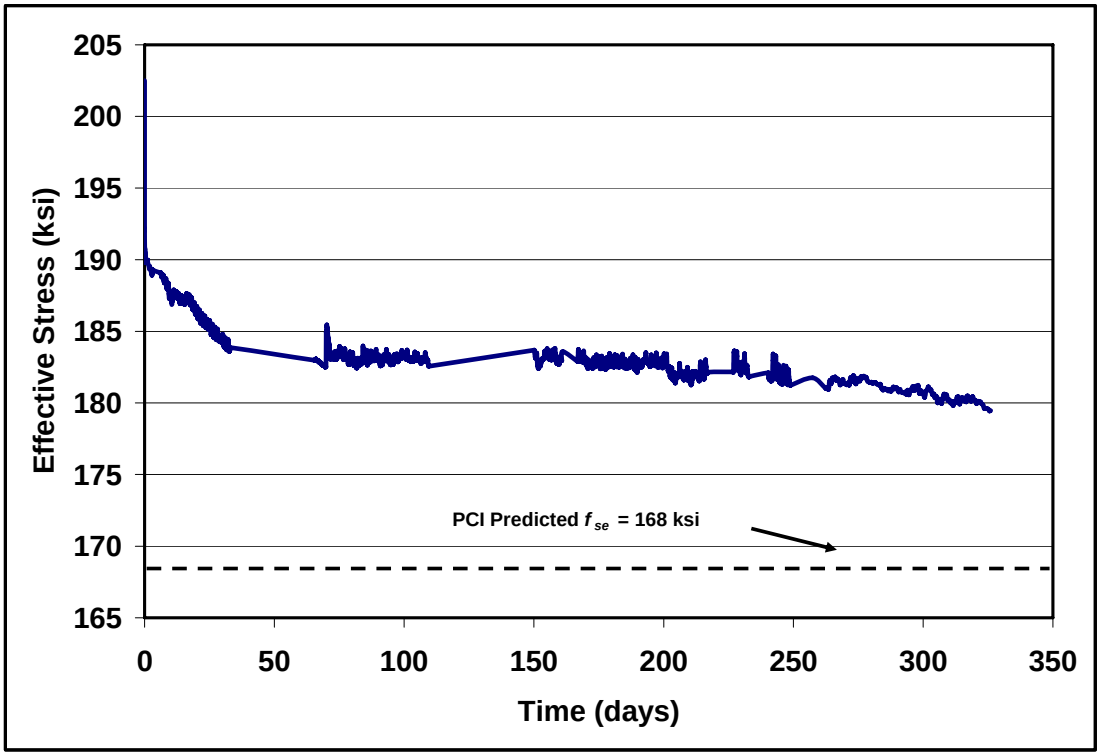

Figure 13.11: Effective stress for girder D1

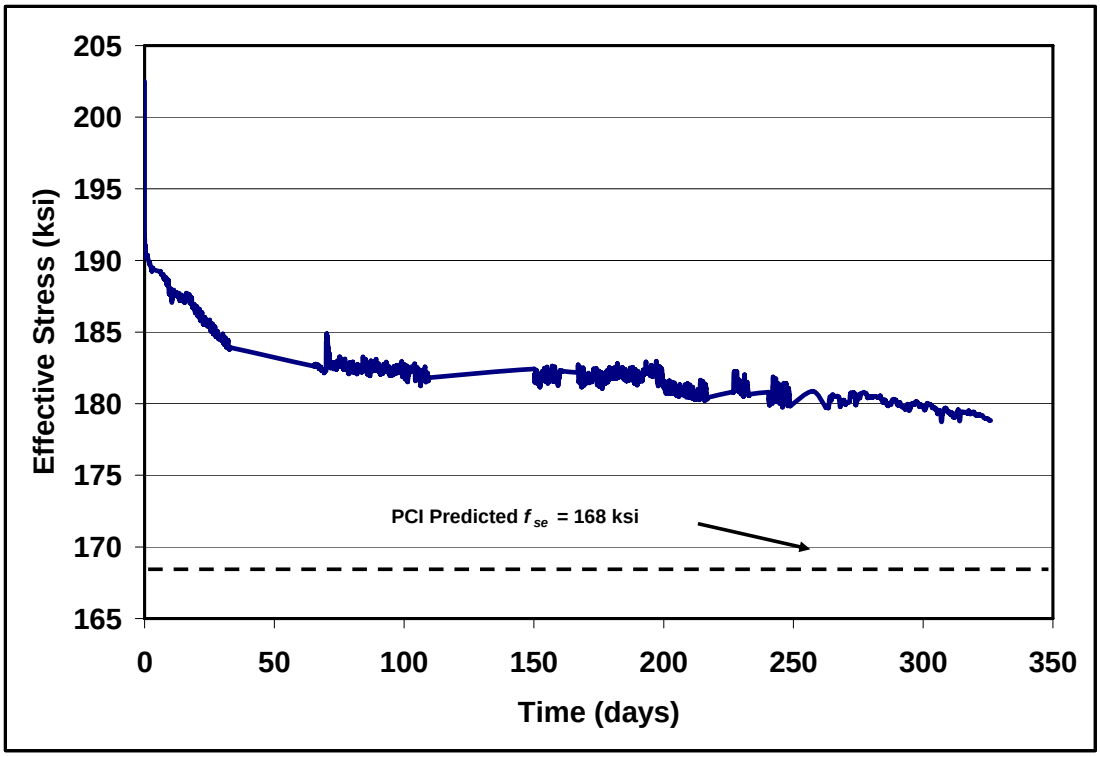

Figure 13.12: Effective stress for girder D3

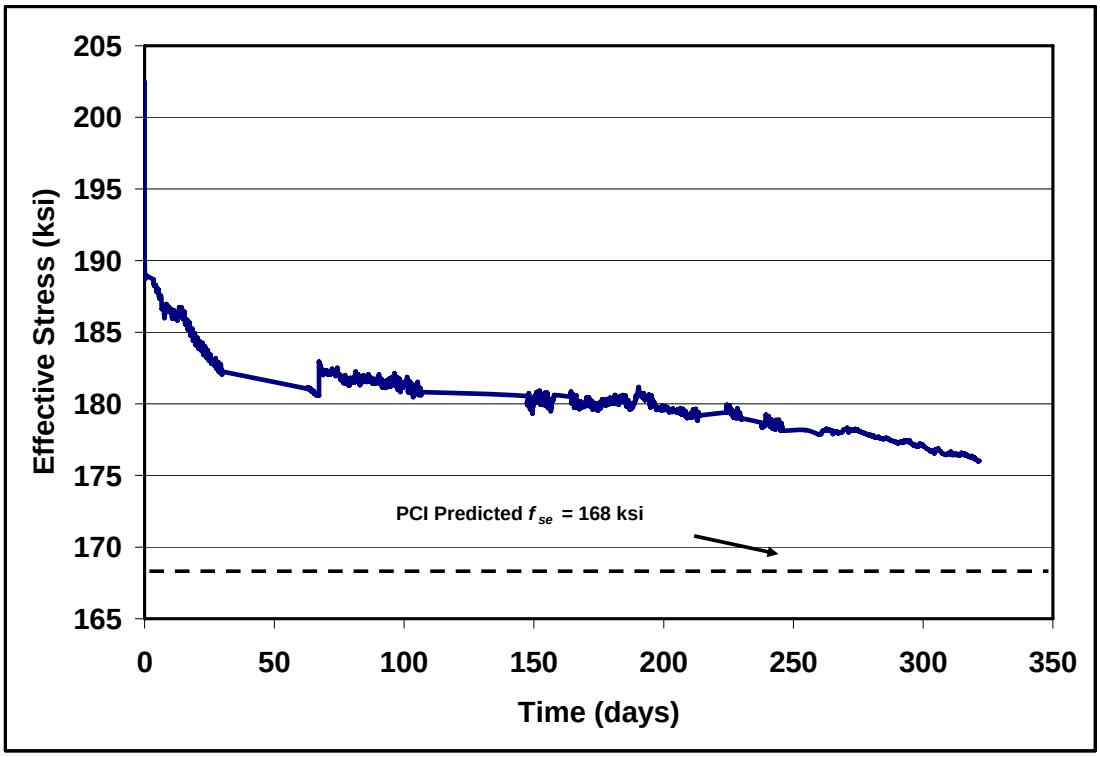

Figure 13.13: Effective stress for girder E3

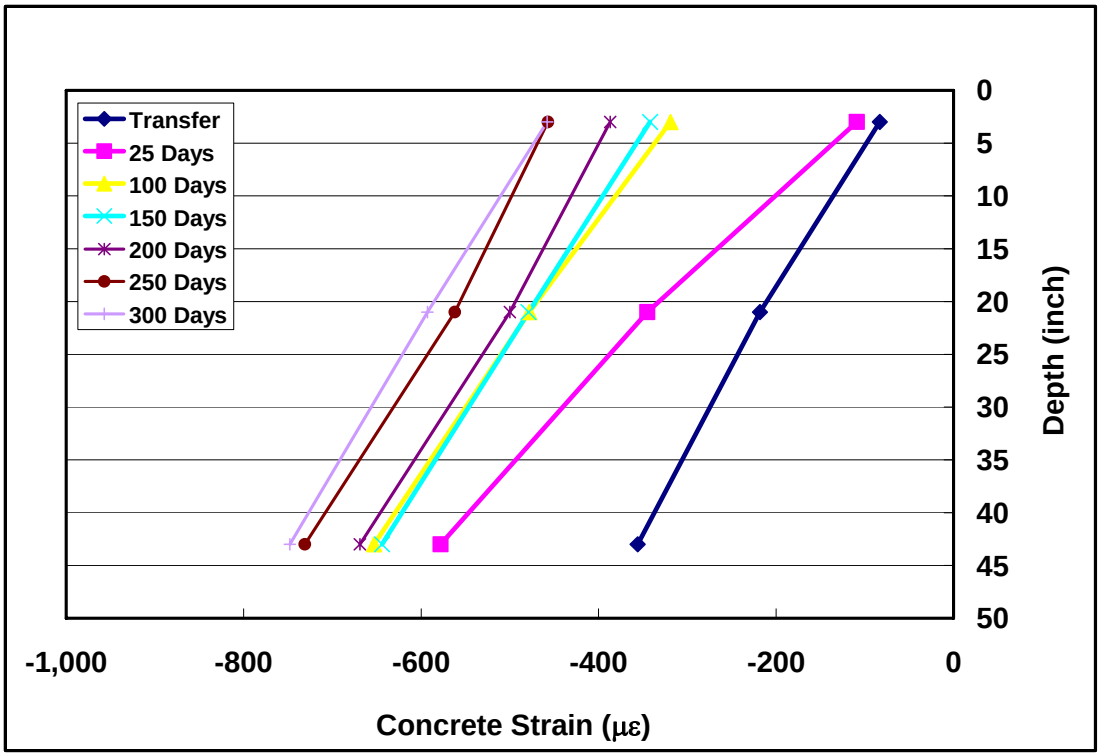

Figure 13.14: Strain versus depth for girder D1

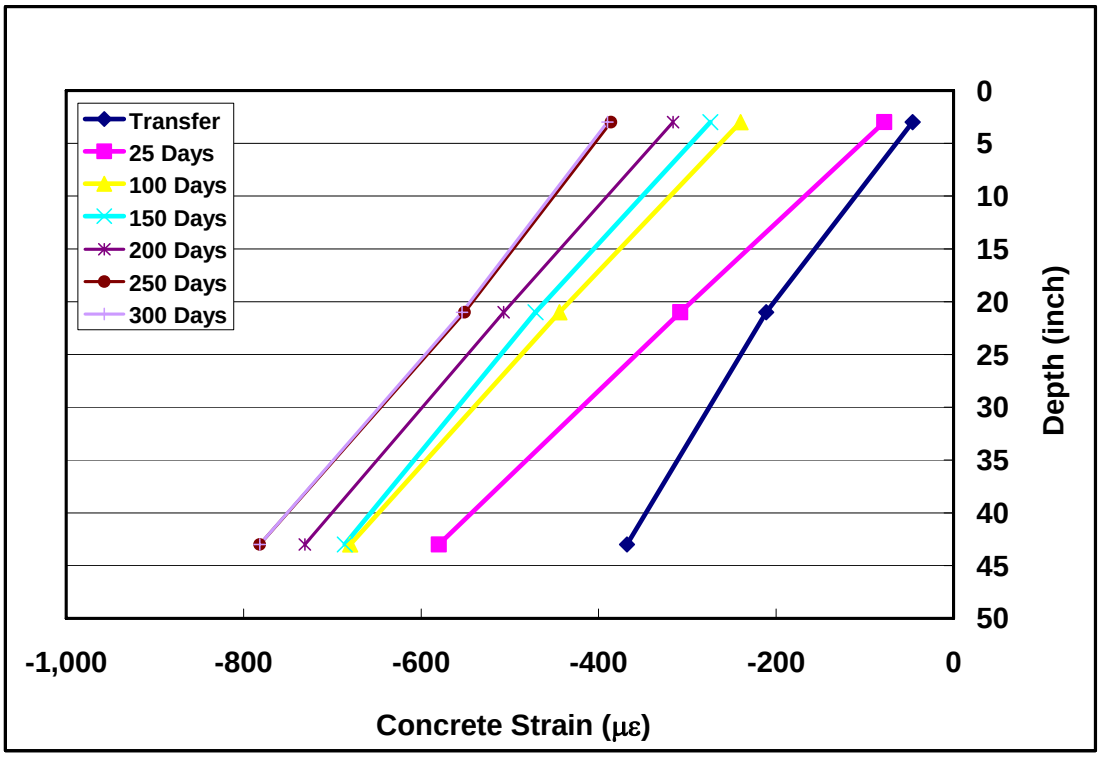

Figure 13.15: Strain versus depth for girder D3

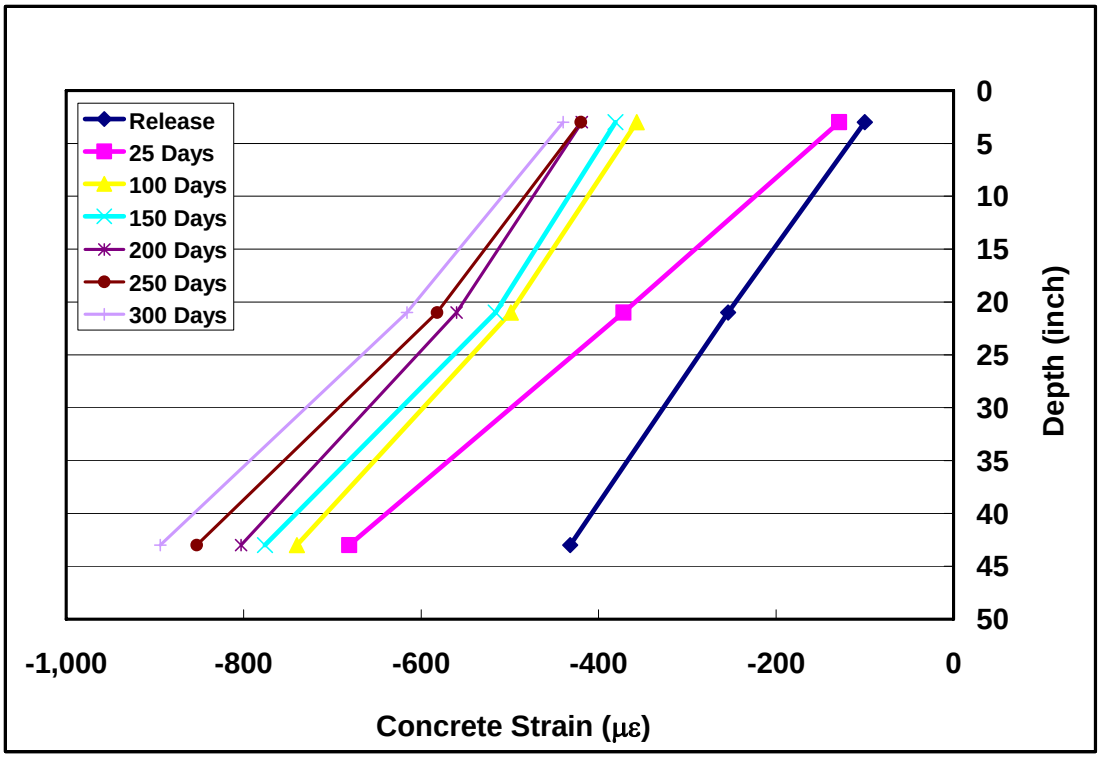

Figure 13.16: Strain versus depth for girder E3

13.3 Comparison with Code Expressions

This section compares experimental stress results with code predictions. Figure 13.17 compares the average effective stress for girders with SCC against those with conventional concrete. It can be seen that girders with conventional concrete have experienced less prestress loss than those with SCC. This can be attributed mainly to differences in the elastic shortening term. Also the creep effect may be larger due to the lower modulus of elasticity of the concrete.

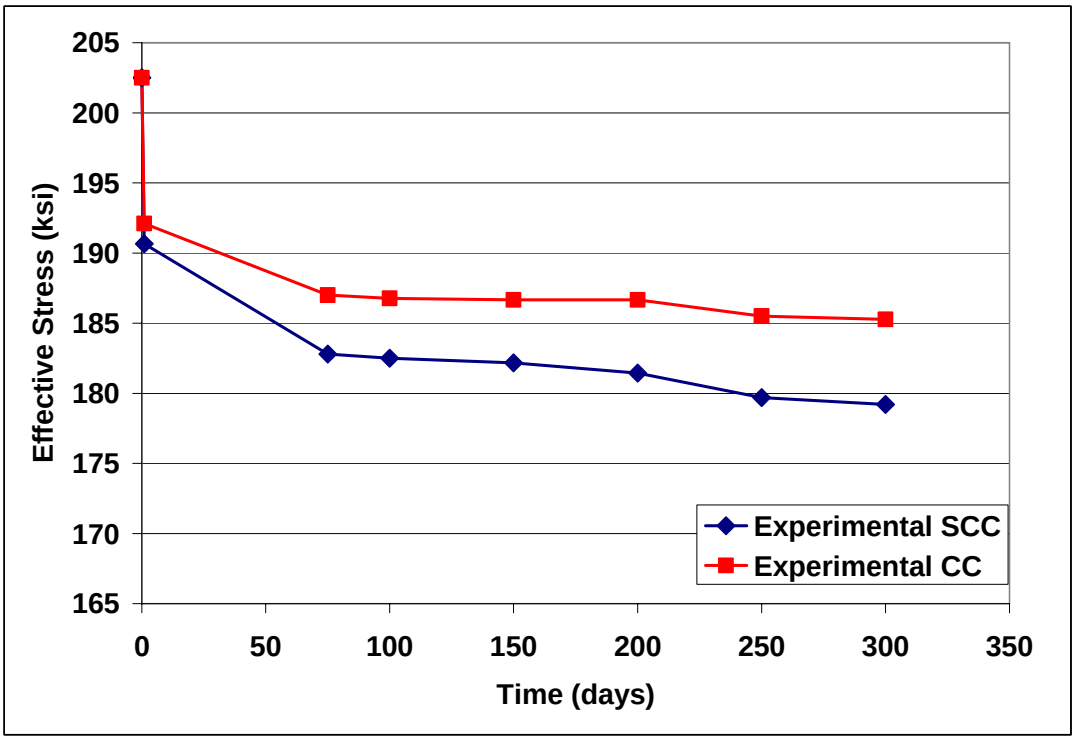

Figure 13.17: Comparison of SCC versus conventional concrete effective stress results

Code predictions were calculated using five different methods. Each method is outlined in section A.2 and calculations are in A.10. The five different methods used were ACI (ACI 318, 2002), PCI (PCI , 2004), AASHTO (LRFD, 2004) , KDOT Design 2003, and ACI-209 (ACI-209, 1997). (It must be noted the ACI and PCI methods give very similar results and they will be presented together.) Resulting values from the first four methods are shown in Table 13.1. Effective stress values for both conventional concrete and SCC girders are shown. Tables 13.2 – 13.7 show the breakdown of each individual prestress loss term for the different methods used. Figures 13.18 and 13.19 present conventional concrete and SCC code predictions versus experimental results. Equation 8.3 was used to calculate loss predictions at intermediate days.

Table 13.1: Predicted effective stress values

Day	Conventional				SCC			
	ACI[4]/PCI[9]	AASHTO[5]	KDOT[8]	Experimental Stress	ACI[4]/PCI[9]	AASHTO[5]	KDOT[8]	Experimental Stress
Release	193.0	191.7	192.1	192.1	190.7	189.2	189.6	190.7
75	180.9	177.5	178.3	187.0	177.3	175.3	176.0	182.8
100	180.2	176.7	177.5	186.8	176.5	174.5	175.2	182.5
150	179.3	175.6	176.4	186.7	175.5	173.4	174.1	182.2
200	178.6	174.8	175.6	186.7	174.7	172.6	173.3	181.4
250	178.1	174.1	174.9	185.5	174.1	171.9	172.6	179.7
300	177.7	173.6	174.4	185.3	173.6	171.4	172.1	179.2
Ultimate	173.1	168.0	168.8	--	168.4	165.8	166.5	--

* all values reported in ksi

Table 13.2: Prestress loss using ACI/PCI method for conventional concrete girders

Day	Elastic Shortening	Creep	Shrinkage	Relaxation	Total Losses	ACI/PCI	Experimental Stress-CC
Release	7.9	0.0	0.0	1.6	9.5	193.0	192.1
75	7.9	6.4	3.6	3.7	21.6	180.9	187.0
100	7.9	6.8	3.9	3.7	22.3	180.2	186.8
150	7.9	7.4	4.2	3.7	23.2	179.3	186.7
200	7.9	7.9	4.4	3.7	23.9	178.6	186.7
250	7.9	8.2	4.6	3.7	24.4	178.1	185.5
300	7.9	8.5	4.8	3.7	24.8	177.7	185.3
Ultimate	7.9	11.4	6.4	3.7	29.4	173.1	--

* all values reported in ksi

Table 13.3: Prestress loss using AASHTO method for conventional concrete girders

Day	Elastic Shortening	Creep	Shrinkage	Relaxation	Total Losses	AASHTO	Experimental Stress-CC
Release	9.0	0.0	0.0	1.8	10.8	191.7	192.1
75	9.0	8.3	4.1	3.6	25.0	177.5	187.0
100	9.0	8.8	4.3	3.6	25.8	176.7	186.8
150	9.0	9.6	4.7	3.6	26.9	175.6	186.7
200	9.0	10.1	5.0	3.6	27.7	174.8	186.7
250	9.0	10.6	5.2	3.6	28.4	174.1	185.5
300	9.0	10.9	5.4	3.6	28.9	173.6	185.3
Ultimate	9.0	14.7	7.3	3.6	34.6	168.0	--

* all values reported in ksi

Table 13.4: Prestress loss method using KDOT method for conventional concrete girders

Day	Elastic Shortening	Creep	Shrinkage	Relaxation	Total Losses	KDOT	Experimental Stress-CC
Release	8.8	0.0	0.0	1.6	10.4	192.1	192.1
75	8.8	8.3	4.1	3.0	24.2	178.3	187.0
100	8.8	8.8	4.3	3.0	25.0	177.5	186.8
150	8.8	9.6	4.7	3.0	26.1	176.4	186.7
200	8.8	10.1	5.0	3.0	26.9	175.6	186.7
250	8.8	10.6	5.2	3.0	27.6	174.9	185.5
300	8.8	10.9	5.4	3.0	28.1	174.4	185.3
Ultimate	8.8	14.7	7.3	3.0	33.8	168.8	--

* all values reported in ksi

Table 13.5: Prestress loss method using ACI/PCI method for SCC girders

Day	Elastic Shortening	Creep	Shrinkage	Relaxation	Total Losses	ACI/PCI	Experimental Stress-SCC
Release	10.2	0.0	0.0	1.6	11.8	190.7	190.7
75	10.2	7.9	3.6	3.5	25.2	177.3	182.8
100	10.2	8.4	3.9	3.5	26.0	176.5	182.5
150	10.2	9.1	4.2	3.5	27.0	175.5	182.2
200	10.2	9.7	4.4	3.5	27.8	174.7	181.4
250	10.2	10.1	4.6	3.5	28.4	174.1	179.7
300	10.2	10.4	4.8	3.5	28.9	173.6	179.2
Ultimate	10.2	14.0	6.4	3.5	34.1	168.4	--

* all values reported in ksi

Table 13.6: Prestress loss method using AASHTO method for SCC girders

Day	Elastic Shortening	Creep	Shrinkage	Relaxation	Total Losses	AASHTO	Experimental Stress-SCC
Release	11.5	0.0	0.0	1.8	13.3	189.2	190.7
75	11.5	8.3	4.1	3.3	27.2	175.3	182.8
100	11.5	8.8	4.3	3.3	28.0	174.5	182.5
150	11.5	9.6	4.7	3.3	29.1	173.4	182.2
200	11.5	10.1	5.0	3.3	29.9	172.6	181.4
250	11.5	10.6	5.2	3.3	30.6	171.9	179.7
300	11.5	10.9	5.4	3.3	31.1	171.4	179.2
Ultimate	11.5	14.7	7.3	3.3	36.8	165.8	--

* all values reported in ksi

Table 13.7: Prestress loss method using KDOT method for SCC girders

Day	Elastic Shortening	Creep	Shrinkage	Relaxation	Total Losses	KDOT	Experimental Stress-SCC
Release	11.3	0.0	0.0	1.6	12.9	189.6	190.7
75	11.3	8.3	4.1	2.8	26.5	176.0	182.8
100	11.3	8.8	4.3	2.8	27.3	175.2	182.5
150	11.3	9.6	4.7	2.8	28.4	174.1	182.2
200	11.3	10.1	5.0	2.8	29.2	173.3	181.4
250	11.3	10.6	5.2	2.8	29.9	172.6	179.7
300	11.3	10.9	5.4	2.8	30.4	172.1	179.2
Ultimate	11.3	14.7	7.3	2.8	36.1	166.5	--

* all values reported in ksi

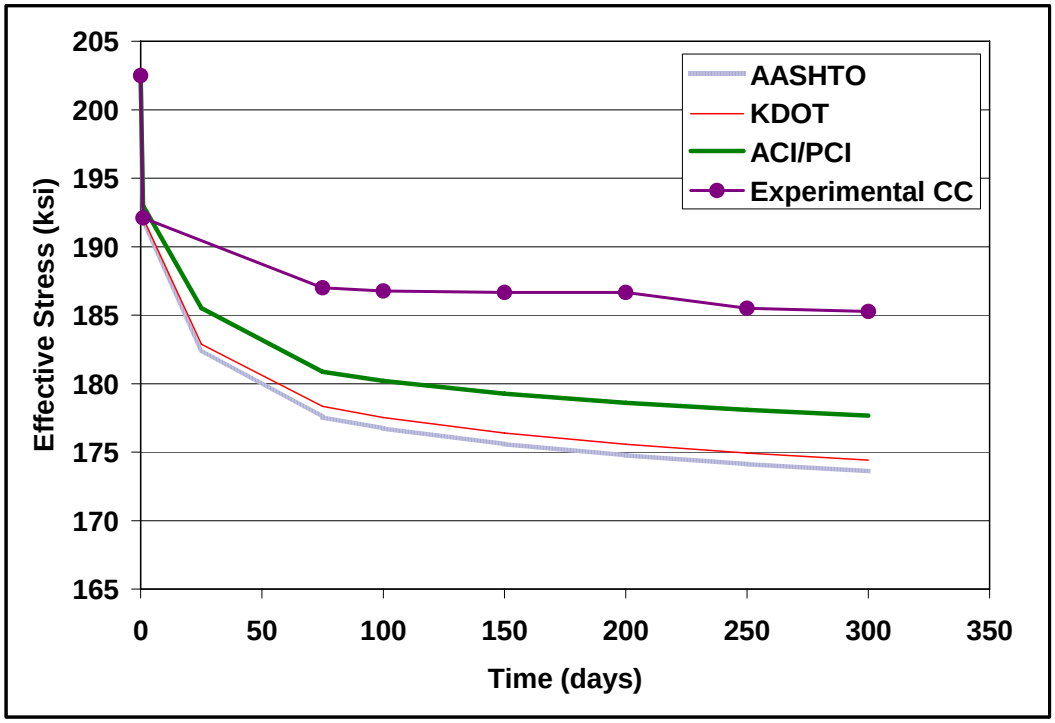

Figure 13.18: Effective stress calculations for conventional concrete girders

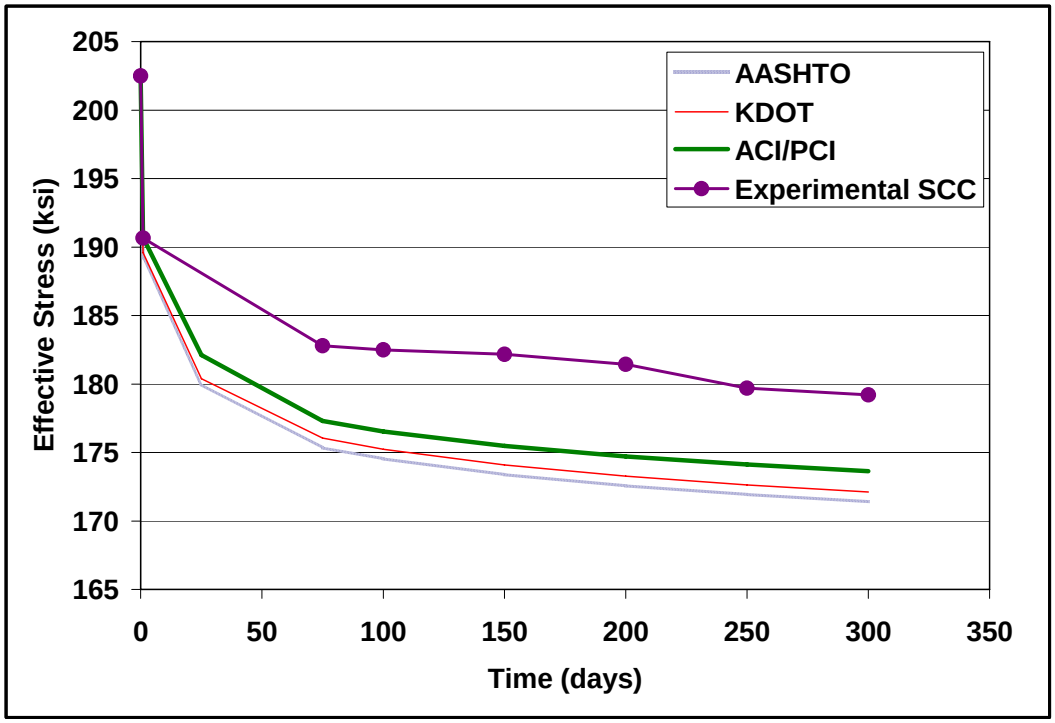

Figure 13.19: Effective stress calculations for girders with SCC

The ACI-209 method for predicting prestress loss was also used for the girders with SCC. Figure 13.20 presents these results. It can be seen that the ACI 209 method is much more conservative than predictions made by using the other four methods. A major difference is the prediction for shrinkage loss. It can be seen in Table 13.8 that the shrinkage loss prediction, using the ACI 209 method, is much greater than that of the other four methods. With a more accurate prediction of shrinkage loss for the ACI 209 method, it is assumed that predicted and experimental values would be much closer.

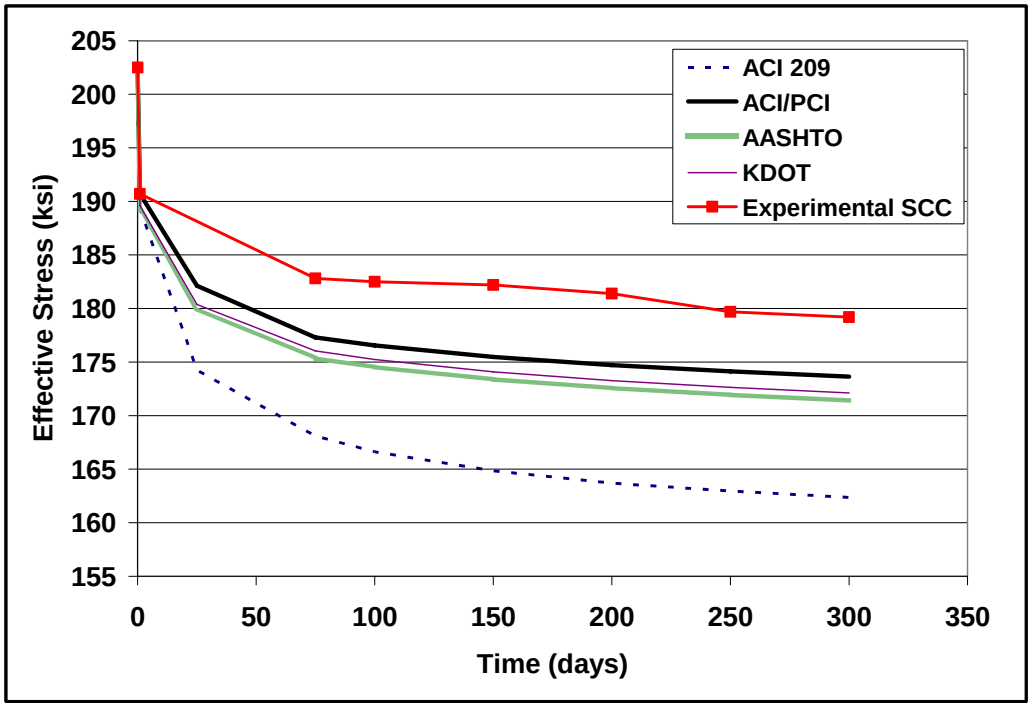

Figure 13.20: Effective stress comparison with all five methods for girders with SCC

Table 13.8: Shrinkage predictions using all five methods

Day	ACI-209	ACI/PCI	AASHTO	KDOT
Release	0.0	0.0	0.0	0.0
75	12.0	3.6	4.1	4.1
100	12.6	3.9	4.3	4.3
150	13.4	4.2	4.7	4.7
200	13.8	4.4	5.0	5.0
250	14.0	4.6	5.2	5.2
300	14.2	4.8	5.4	5.4
Ultimate	15.2	6.4	7.3	7.3

* all values reported in ksi

CHAPTER FOURTEEN - CONCLUSIONS AND RECOMMENDATIONS

14.1 Introduction

A three-phase comprehensive experimental and analytical research program was conducted to evaluate a proposed self-consolidating concrete (SCC) mixture in prestressed bridge applications. Phase I consisted of analyzing transfer lengths and development lengths of flexural specimens. Phase II evaluated the transfer length of an IT specimen by use of concrete surface strains along with monitoring long-term, time-dependent deformations. The primary objective of phase III was to monitor long-term prestress losses of bridge girders cast with both conventional concrete and self-consolidating concrete as placed in the field.

The test program was undertaken due to concerns for the low pullout values while performing large-block pullout tests (LBPTs) with prestressing strand in SCC. It must be noted that results obtained in this study are for the proposed SCC mixture, and other SCC mixtures may perform differently than the one evaluated in this program. While developing a new SCC mixture, it is not necessary to perform an extensive test program like the one carried out with this proposed SCC mixture, but it is imperative to confirm the long-term transfer length of the new SCC mixture. It has been shown that, in some cases, transfer lengths at release gave satisfactory results but then significantly increased with time. For the early age of the member, this will not be a problem; however, long-term issues could arise in the form of either shear or development length problems if strands continue to slip with time.

14.2 Conclusion Based on Flexural Specimens

The following can be concluded from the experimental studies conducted on the flexural specimens.

1. Large-block pullout test (LBPT) results for the strand used in this project and conducted with the mixture stipulated by Logan were above recommended minimum values for first-observed slip and maximum pullout force. Subsequent flexural beams fabricated with this strand and the proposed SCC all exhibited satisfactory flexural performance.
2. Recommended values for first-observed slip and maximum pullout force for 0.5-inch-diameter strand of 16 kip and 36 kip should not be used with LBPTs conducted with SCC. These values should be applied only when using a concrete mixture similar to the one stipulated by Logan.
3. Flexural tests indicated that current AASHTO (and also the ACI 318) equations for strand development length were conservative for the SCC mixture and specimen geometry used in this study. Moreover, all specimens with an embedment length equal to 80% of the ACI development length, including those with more than 12 inches of concrete below the strand, failed in flexure by strand rupture.
4. Transfer lengths estimated from 18-day strand end-slip measurements were in general agreement with the values assumed by the AASHTO and ACI 318 specifications. Average implied transfer lengths for top-strand beams at 18 days and at the time of testing were approximately 30% greater than those for the corresponding bottom-strand beams for all specimens with one strand.

5. For all flexural specimens in this study there was an increase in implied transfer lengths during the first 18 days after detensioning. For specimens with strand cast two inches from the bottom, the average increase was 10 to 20%, while for specimens with strands cast 22 inches above the bottom the increase was close to 100%. This suggests there is a reduction in bond for specimens with strand cast near the top surface of deep members.
6. Although a top-strand effect is present for members with this proposed SCC mixture, there was no evidence that it affected the development length for the members, just the transfer length.
7. No considerable increase in transfer length was measured after 18 days for the proposed SCC mixture.

14.3 Conclusions Based on IT Specimens

The following can be concluded from the experimental and analytical studies conducted on the IT specimens, along with the creep and shrinkage prisms.

1. Total observed losses for the experimental specimens were slightly less than those predicted by the current AASHTO, ACI/PCI, and KDOT design expressions.
2. Measured transfer lengths for the proposed SCC mixture and specimen geometry (IT) were in general agreement with the current AASHTO and ACI/PCI design assumptions, with the maximum measured transfer lengths being 33% larger than the calculated value using equation 1.1, and close to values stipulated by AASHTO (60 d_b) and ACI (50 d_b) for shear design.

3. Using the proposed SCC mixture, it was found that effective prestress losses were in general accordance with current AASHTO, ACI/PCI, and KDOT code equations. Therefore, no special design considerations are necessary when estimating losses in pretensioned members with this SCC mixture.
4. Creep coefficient and ultimate shrinkage strains obtained from companion laboratory samples were within general accordance with the values suggested by ACI Committee 209.
5. The ACI Committee 209 expression overestimated shrinkage for the IT specimens cast with the proposed SCC mixture.

14.4 Conclusions Based on Cowley County Bridge

The following can be concluded from the experimental and analytical studies conducted on the girders used in the Cowley County Bridge.

1. Total observed losses for the bridge girders were slightly less than those predicted by current PCI design expressions.
2. Girders containing SCC had slightly larger prestress losses, and this can be attributed to a smaller modulus of elasticity of concrete for the SCC mixture.
3. Time-dependent deformations for the proposed SCC mixture are within acceptable range of design guideline equations recommended by the ACI, AASHTO, and KDOT, and no special design considerations need to be used when estimating losses in pretensioned members cast with this SCC mixture.
4. The current conventional concrete mixture is exhibiting satisfactory performance in prestressed bridge girders.

5. At time of publication, none of the girders instrumented with VWSGs had time-dependent deformations exceeding those predicted by code equations.

14.5 Recommendations Based on Experimental Results

As with any experimental program involving a limited number of tests, it is difficult to draw universal conclusions and recommendations. However, the following recommendations are made to the state of Kansas regarding the experimental procedure used when evaluating the proposed SCC mixture in state bridge girders.

1. Current KDOT design guidelines should be used when SCC is to be used in state girders and no changes should be made.
2. General code equations for predicting modulus of elasticity (E_c) for the SCC mixture should not be used. The current equation overestimates the modulus of elasticity for the proposed SCC mixture. For this reason, experimental results for modulus should be used until a more accurate model is developed for the proposed SCC mixture.
3. Further tests should be completed to examine the top-strand effect to determine if the increased transfer lengths are due to the amount of concrete above or below the strand. It is believed that the pressure being applied by the concrete above the strand is contributing to smaller transfer lengths than those members with less concrete above the strand. The following test would confirm if the amount of concrete above the strand has a significant affect on bond.
    - Perform LBPTs on specimens in which the strand is cast and cured in the horizontal position.

- Have blocks with the strand at various amounts of concrete above and below the stand.
- For one of the blocks place a dead weight over the curing concrete to test if the consolidation pressure above is affecting pullout values.
- The following three blocks would be cast and tested to evaluation the bleed water effect and the amount of concrete above the strand. The side view of each block will be shown with the depth of each block being 24 inches. Block #1 (Figure 14.1) would be the control. Block #2 (Figure 14.2) would have two rows of strands to evaluate both the bleed water and amount of concrete above the strand. Block #3 (Figure 14.3 would have the same dimensions as Block #1, however it would have a dead load of 1400 pounds, the exact weight of concrete above the bottom row of strands of Block #2.

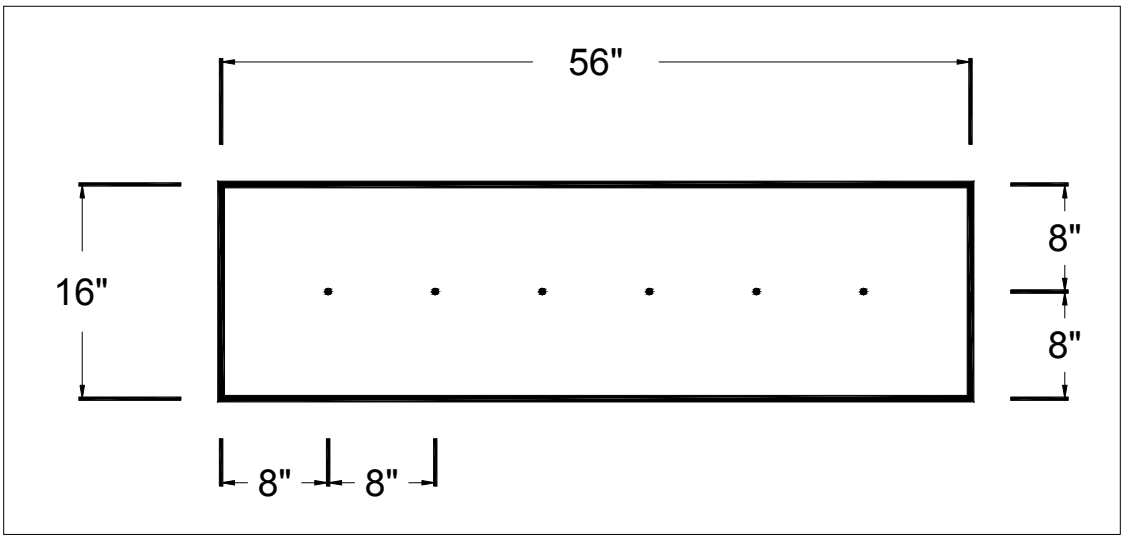

Figure 14.1: Block #1

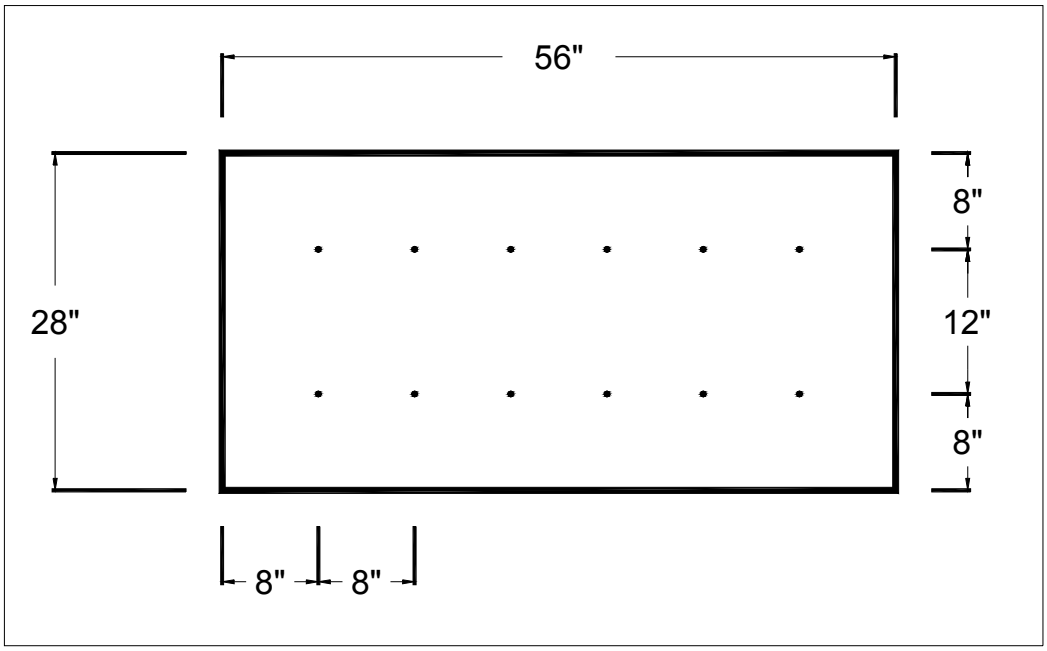

Figure 14.2: Block #2

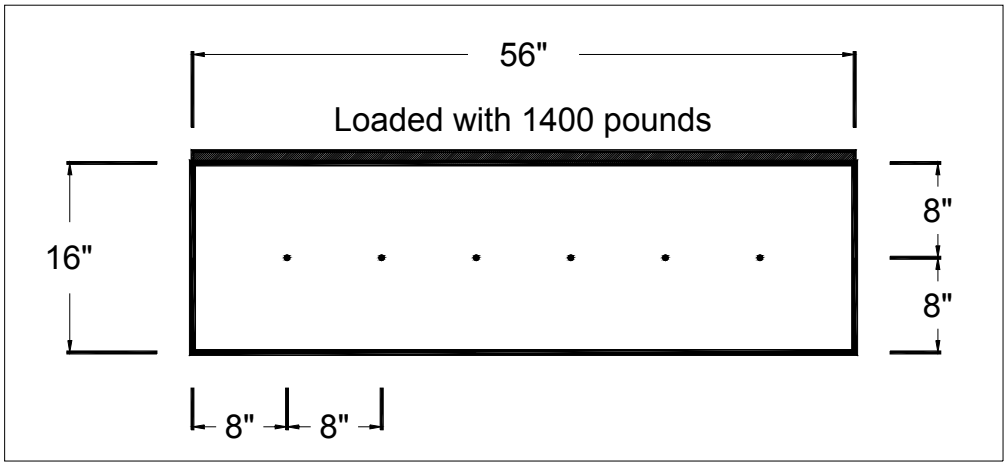

Figure 14.3: Block #3 (Loaded with 1400 pounds)

The following conclusions could be made depending of the results of the tests performed.

1. If the amount of concrete below the strand was the causing the poor bond of the top strands, then the pullout values of Blocks #1 and #3 would act the same as the bottom row of Block #2, having higher pullout values the top row of Block #2.
2. If the amount of concrete above the strand is the major contributing factor to bond, then Block #1 and the top row of Block #2 would have similar results, while Block #3 and the bottom row of Block #2 would act in a similar manner.

CHAPTER FIFTEEN - IMPLEMENTATION

The following are suggested policies KDOT should consider when using SCC in state bridge girders.

15.1 Recommendations Based on Plant Observations

1. LBPT testes have shown that the bond capacity of vertical, untensioned strand in SCC may be significantly less than that of the same strand in a conventional concrete mixture. This result could have significant implications for lifting devices in members cast with SCC. It is recommended that lifting devices used in KDOT girders be evaluated in SCC to ensure appropriate factors of safety are met.
2. Consistency in the SCC mixture needs to be maintained throughout the placement of concrete. A 25 +/- 2 inch spread should be targeted when using the proposed SCC mixture. It has been observed that when the SCC spread gets below 23 inches the development of “bug” holes at the surface occur. This spread measurement needs to be taken at the site of the prestressing bed, not the batch plant. A mixture can look good (spread and VSI) at the batch plant but segregation during transportation can adversely affect the concrete mix.
3. Long delays between placement of the SCC into the same girder need to be eliminated. Cast lines can develop if too much time elapses between placement of concrete from different batches into the same girder. One way to eliminate these cast lines is to dispense the concrete at a slower rate, thus eliminating long breaks between delivery.

4. When hot temperatures exist (more than 90 degrees F), special precautions need to be made to prevent major (+6 inch) spread loss from batch plant to prestressing beds.
5. The state inspector should be trained in determining whether or not an SCC mixture is acceptable for use in girders.

15.2 Recommendations to Evaluate Other SCC Mixtures

The research program that was completed to evaluate the proposed SCC mixture was a long process. The following recommendations are made to evaluate other mixtures that are to be used in bridge girders.

1. The Large Block Pullout Tests fabricated with SCC are not a good indicator on whether the SCC mixture will perform well when the strand is tensioned and cast in the horizontal position. LBPTs should only be used to determine strand-bond quality and should be conducted with a concrete mixture similar to the one stipulated by Logan.
2. Performing transfer length measurements on flexural specimens should be used when evaluating a potential SCC mixture. It is important to take readings well after detensioning to determine if the strand is continuing to “draw” in to the beam and the transfer length is getting longer over time. The use of Whittemore points to measure surface strains to determine transfer length was a lengthy process and could be eliminated since transfer lengths estimated from strand end-slip yielded similar results.
3. Evaluating specimens with strands cast near the bottom and top surface is important. However having three specimens for each embedment length was not

needed. If one specimen (not three) was loaded similar to the 100% M_n loading condition and the beam had not failed after the 24 hour hold then it could be concluded that the mix would perform well in flexure. Additionally, only 80% embedment length specimens could be tested and if no failure before nominal capacity were seen then there would be no need to run the 100% embedment length specimens.

4. The placement of three VWSG's into a potential bridge girder cast with SCC would be a good indictor of determining long-term prestress losses. If any major differences are seen between the girder cast with SCC and those of code expressions then designs accounting for long-term losses should be based on experimental measurements for the actual SCC mixture, rather then code expressions. The casting of separate girders to isolate shrinkage alone is not needed to determine total losses

Notations

A	-	Cross-sectional area of member
AASHTO	-	American Association of State Highway Transportation Officials
ACI	-	American Concrete Institute
A_{ps}	-	Area of prestressing strand
CC	-	Conventional concrete
d_b	-	Diameter of prestressing strand
d_p	-	Depth of prestressing strand
E	-	Eccentricity
E_c	-	28-day modulus of elasticity of concrete
E_{ci}	-	Release modulus of elasticity of concrete
E_{ps}	-	Modulus of elasticity of prestressing strand
f'_c	-	28-day compressive concrete strength
f'_{ci}	-	Release compressive concrete strength
f_{pj}	-	Stress in strand after tensioning
f_{ps}	-	Stress in prestressing strand at failure
f_{se}	-	Effective prestress, after all time-dependent deformations
f_{si}	-	Prestress after transfer before time-dependent losses
FT	-	Fully tensioned
KDOT	-	Kansas Department of Transportation
LBPT	-	Large-block pullout test
RH	-	Relative humidity
I	-	Moment of inertia of cross section
IT	-	Inverted-T
L	-	Length of member
L_{dev}	-	Development length
L_e	-	Embedment length
L_{tr}	-	Transfer length
M_n	-	Nominal moment
M_{sw}	-	Moment due to self weight of member
P	-	Force in prestressing strand after release
PCI	-	Prestressed/Precast Concrete Institute
SCC	-	Self-consolidating concrete
SSB	-	Single-strand beam
TB	-	T-beam
TSB	-	Top-strand beam
UT	-	Untensioned
V/S	-	Volume-to-surface ratio
v_t	-	Creep coefficient at any given time
v_u	-	Ultimate creep coefficient
VWSG	-	Vibrating wire strain gage
Y	-	Distance to neutral axis
□	-	Measured end slip
□	-	Strain
$(\square_{sh})_t$	-	Shrinkage strain at any time

$(\square_{sh})_u$ - Ultimate shrinkage strain
$\square$ - stress

References

1. Interim Guidelines for the Use of Self-Consolidating Concrete in Precast/ Prestressed Concrete Institute Member Plants, First Edition, Chicago, IL, 2003.

2. Russell, B.W., and Burns, N. H., "Design Guidelines for Transfer, Development and Debonding of Large Diameter Seven Wire Strands in Pretensioned Concrete Girders," Texas Department of Transportation, Research Project 3-5-89/2-1210, 286 pp., January 1993.

3. Peterman, R. J., Ramirez, J. A., and Olek, J., "Influence of Flexure-Shear Cracking on Strand Development Length in Prestressed Concrete Members," *PCI Journal*, V. 45, No. 5, September-October 2000, pp. 76-94.

4. ACI Committee 318, "Building Code Requirements for Structural Concrete (ACI 318-02) and Commentary (ACI 318R-02)," American Concrete Institute, Farmington Hills, MI, 2002.

5. AASHTO, *LRFD Bridge Design Specifications*, 3rd Ed., American Association of State Highway and Transportation Officials, Washington, DC, 2004.

6. Logan, Donald R., "Acceptance Criteria for Bond Quality of Strand for Pretensioned Prestressed Concrete Applications," *PCI Journal*, V.42, No. 2, March-April 1997, pp.52-90.

7. Nilson, A., *Design of Prestressed Concrete*, Second Edition, John Wiley & Sons, New York, New York, 1987.

8. Kansas Department of Transportation Design Manual, Bridge Section, V. 3, Version September 2003.

9. *PCI Design Handbook*, Sixth Edition, Precast/Prestressed Concrete Institute, Chicago, IL, 2004.

10. ACI Committee 209, "Prediction of Creep, Shrinkage, and Temperature Effects in Concrete Structures," American Concrete Institute, Farmington Hills, Mich., 1997.

11. Ouchi, M., "Self-Compacting Concrete Development, Applications and Investigations," *Proceedings of the Fourth International Conference on Materials Engineering for Resources*, V. 1, 2001, pp. 53-58.

12. Bury, A., and Christensen, B., "The Role of Innovative Chemical Admixtures in Producing Self-Consolidating Concrete," First North American Conference on the Design and Use of Self-Consolidating Concrete, 2002, pp. 137-140.

13. Ouchi, M.; Nakamura, S.; Osterberg, T.; Hallberg, S.; Lwin, M., “Applications of Self-Compacting Concrete in Japan, Europe, and the United States,” 2003 ISHPC.

14. Janney, J., “Nature of Bond in Pre-tensioned Prestressed Concrete,” *Journal of the American Concrete Institute*, May 1954, pp717-736.

15. Hanson, N., and Kaar, P., “Flexural Bond Tests of Pretensioned Prestressed Beams,” *Journal of the American Concrete Institute*, V. 55, n. 51, January 1959, pp. 783-802.

16. Kaar, P., LaFraugh, R., and Mass, M., “Influence of Concrete Strength on Strand Transfer Length,” *Ninth Annual Convention of the Prestressed Concrete Institute*, October 1963, pp. 47-67.

17. Janney, J., “Report of Stress Transfer Length Studies on 270 k Prestressing Strand,” *PCI Journal*, February 1963, pp. 41-45.

18. Kaar, P., and Hanson, N., “Bond Fatigue Tests of Beams Simulating Pretensioned Concrete Crossties,” *PCI Journal*, V. 20, n. 5, September- October 1975, pp 65-80.

19. Martin, L., and Scott, N., “Development of Prestressing Strand in Pretensioned Members,” *ACI Journal*, V. 73, n. 8, August 1976, pp 453-453.

20. Zia, P., and Mostafa, T., Development Length of Prestressing Strands,” *Journal of Prestressed Concrete Institute*, V. 22, n. 5, September-October 1977, pp. 54-65.

21. Cousins, T., Johnston, D., and Zia, P., “Transfer and Development Length of Epoxy Coated and Uncoated Prestressing Strand,” *PCI Journal*, V. 35, n. 4, July-August 1990, pp. 92-103.

22. Cousin, T., Badeaux, M., and Moustafa, S., “Proposed Test for Determining Bond Characteristics of Prestressing Strand,” *PCI Journal*, V. 37, n.1, January-Febuaury1992, pp. 66-73.

23. Shahawy, M., Issa, M., and Batchelor, B., “Strand Transfer Lengths in Full Scale AASHTO Prestressed Concrete Girders,” *PCI Journal*, V. 37, n. 3, May-June 1992, pp. 84-96.

24. Mitchell, D., Cook, W., Khan, A., and Tham, T., “Influence of High Strength Concrete on Transfer and Development Length of Pretensioning Strand,” PCI *Journal*, V. 38, n. 3, May-June 1993, pp. 52-66.

25. Buckner, D., “A Review of Strand Development Length for Pretensioned Concrete Members,” *PCI Journal*, V. 40, No. 2, March-April 1995, pp.84-105.

26. Martin, L., and Korkosz, W., “Strength of Prestressed Concrete Members at Sections Where Strands are not Fully Developed,” *PCI Journal*, V. 40, n. 5, September- October 1995, pp. 58-66.

27. Russell, B., and Burns, N., “Measured Transfer Lengths of 0.5 and 0.6 in. Strands in Pretensioned Concrete,” *PCI Journal*, V. 41, n. 5, September-October 1996, pp. 44-64.

28. Rose, D., and Russell, B., “Investigation of Standardized Tests to Measure the Bond Performance of Prestressing Strand,” *PCI Journal*, V. 42, n. 4, July-August 1997, pp. 44-66.

29. Lane, S., “A New Development Length Equation for Pretensioned Strands in Bridge Beams and Piles,” Publication No. FHWA-RD-98-116, December 1996, pp. 123.

30. Steinberg, E., Beier, J., and Sargand, S., “Effects of Sudden Prestress Force Transfer in Pretensioned Concrete Beams,” *PCI Journal*, V. 46, n. 1, January-February 2001, pp.64-75.

31. Oh, B., Kim, E., and Kim, K., “Correct Prediction of Transfer Lengths in Pretensioned Prestressed Concrete Structures,” SmiRT 16, Washington DC, August 2001 pp. 1-8.

32. Barnes, R. W., Grove, J. W., and Burns, N. H., “Experimental Assessment of Factors Affecting Transfer Length,” *ACI Structural Journal*, V. 100, No. 6, November-December 2004, pp. 740-748.

33. Khayat, K., Petrov, N., Attiogbe, E., and See, H., “Uniformity of Bond Strength of Prestressing Strands in Conventional Flowable and Self-Consolidating Concrete Mixtures,” *3rd International Symposium on Self-Compacting Concrete*, August 17-20, 2003, Iceland, pp. 703-712.

34. Girgis, A., and Tuan, C., “Bond Strength and Transfer Length of Pretensioned Bridge Girders Cast with Self-Consolidating Concrete,” *PCI Journal*, V. 50, n. 6, November-December 2005, pp. 72-87.

35. Burgueno, R., and Haq, M., “Transfer and Development Length of Prestressing Strands in Precast/Prestressed Girders using Self-Consolidating Concrete,” SCC 2005 Proceedings, 6 pp.

36. The European Guidelines for Self-Compacting Concrete: Specification, Production and Use, May 2005.
37. Tabatabai, H.; Dickson, T., "The History of the Prestressing Strand Development Length Equation," *PCI Journal*, V. 38, No. 6. pp. 64-75.

38. Ahlborn, T., French, C., and Shield, C., "High-Strength Concrete Prestressed Bridge Girders: Long Term and Flexural Behavior," Final Report 2000-32, Minnesota Department of Transportation, Nov 2000, 357 pp.

39. Barr, E., Fekete, M., Eberhard, J., Stanton, B., Khaleghi, J., and Hsieh, J., "High Performance Concrete in Washington State SR 18/SR 516 Overcrossing: Interim Report on Girder Monitoring," Interim Report Jan 1996- Nov1998, Washington State Department of Transportation, April 2000 129 pp.

40. Ramakrishnan, V., and Sigi, A., "Evaluation of High Performance Concrete in Four Bridge Decks as well as Prestressed Girders for Two Bridges," Final Report Study SD98-06, South Dakota Department of Transportation, December 2001, 180 pp.

41. Onyemelukwe, O., Issa, M., and Mills, C., "Field Measured Pre-Stress Concrete Losses Versus Design Code Estimates," Experimental Mechanics, V. 43, n. 2, June 2003, pp.201-215.

42. Yang, Y., and Myers, J., "Prestress Loss Measurements in Missouri's First Fully Instrumented High-Performance Concrete Bridge," *Transportation Research Record: Journal of the Transportation Research Board*, No. 1928, 2005, pp.118-125.

43. ASTM C1611 Standard Test Method for Slump Flow of Self-Consolidating Concrete.

44. ASTM C1621 Standard Test Method for Passing Ability of Self-Consolidating Concrete by J-Ring.

45. Khayat, K. H., Assaad, J., and Daczko, J., "Comparison of Field-Oriented Test Methods to Assess Dynamic Stability of Self-Consolidating Concrete," ACI Materials Journal, V. 101, No. 2, March-April 2004, pp. 168-176.

46. Geokon Inc., "Installation Manual: Models VCE-4200/4202/4210 Vibrating Wire Strain Gages," Nebanon, New Hampshire, 2004.

47. Corley, W.G., and Sozen, M.A., "Time Dependent Deflections of Reinforced Concrete Beams," *Journal of the American Concrete Institute*, Proceedings V. 63, No. 3, March 1966, pp. 373-386.

48. Mokhtarzadeh, A., and French, C., “Time-Dependent Properties of High-Strength Concrete with Consideration for Precast Application,” *ACI Materials Journal*, V. 97, No. 3. May-June 2000, pp. 263-271.

49. ASTM C512 Standard Test Method for Creep of Concrete in Compression.

APPENDIX

A.1 LBPT Tables

Table A.1: Mixture proportions stipulated by Logan

Materials	Quantity per yd^3
Cement (Type III)	660 lb
Concrete Sand	1100 lb
Crushed Gravel (Max 3/4")	1900 lb
Normal Range Water Reducer	26 oz
Air-Entraining Agent	0 oz
High Range Water Reducer	0 oz
Water	35 gal
w/c ratio	0.44

Note: The coarse aggregate had a maximum size of ¾" and an average Moh's hardness of 6.2 and the fineaggregate had a fineness modulus of 2.83

Table A.2: LBPT with SCC and control strand

SCC with Control Strand		
Specimen	**Max Load (kip)**	**Load at 1st Slip (kip)**
1	21.8	11.8
2	21.4	12.5
3	19.7	12.4
4	27.5	10.7
5	23.2	12.7
6	21.4	10.7
Average	**22.5**	**11.8**
Coeff of Var	**12.0%**	**7.7%**

Table A.1: LBPT with Logan concrete and control strand

Logan Concrete with Control Strand		
Specimen	**Max Load (kip)**	**Load at 1st Slip (kip)**
1	42.0	28.2
2	41.7	27.8
3	40.4	27.3
4	36.5	24.9
5	36.9	24.2
6	39.9	25.0
Average	**39.5**	**26.2**
Coeff of Var	**6.0%**	**6.6%**

A.2 Prestress Loss Equations

ACI and PCI METHOD

Elastic Shortening of Concrete (ES)

For members with bonded tendons,

$$ES = K_{es} E_s \frac{f_{cir}}{E_{ci}}$$

in which

K_{es} = 1.0 for pretensioned members
K_{es} = 0.5 for post-tensioned members when tendons are tensioned in sequential order to the same tension. With other post-tensioning procedures, the value for K_{es} may vary from 0 to 0.5.

$$f_{cir} = K_{cir} f_{cpi} - f_g$$

in which

K_{cir} = 1.0 for post-tensioned members.
K_{cir} = 0.9 for pretensioned members.

Creep of Concrete (CR)

For members with bonded tendons,

$$CR = K_{cr}\frac{E_s}{E_c}\left(f_{cir} - f_{cds}\right)$$

in which

K_{cr} = 2.0 for pretensioned members
K_{cr} = 1.6 for post-tensioned members

Shrinkage of Concrete (SH)

$$SH = 8.2x10^{-6}K_{sh}E_s\left(1 - 0.06\frac{V}{S}\right)\left(100 - RH\right)$$

in which

K_{sh} = 1.0 for pretensioned members
or
K_{sh} is taken from Table 1[9] for post-tensioned members.

Relaxation of Tendons (RE)

$$RE = \left[K_{re} - J\left(SH + CR + ES\right)\right]C$$

in which the values of K_{re}, J, and C are taken from Tables 2 and 3.[9]

AASHTO METHOD

Taken from the Third Edition[5] for pretensioned members

$$\Delta f_{pT} = \Delta f_{pES} + \Delta f_{pSR} + \Delta f_{pCR} + \Delta f_{pR2}$$

where:
- f_{pT} = total loss (ksi)
- f_{pES} = loss due to elastic shortening (ksi)

Δf_{pSR} = loss due to shrinkage (ksi)
Δf_{pCR} = loss due to creep of concrete (ksi)
Δf_{pR2} = loss due to relaxation of steel after transfer (ksi)

<u>Elastic Shortening (Δf_{pES})</u>

$$\Delta f_{pES} = \frac{E_p}{E_{ci}} f_{cgp}$$

where:
f_{cgp} = sum of concrete stresses at the center of gravity of prestressing tendons due to the prestressing force at transfer and the self-weight of the member at the sections of maximum moment (ksi)
E_p = modulus of elasticity of prestressing steel (ksi)
E_{ci} = modulus of elasticity of concrete at transfer (ksi)

<u>Shrinkage (Δf_{pSR})</u>

$$\Delta f_{pSR} = (17.0 - 0.150H)$$

where:
H = the average annual ambient relative humidity (percent)

<u>Creep (Δf_{pCR})</u>

$$\Delta f_{pCR} = 12.0 f_{cgp} - 7.0 \Delta f_{cdp} \geq 0$$

where:
f_{cgp} = concrete stress at center of gravity of prestressing steel at transfer (ksi)
Δf_{cdp} = change in concrete stress at center of gravity of prestressing steel due to permanent loads with the exception of the load acting at the time the prestressing force is applied. Values of Δf_{cdp} should be calculated at the same section or at sections for which f_{cgp} is calculated (ksi)

<u>Relaxation (Δf_{pR2})</u>

At transfer

In pretensioned members, the relaxation loss in prestressing steel, initially stressed in excess of 0.50 f_{pu}, may be taken as:

For stress-relieved strand:

$$\Delta f_{pR1} = \frac{\log(24.0t)}{10.0}\left[\frac{f_{pj}}{f_{py}} - 0.55\right] f_{pj}$$

For low-relaxation strand:

$$\Delta f_{pR1} = \frac{\log(24.0t)}{40.0}\left[\frac{f_{pj}}{f_{py}} - 0.55\right] f_{pj}$$

where:

t = time estimated in days from stressing to transfer (days)
f_{pj} = initial stress in the tendon at the end of the stressing (ksi)
f_{py} = specified yield strength of prestressing steel (ksi)

After Transfer

Losses due to relaxation of prestressing steel may be taken as:

For pretensioning with stress-relieved strands:

$$\Delta f_{pR2} = 20.0 - 0.4\Delta f_{pES} - 0.2\left(\Delta f_{pSR} + \Delta f_{pCR}\right)$$

where:
□f_{pES} = loss due to elastic shortening (ksi)
□f_{pSR} = loss due to shrinkage (ksi)
□f_{pCR} = loss due to creep of concrete (ksi)

For prestressing steels with low relaxation properties conforming to AASHTO M 203 (ASTM A 416 or E 328):

Use 30 percent of □f_{pR2} given by equation 12.

KDOT METHOD

As described in the 2003 release[8].

The loss of stress in the prestressing steel is as follows:

□f_S = SH + ES + CR_C +CR_S
□f_S = Loss of stress, psi
SH = Loss due to concrete shrinkage, psi
ES = Loss due to elastic shortening, psi
CR_C = Loss due to creep of concrete, psi
CR_S = Loss due to relaxation of steel, psi

<u>Shrinkage</u>

The shrinkage loss is computed as follows,

$$SH = 17,000 - 150RH$$

Where RH is the average relative humidity in percent. For Kansas, the humidity may be assumed at 65 percent.

Elastic Shortening

Elastic shortening is computed as follows:

$$ES = \left(E_s / E_{ci} \right) f_{cir}$$

in which

E_s = 28 x 10^6 psi

E_{ci} = Modulus of elasticity of concrete at transfer of stress ($33W^{3/2} \sqrt{f'_{ci}}$ psi.)

W = 145 pcf for normal weight concrete

f_{cir} = Concrete stress at the center of gravity of the prestressing steel due top prestressing force and dead load of the beam immediately after transfer. (At this stage, the initial stress in the tendon has been reduced by elastic shortening of the concrete and tendon relaxation during placing and curing of the concrete.)

Creep of Concrete:

For pretensioned and post-tensioned members

$$CR_C = 12 f_{cir} - 7 f_{cds}$$

Where f_{cds} is the concrete stress at the center of gravity of prestressing steel due to all dead loads except the dead loads present at the time prestressing force is applied.

Relaxation of Prestressing Steel – (Low Relaxation Strand)

$$CR_S = 5,000 - 0.10ES - 0.05\left(SH + CR_C\right)$$

The values of *ES*, *SH*, and CR_C are those computed previously,

Total losses: $\Delta f = SH + ES + CR_C + CR_S$

The minimum loss of prestress to be used when computing service load stresses shall be 35,000 psi.

ACI 209 COMMITTEE

$$\lambda_t = (nf_c) + (nf_c)v_t\left(1 - \frac{F_t}{2F_0}\right) + \frac{(\varepsilon_{sh})_t E_s}{1 + n\rho\xi_s} + (f_{sr})_t$$

where

λ_t = total losses

n = modular ratio, E_S/E_{ci} at the time of loading;

f_c = concrete stress such as at steel c.g.s. due to prestress and precast beam dead load in the prestress loss equations;

v_t = creep coefficient at any time;

F_t = total loss of prestress at any time minus the inital elastic loss;

F_o = prestress force at transfer, after elastic loss;

$(\varepsilon_{sh})_t$ = shrinkage strain at any time;

E_s = modulus of elasticty of steel;

ρ = reinforcement ratio;

ξ_s = cross section shape coefficient;

$(f_{sr})_t$ = stress loss due to steel relaxation in prestressed member at any time.

A.3 Shear Calculations for Single Strand Specimens

Test Span $L_{test} = 12.83$ ft

Shear Span $a_{test} = 5.92$ ft

$M_D + M_L = 32.9$ kip-ft

$$\frac{(0.0933)\text{ x }(12.83)^2}{8} + \frac{P_F}{2}(5.92) = 32.9$$

$P_F = 10.5$ kips

$$V_{\max} = 0.0933\text{ x }(6) + \frac{10.5}{2} = 5.8\text{ kip}$$

$$V_c = 2 * \sqrt{f_c^{'}}\text{ x }b\text{ x }d_p = 2\text{ x }\sqrt{8,000}\text{ x }8\text{ x }10 = 14.3\text{ kip}$$

$V_c > V_{\max}$ (Good)

A.4 Nominal Moment Calculations for Single Strand Specimens

$$P_e = f_{se} \text{ x } A_{ps} = 185 \text{ x } 0.153 = 28.3 \text{ kip}$$

$$\varepsilon_1 = f_{se} / E_p = 185 / 28,500 = 0.00649$$

$$\varepsilon_2 = \frac{1}{E_c}\left[\frac{P_e}{A} + \frac{P_e \text{ x } e^2}{I}\right] = \frac{1}{5000}\left[\frac{28.3}{96} + \frac{28.3 \text{ x } 4^2}{1152}\right] = .000138$$

Assume $f_{ps} = 268.2 \text{ ksi}$

$$a = \frac{A_{ps} \text{ x } f_{ps}}{0.85 \text{ x } f_c^{'} * b} = \frac{0.153 \text{ x } 268.2}{0.85 \text{ x } 8 \text{ x } 8} = 0.754$$

$$c = a / \beta_1 = 0.754 / 0.65 = 1.16$$

$$\varepsilon_3 = \left(\frac{d_p - c}{c}\right) \text{x } \varepsilon_c = \left(\frac{10 - 1.16}{1.16}\right) \text{x } 0.003 = 0.0229$$

$$\varepsilon_{ps} = \varepsilon_1 + \varepsilon_2 + \varepsilon_3 = 0.00649 + 0.000138 + 0.0229 = 0.0295$$

From strand stress-strain curve in PCI Design Handbook

$$f_{ps} = 270 - \frac{0.04}{\varepsilon_{ps} - 0.007} = 268.2 \text{ ksi (Equals assumed value)}$$

$$M_n = A_{ps} \text{ x } f_{ps} \text{ x}\left(d_p - \frac{a}{2}\right) = 0.153 \text{ x } 268.2 \text{ x}\left(10 - \frac{.754}{2}\right) = 394.9 \text{ kip-in.}$$

$$= 32.9 \text{ kip-ft}$$

A.5 Nominal Moment Calculations for TB Specimens

$$P_e = f_{se} \text{ x } A_{ps} = 181\left((5)0.153\right) = 138.5 \text{ kip}$$

$$\varepsilon_1 = f_{se} / E_p = 181/28{,}500 = 0.00635$$

$$\varepsilon_2 = \frac{1}{E_c}\left[\frac{P_e}{A} + \frac{P_e \text{ x } e^2}{I}\right] = \frac{1}{5000}\left[\frac{138.5}{466} + \frac{138.5 \text{ x } 10.52^2}{17733}\right] = .000232$$

Assume $f_{ps} = 268.8$ ksi and compression in flange

$$a = \frac{A_{ps} \text{ x } f_{ps}}{0.85 \text{ x } f_c^{'} * b} = \frac{(5)0.153 \text{ x } 268.8}{0.85 \text{ x } 8 \text{ x } 36} = 0.84$$

$$c = a / \beta_1 = 0.84 / 0.65 = 1.29$$

$$\varepsilon_3 = \left(\frac{d_p - c}{c}\right) \text{x } \varepsilon_c = \left(\frac{19 - 1.29}{1.29}\right) \text{x } 0.003 = 0.0411$$

$$\varepsilon_{ps} = \varepsilon_1 + \varepsilon_2 + \varepsilon_3 = 0.00635 + .000232 + .0411 = 0.0477$$

From strand stress-strain curve in PCI Design Handbook

$$f_{ps} = 270 - \frac{0.04}{\varepsilon_{ps} - 0.007} \approx 268.8 \text{ ksi (Equals assumed value)}$$

$$M_n = A_{ps} \text{ x } f_{ps} \text{ x}\left(d_p - \frac{a}{2}\right) = (5)0.153 \text{ x } 268.8 \text{ x}\left(19 - \frac{.84}{2}\right) = 3821 \text{ kip-in.}$$

$$= 318 \text{ kip-ft}$$

A.6 Calculations of Losses for Flexural Specimens

(using PCI Method)

Single-strand specimens

<u>Elastic Shortening of Concrete (ES)</u>

$$ES = K_{es} E_s \frac{f_{cir}}{E_{ci}}$$

K_{es} = 1.0 for pretensioned members
E_{ci} = 3,600 ksi
Es = 28,500 ksi

$$f_{cir} = K_{cir} f_{cpi} - f_g$$

K_{cir} = 0.9 for pretensioned members.

$$f_{cpi} = 0.9\left(\frac{31}{96} + \frac{31(4)^2}{1152}\right) = .68\,ksi$$

$$f_g = \frac{2.0(12)4}{1152} = 0.08\,ksi$$

$$f_{cir} = 1.0(.68) - .08 = 0.6\,ksi$$

$$ES = 1.0(28500)\frac{0.6}{3600} = 4.8\,ksi$$

<u>Creep of Concrete (CR)</u>

For members with bonded tendons,

$$CR = K_{cr}\frac{E_s}{E_c}(f_{cir} - f_{cds})$$

K_{cr} = 2.0 for pretensioned members

$$f_{cds} = 0\,ksi$$

$$CR = 2\frac{28500}{5000}(0.6 - 0) = 6.8\,ksi$$

<u>Shrinkage of Concrete (SH)</u>

$$SH = 8.2x10^{-6}K_{sh}E_s\left(1 - 0.06\frac{V}{S}\right)(100 - RH)$$

K_{sh} = 1.0 for pretensioned members

$V/S = 2.33$

RH = 65%

$$SH = 8.2x10^{-6}(1.0)28500(1 - .06(2.33))(100 - 65) = 7.0\,ksi$$

<u>Relaxation of Tendons (RE)</u>

$$RE = \left[K_{re} - J(SH + CR + ES)\right]C$$

K_{re} = 5.0

J = 0.04

C = 1.0

$$RE_L = \left[5.0 - .04\left(4.8 + 6.8 + 7.0\right)\right]1 = 4.3\,ksi$$

$$RE_i = f_{st}\left\{\left[\log 24t - \log 24t_1\right]/24\right\} \text{x} \left[f_{st}/f_{py} - .55\right]$$

$$= 202{,}500 \text{ x} \left[\log 18\right]/45 \text{ x} \left[202{,}500/243{,}000 - .55\right] = 1.60 \text{ ksi}$$

<u>Total Losses</u>

$$f_{si} = f_{pj} - ES - RE_i$$

$$= 202.5 - 4.8 - 1.6 \approx 196 \text{ ksi}$$

$$f_{se} = f_{pj} - ES - CR - SH - RE_L$$

$$= 202.5 - 4.8 + 6.8 + 7.0 + 4.3 \approx 180 \text{ ksi}$$

$$f_{se@90} = 185 \text{ ksi}^*$$

$^*f_{se}$ of 90 days was used for calculations because that was the average age of the specimens at the time of testing.

Calculated Transfer Length (using equation 1.1)

$$L_{tr} = f_{se} d_b / 3$$

$$185 \text{ x} .5/3 = 31 \text{ in.}$$

Calculated Development Length (using equation 1.2)

$$L_{dev} = f_{se} d_b / 3 + (f_{ps} - f_{se}) d_b$$

$$= 185 \text{ x} .5/3 + \left(268.2 - 185\right) \text{x} .5 = 72.5 \text{ in.} \approx 6'\text{-}1''$$

Multiple-strand specimens

<u>Elastic Shortening of Concrete (ES)</u>

$$ES = K_{es} E_s \frac{f_{cir}}{E_{ci}}$$

K_{es} = 1.0 for pretensioned members
E_{ci} = 3,600 ksi
Es = 28,500 ksi

$$f_{cir} = K_{cir} f_{cpi} - f_g$$

K_{cir} = 0.9 for pretensioned members.

$$f_{cpi} = 0.9\left(\frac{155}{466} + \frac{155(10.52)^2}{17733}\right) = 1.17\,ksi$$

$$f_g = \frac{11.4(12)10.52}{17733} = 0.08\,ksi$$

$$f_{cir} = 1.0(1.17) - .08 = 1.09\,ksi$$

$$ES = 1.0(28500)\frac{1.08}{3600} = 8.55\,ksi$$

<u>Creep of Concrete (CR)</u>

For members with bonded tendons,

$$CR = K_{cr}\frac{E_s}{E_c}(f_{cir} - f_{cds})$$

K_{cr} = 2.0 for pretensioned members

$$f_{cds} = 0\,ksi$$

$$CR = 2\frac{28500}{5000}(1.09 - 0) = 12.4\,ksi$$

<u>Shrinkage of Concrete (SH)</u>

$$SH = 8.2x10^{-6} K_{sh} E_s \left(1 - 0.06\frac{V}{S}\right)(100 - RH)$$

K_{sh} = 1.0 for pretensioned members

$V/S = 3.91$

RH = 65%

$$SH = 8.2x10^{-6}(1.0)28500(1 - .06(3.91))(100 - 65) = 6.3\,ksi$$

<u>Relaxation of Tendons (RE)</u>

$$RE = \left[K_{re} - J(SH + CR + ES)\right]C$$

K_{re} = 5.0
J = 0.04
C = 1.0

$$RE_L = \left[5.0 - .04\left(8.6 + 12.4 + 6.3\right)\right]1 = 3.9\,ksi$$

$$RE_i = f_{st}\left\{\left[\log 24t - \log 24t_1\right]/24\right\} \text{x} \left[f_{st}/f_{py} - .55\right]$$

$$= 202{,}500 \text{ x} \left[\log 18\right]/45 \text{ x} \left[202{,}500/243{,}000 - .55\right] = 1.60 \text{ ksi}$$

<u>Total Losses</u>

$$f_{si} = f_{pj} - ES - RE_i$$

$$= 202.5 - 8.6 - 1.6 \approx 192 \text{ ksi}$$

$$f_{se} = f_{pj} - ES - CR - SH - RE_L$$

$$= 202.5 - 8.6 - 12.4 - 6.3 - 3.9 \approx 171 \text{ ksi}$$

$$f_{se@90} = 181 \text{ ksi}^*$$

*f_{se} of 90 days was used for calculations because that was the average age of the specimens at the time of testing.

Calculated Transfer Length (using equation 1.1)

$$L_{tr} = f_{se} d_b / 3$$

$$181 \text{ x} .5/3 = 30 \text{ in.}$$

Calculated Development Length (using equation 1.2)

$$L_{dev} = f_{se} d_b / 3 + (f_{ps} - f_{se}) d_b$$

$$= 181 \text{ x} .5/3 + \left(268.8 - 181\right) \text{x} .5 = 73 \text{ inch} \approx 6'\text{-}1''$$

A.7 As-Built Dimensions for Flexural Specimens

Table A.4: As-built dimensions for SSB specimens

Specimen	Heigth (inch)	Width (inch)	Strand Depth (inch)
SSB A	12	8.25	9.88
SSB C	12	8.25	9.88
SSB D	12	8.25	10
SSB E	12	8.25	9.88
SSB F	12	8.25	10

Table A.5: As-built dimensions for TSB specimens

Specimen	Heigth (inch)	Width (inch)	Strand Depth (inch)
TSB A	12.5	8	10
TSB B	12.5	8	10
TSB C	12.5	8	10
TSB D	12.25	8.13	9.75
TSB E	12	8.25	9.5
TSB F	12	7.88	9.5

Table A.6:2 As-built dimensions for TB specimens

Specimen	Height (inch)	Flange Width (inch)	Flange Heigth (inch)	Web Width (inch)	Strand Depth (inch)
TB A	20.63	36	6.38	16.06	18.63
TB B	21.63	35.88	6.75	15.94	19.63
TB C	20.63	36	6.38	16.06	18.63
TB D	21.63	35.88	6.75	15.94	19.63

A.8 Calculations of Prestress Losses for IT Specimens

ACI and PCI METHOD

Elastic Shortening of Concrete (ES)

$$ES = K_{es} E_s \frac{f_{cir}}{E_{ci}}$$

K_{es} = 1.0 for pretensioned members
E_{ci} = 3,600 ksi
Es = 28,500 ksi

$$f_{cir} = K_{cir} f_{cpi} - f_g$$

K_{cir} = 0.9 for pretensioned members.

$$f_{cpi} = 0.9\left(\frac{484}{256} + \frac{484(3.86)^2}{12822}\right) = 2.21\,ksi$$

$$f_g = \frac{4.41(12)3.86}{12822} = 0.02\,ksi$$

$$f_{cir} = 1.0(2.21) - .02 = 2.19\,ksi$$

$$ES = 1.0(28500)\frac{2.19}{3600} = 17.3\,ksi$$

Creep of Concrete (CR)

For members with bonded tendons,

$$CR = K_{cr} \frac{E_s}{E_c}(f_{cir} - f_{cds})$$

K_{cr} = 2.0 for pretensioned members

$$f_{cds} = 0\,ksi$$

$$CR = 2\frac{28500}{5300}(2.19 - 0) = 23.6\,ksi$$

Shrinkage of Concrete (SH)

$$SH = 8.2x10^{-6} K_{sh} E_s \left(1 - 0.06\frac{V}{S}\right)(100 - RH)$$

K_{sh} = 1.0 for pretensioned members
$V/S = 2.87$
RH = 65%

$$SH = 8.2x10^{-6}(1.0)28500(1 - .06(2.87))(100 - 65) = 6.8\,ksi$$

<u>Relaxation of Tendons (RE)</u>

$$RE = \left[K_{re} - J\left(SH + CR + ES\right)\right]C$$

K_{re} = 5.0
J = 0.04
C = 1.0

$$RE = \left[5.0 - .04(17.3 + 23.6 + 6.8)\right]1 = 3.1\,ksi$$

<u>Total Losses</u>

$$TL = 17.3 + 23.6 + 6.8 + 3.1 = 50.8\,ksi$$
$$f_{se} = 198 - 50.8 \approx 147\,ksi$$

AASHTO METHOD

$$\Delta f_{pT} = \Delta f_{pES} + \Delta f_{pSR} + \Delta f_{pCR} + \Delta f_{pR2}$$

<u>Elastic Shortening (□f_{pES})</u>

$$\Delta f_{pES} = \frac{E_p}{E_{ci}} f_{cgp}$$

f_{cgp} = $$\left(\frac{484}{256} + \frac{484(3.86)^2}{12822}\right) - \frac{4.41(12)3.86}{12822} = 2.44\,ksi$$

$$\Delta f_{pES} = \frac{28500}{3600} 2.44 = 19.3\,ksi$$

<u>Shrinkage (□f_{pSR})</u>

$$\Delta f_{pSR} = \left(17.0 - 0.150H\right)$$

H = 65

$$\Delta f_{pSR} = \left(17.0 - 0.150\left(65\right)\right) = 7.25\,ksi$$

<u>Creep (□f_{pCR})</u>

$$\Delta f_{pCR} = 12.0\,f_{cgp} - 7.0\Delta f_{cdp} \geq 0$$

f_{cgp} = 2.44 ksi
□f_{cdp} =0 ksi

$$\Delta f_{pCR} = 12.0\left(2.44\right) - 7.0\left(0\right) = 29.3\,ksi$$

<u>Relaxation (□f_{pR2})</u>

After Transfer

$$\Delta f_{pR2} = \left(20.0 - 0.4\Delta f_{pES} - 0.2\left(\Delta f_{pSR} + \Delta f_{pCR}\right)\right).30$$

$$\Delta f_{pR2} = \left(20.0 - 0.4\left(19.3\right) - 0.2\left(7.25 + 29.3\right)\right).30 = 1.5\,ksi$$

<u>Total Losses</u>

$$TL = 19.3 + 29.3 + 7.3 + 1.5 = 57.4$$
$$f_{se} = 198 - 57.4 \approx 141\,ksi$$

KDOT METHOD

<u>Shrinkage</u>

$$SH = 17,000 - 150RH$$

H =65

$$SH = 17,000 - 150\left(65\right) = 7250\ psi = 7.3\,ksi$$

<u>Elastic Shortening</u>

$$ES = \left({E_s}/{E_{ci}} \right) f_{cir}$$

E_s = 28 x 10^6 psi
f_{cir} = 2440 psi

$$ES = \left(28000/3600\right)2440 = 18900\ psi = 18.9\,ksi$$

Creep of Concrete:

$$CR_C = 12\,f_{cir} - 7\,f_{cds}$$

f_{cds} = 0 ksi

$$CR_c = 12\left(2.44\right) - 7\left(0\right) = 29.3\,ksi$$

Relaxation of Prestressing Steel

$$CR_S = 5{,}000 - 0.10ES - 0.05\left(SH + CR_C\right)$$

$$CR_s = 5 - .1\left(18.9\right) - .05\left(7.3 + 29.3\right) = 1.3\,ksi$$

Total Losses

$$TL = 18.9 + 29.3 + 7.3 + 1.3 = 56.8$$
$$f_{se} = 198 - 56.8 \approx 141\,ksi$$

A.9 Calculation of ACI 209 Prestress Losses for IT specimen

Elastic shortening

$$ES = nf_c$$

$$n = 28500/3500 = 8.14$$

$$f_c = \frac{484}{256} + \frac{484\left(3.86\right)^2}{12822} - \frac{4.41\left(12\right)3.86}{12822} = 2.44\,ksi$$

$$ES = 8.14\left(2.44\right) = 19.9\,ksi$$

Creep

$$CR = (nf_c)v_u\left[1 - \Delta F_t / 2F_o\right]$$

$$n = 28500/3750 = 7.6$$

$$f_c = 2.44\,ksi$$

$$v_u = 1.75$$

$$\Delta F_t / F_o = .18$$

$$CR = (7.6(2.44))1.75\left[1 - .18/2\right] = 29.5\,ksi$$

<u>Shrinkage</u>

$$SH = \frac{(\varepsilon_{sh})_u E_s}{1 + n\rho k_s}$$

$$(\varepsilon_{sh})_u = 550\,\mu\varepsilon$$

$$E_s = 28500\,ksi$$

$$n = 28500/3750 = 7.6$$

$$\rho = \frac{14(.153)}{6.35(21)} = 0.016$$

$$k_s = 1 + e^2/r^2 = 1 + 3.86^2 / \left(12822/256\right) = 1.30$$

$$SH = \frac{550/10^6\ 28500}{1 + 7.6(.016)1.3} = 13.5\,ksi$$

<u>Relaxation</u>

$$RE = (f_{sr})_t$$

$$\left(f_{sr}\right)_u = .025(198) = 5.0$$

$$RE = 5.0\,ksi$$

Total Losses

$$TL = 19.9 + 29.5 + 13.5 + 5 = 67.9\,ksi$$
$$f_{se} = 198 - 67.9 \approx 130\,ksi$$

A.10 Calculation of Prestress Losses for K3 Girders

ACI and PCI METHOD (Conventional Concrete)

Elastic Shortening of Concrete (ES)

$$ES = K_{es} E_s \frac{f_{cir}}{E_{ci}}$$

K_{es} = 1.0 for pretensioned members
E_{ci} = 4,500 ksi
Es = 28,500 ksi

$$f_{cir} = K_{cir} f_{cpi} - f_g$$

K_{cir} = 0.9 for pretensioned members.

$$f_{cpi} = 0.9\left(\frac{496}{525} + \frac{496(13.27)^2}{127490}\right) = 1.47\,ksi$$

$$f_g = \frac{171(12)13.27}{127490} = 0.21\,ksi$$

$$f_{cir} = 1.0(1.47) - .21 = 1.26\,ksi$$

$$ES = 1.0(28500)\frac{1.26}{4500} = 8.0\,ksi$$

Creep of Concrete (CR)

For members with bonded tendons,

$$CR = K_{cr}\frac{E_s}{E_c}\left(f_{cir} - f_{cds}\right)$$

K_{cr} = 2.0 for pretensioned members

$$f_{cds} = \frac{850(50)^2 12(13.27)}{8(127490)} = .33\,ksi$$

$$CR = 2\frac{28500}{4600}(1.26 - .33) = 11.5\,ksi$$

<u>Shrinkage of Concrete (SH)</u>

$$SH = 8.2x10^{-6} K_{sh} E_s \left(1 - 0.06\frac{V}{S}\right)(100 - RH)$$

K_{sh} = 1.0 for pretensioned members
$V/S = 3.56$
RH = 65%

$$SH = 8.2x10^{-6}(1.0)28500(1 - .06(3.56))(100 - 65) = 6.4\,ksi$$

<u>Relaxation of Tendons (RE)</u>

$$RE = \left[K_{re} - J\left(SH + CR + ES\right)\right]C$$

K_{re} = 5.0
J = 0.04
C = 1.0

$$RE = \left[5.0 - .04(8.0 + 11.5 + 6.4)\right]1 = 4.0\,ksi$$

<u>Total Losses</u>

$$TL = 8.0 + 11.5 + 6.4 + 4.0 = 29.9\,ksi$$
$$f_{se} = 202.5 - 29.9 \approx 173\,ksi$$

AASHTO METHOD (Conventional Concrete)

$$\Delta f_{pT} = \Delta f_{pES} + \Delta f_{pSR} + \Delta f_{pCR} + \Delta f_{pR2}$$

<u>Elastic Shortening (Δf_{pES})</u>

$$\Delta f_{pES} = \frac{E_p}{E_{ci}} f_{cgp}$$

f_{cgp} = $$\left(\frac{496}{525} + \frac{496(13.27)^2}{127490}\right) - \frac{171(12)13.27}{127490} = 1.42\,ksi$$

$$\Delta f_{pES} = \frac{28500}{4500} 1.42 = 9.0\,ksi$$

<u>Shrinkage (□f_{pSR})</u>

$$\Delta f_{pSR} = (17.0 - 0.150H)$$

H = 65

$$\Delta f_{pSR} = (17.0 - 0.150(65)) = 7.25\,ksi$$

<u>Creep (□f_{pCR})</u>

$$\Delta f_{pCR} = 12.0 f_{cgp} - 7.0\Delta f_{cdp} \geq 0$$

f_{cgp} = 1.42 ksi
□f_{cdp} =.33 ksi

$$\Delta f_{pCR} = 12.0(1.42) - 7.0(.33) = 14.7\,ksi$$

<u>Relaxation (□f_{pR2})</u>

After Transfer

$$\Delta f_{pR2} = \left(20.0 - 0.4\Delta f_{pES} - 0.2\left(\Delta f_{pSR} + \Delta f_{pCR}\right)\right).30$$

$$\Delta f_{pR2} = \left(20.0 - 0.4(9.0) - 0.2(7.25 + 14.7)\right).30 = 3.6\,ksi$$

<u>Total Losses</u>

$$TL = 9.0 + 14.7 + 7.3 + 3.6 = 34.6$$
$$f_{se} = 202.5 - 34.6 \approx 168\,ksi$$

KDOT METHOD (Conventional Concrete)

Shrinkage

$$SH = 17,000 - 150RH$$

H =65

$$SH = 17,000 - 150(65) = 7250\ psi = 7.3\,ksi$$

Elastic Shortening

$$ES = \left(E_s / E_{ci} \right) f_{cir}$$

E_s = 28 x 10^6 psi
f_{cir} = 1420 psi

$$ES = \left(28000 / 4500 \right) 1420 = 8840\ psi = 8.8\,ksi$$

Creep of Concrete:

$$CR_C = 12 f_{cir} - 7 f_{cds}$$

f_{cds} = .33 ksi

$$CR_c = 12(1.42) - 7(.33) = 14.7\,ksi$$

Relaxation of Prestressing Steel

$$CR_S = 5,000 - 0.10ES - 0.05(SH + CR_C)$$

$$CR_s = 5 - .1(8.8) - .05(7.3 + 14.7) = 3.0\,ksi$$

Total Losses

$$TL = 8.8 + 14.7 + 7.3 + 3.0 = 33.8$$
$$f_{se} = 202.5 - 33.8 \approx 169\,ksi$$

ACI and PCI METHOD (SCC)

Elastic Shortening of Concrete (ES)

$$ES = K_{es} E_s \frac{f_{cir}}{E_{ci}}$$

K_{es} = 1.0 for pretensioned members
E_{ci} = 3,500 ksi
Es = 28,500 ksi

$$f_{cir} = K_{cir} f_{cpi} - f_g$$

K_{cir} = 0.9 for pretensioned members.

$$f_{cpi} = 0.9\left(\frac{496}{525} + \frac{496(13.27)^2}{127490}\right) = 1.47 ksi$$

$$f_g = \frac{171(12)13.27}{127490} = 0.21 ksi$$

$$f_{cir} = 1.0(1.47) - .21 = 1.26 ksi$$

$$ES = 1.0(28500)\frac{1.26}{3500} = 10.3 ksi$$

Creep of Concrete (CR)

For members with bonded tendons,

$$CR = K_{cr} \frac{E_s}{E_c}(f_{cir} - f_{cds})$$

K_{cr} = 2.0 for pretensioned members

$$f_{cds} = \frac{850(50)^2 12(13.27)}{8(127490)} = .33 ksi$$

$$CR = 2\frac{28500}{3750}(1.26 - .33) = 14.1 ksi$$

Shrinkage of Concrete (SH)

$$SH = 8.2x10^{-6} K_{sh} E_s \left(1 - 0.06\frac{V}{S}\right)(100 - RH)$$

K_{sh} = 1.0 for pretensioned members
$V/S = 3.56$
RH = 65%

$$SH = 8.2x10^{-6}(1.0)28500(1 - .06(3.56))(100 - 65) = 6.4\,ksi$$

<u>Relaxation of Tendons (RE)</u>

$$RE = \left[K_{re} - J\left(SH + CR + ES\right)\right]C$$

K_{re} = 5.0
J = 0.04
C = 1.0

$$RE = \left[5.0 - .04(10.3 + 14.1 + 6.4)\right]1 = 3.8\,ksi$$

<u>Total Losses</u>

$$TL = 10.3 + 14.1 + 6.4 + 3.8 = 34.6\,ksi$$
$$f_{se} = 202.5 - 34.6 \approx 168\,ksi$$

AASHTO METHOD (SCC)

$$\Delta f_{pT} = \Delta f_{pES} + \Delta f_{pSR} + \Delta f_{pCR} + \Delta f_{pR2}$$

<u>Elastic Shortening (□f_{pES})</u>

$$\Delta f_{pES} = \frac{E_p}{E_{ci}} f_{cgp}$$

f_{cgp} = $$\left(\frac{496}{525} + \frac{496(13.27)^2}{127490}\right) - \frac{171(12)13.27}{127490} = 1.42\,ksi$$

$$\Delta f_{pES} = \frac{28500}{3500}1.42 = 11.6\,ksi$$

<u>Shrinkage (□f_{pSR})</u>

$$\Delta f_{pSR} = (17.0 - 0.150H)$$

H = 65

$$\Delta f_{pSR} = (17.0 - 0.150(65)) = 7.25\,ksi$$

<u>Creep (□f_{pCR})</u>

$$\Delta f_{pCR} = 12.0\,f_{cgp} - 7.0\Delta f_{cdp} \geq 0$$

f_{cgp} = 1.42 ksi
□f_{cdp} =.33 ksi

$$\Delta f_{pCR} = 12.0(1.42) - 7.0(.33) = 14.7\,ksi$$

<u>Relaxation (□f_{pR2})</u>

After Transfer

$$\Delta f_{pR2} = \left(20.0 - 0.4\Delta f_{pES} - 0.2\left(\Delta f_{pSR} + \Delta f_{pCR}\right)\right).30$$

$$\Delta f_{pR2} = \left(20.0 - 0.4(11.6) - 0.2(7.25 + 14.7)\right).30 = 3.3\,ksi$$

<u>Total Losses</u>

$$TL = 11.6 + 14.7 + 7.3 + 3.3 = 36.9$$
$$f_{se} = 202.5 - 36.9 \approx 166\,ksi$$

KDOT METHOD (SCC)

<u>Shrinkage</u>

$$SH = 17,000 - 150RH$$

H =65

$$SH = 17,000 - 150(65) = 7250\ psi = 7.3\,ksi$$

<u>Elastic Shortening</u>

$$ES = \left(E_s / E_{ci} \right) f_{cir}$$

E_s = 28 x 10^6 psi
f_{cir} = 1420 psi

$$ES = \left(28000/3500\right)1420 = 11360\ psi = 11.4\,ksi$$

Creep of Concrete:

$$CR_C = 12\,f_{cir} - 7\,f_{cds}$$

f_{cds} = .33 ksi

$$CR_c = 12(1.42) - 7(.33) = 14.7\,ksi$$

Relaxation of Prestressing Steel

$$CR_S = 5{,}000 - 0.10ES - 0.05(SH + CR_C)$$

$$CR_s = 5 - .1(11.4) - .05(7.3 + 14.7) = 2.8\,ksi$$

Total Losses

$$TL = 11.4 + 14.7 + 7.3 + 2.8 = 36.2$$
$$f_{se} = 202.5 - 36.2 \approx 166\,ksi$$

ACI 209 METHOD (SCC)

Elastic shortening

$$ES = nf_c$$

$$n = 28500/3500 = 8.14$$

$$f_c = \frac{496}{525} + \frac{496(13.27)^2}{127490} - \frac{171(12)13.27}{127490} = ksi$$

$$ES = 8.14(1.42) = 11.6\,ksi$$

Creep

$$CR = (nf_c)v_u\left[1 - \Delta F_t / 2F_o\right]$$

$$n = 28500/3750 = 7.6$$

$$f_c = 1.42 - \frac{266(12)13.27}{127490} = 1.09\,ksi$$

$$v_u = 1.75$$

$$\Delta F_t / F_o = .14$$

$$CR = \left(7.6(1.09)\right)1.75\left[1 - .14/2\right] = 13.5\,ksi$$

<u>Shrinkage</u>

$$SH = \frac{(\varepsilon_{sh})_u E_s}{1 + n\rho k_s}$$

$$(\varepsilon_{sh})_u = 550\,\mu\varepsilon$$

$$E_s = 28500\,ksi$$

$$n = 28500/3750 = 7.6$$

$$\rho = \frac{16(.153)}{22(42)} = 0.0026$$

$$k_s = 1 + e^2/r^2 = 1 + 13.27^2 \Big/ \frac{127490}{525} = 1.73$$

$$SH = \frac{550/10^6\ 28500}{1 + 7.6(.0026)1.73} = 15.2\,ksi$$

<u>Relaxation</u>

$$RE = (f_{sr})_t$$

$$\left(f_{sr}\right)_u = .025(198) = 5.0$$

$$RE = 5.0\,ksi$$

<u>Total Losses</u>

$$TL = 11.6 + 13.5 + 15.2 + 5 = 45.3\,ksi$$
$$f_{se} = 202.5 - 45.3 \approx 157\,ksi$$

DEPARTMENT OF TRANSPORTATION
KANSAS